SEASONAL VARIATION OF TWILIGHT SODIUM EMISSION AT VICTORIA, B.C., 1967-68

by

MICHAEL GEORGE ROBERTS

B.Sc., University of British Columbia
at Victoria College, 1963

A THESIS SUBMITTED IN PARTIAL FULFILLMENT

OF THE REQUIREMENTS FOR THE DEGREE OF

MASTER OF SCIENCE

in the Department

of

Physics

We accept this thesis as conforming
to the required standard

[redacted]

. . . . . .

. . . . . .

April 1969

ABSTRACT

Supervisor: Professor Harry M. Sullivan

Twilight sodium emission from the upper atmosphere has been studied at Victoria, B.C. for a period of more than one year from February 4, 1967 to February 29, 1968 using a birefringent photometer directed towards the zenith sky.

The observations have shown that the emission intensity increased to a maximum in March 1967, decreased rapidly during this month to a summer time low in June and then increased to a broad maximum in October, November and December. After December, the intensity appeared to decrease to a minimum during the early part of February and then to rise to a secondary maximum in early March. Thus the pattern of the seasonal intensity variation obtained during the first part of 1967 was repeated in 1968.

In addition to the winter-summer seasonal intensity variation, more rapid fluctuations were observed over periods of several weeks during the autumn and winter months. These fluctuations may be due to local conditions, the global effect being simply a high intensity during the winter and a low intensity during the summer. Since the secondary intensity maximum observed in March could be due to similar local conditions which occurred at the same time of year, before it can be concluded that the typical seasonal variation exhibits two maxima and two

minima, more observations should be made, especially during the autumn and winter months.

Seasonal variations of both the morning and evening heights of maximum density were also studied. The morning heights appeared to exhibit maxima in April and November and minima in September and January whereas the evening heights appeared to exhibit maxima in March and October and minima in June and December. The apparent phase difference of approximately six to eight weeks between the two height variations is unexplained.

Although the mean monthly evening-morning intensity ratios did not differ from unity by more than ± 20%, and no seasonal trend could be detected, an interesting evening-morning variation of the height of maximum density was observed, the evening heights being generally greater than the morning ones. This evening-morning height difference variation appears to show a symmetry about the solstices, the difference being least at these times, but greatest near the 90 km. equinoxes.

Although the evening-morning height effect indicates apparent vertical motions it is difficult to explain the effect on the basis of subsidence due to overnight cooling, in view of the seasonal height variation. An alternative explanation might be found in a change in the value of the screening height between evening and morning. This would be reflected by a change in the abundance or distribution of atmospheric ozone during the

night. If the latter explanation is correct the height of the sodium layer may not vary appreciably from evening to morning.

In this thesis comparisons with temperature variations at the 90 km. level were made and a weak correlation was found with the seasonal evening height variations; however, the sparseness of the temperature data at high levels, makes the correlation somewhat uncertain.

Comparisons have been made in the past, by other workers, between stratospheric temperature variations and the seasonal variations of the intensity of the sodium twilight emissions, but again, the correlation has been very uncertain.

If the intensity and the height variations of the sodium layer are reflected by temperature changes or vertical motions of the upper atmosphere, or by changes in the vertical distribution of atmospheric ozone, such variations would be of considerable interest to meteorologists who may be led to a better understanding of atmospheric dynamics in the 90 km. region and thence to a more complete comprehension of the general circulation of the earth's atmosphere.

TABLE OF CONTENTS

LIST OF TABLES

LIST OF FIGURES

ACKNOWLEDGMENTS

The author would like to express his sincere thanks to Dr. H. M. Sullivan for his many helpful suggestions both in the experimental and theoretical aspects of this work. His suggestions concerning the methods of analysis of the observations and the interpretation of the results are greatly appreciated.

In addition, the author wishes to thank Mr. J. Sommers who made all the morning observations and many of the evening ones. Mr. Sommers' familiarity with the instrument made it possible to obtain many excellent twilight intensity records.

The kind assistance of Dr. H. N. Rundle of the Physics Department at the University of Saskatchewan, who made available special equipment required for the calibration of a spectral low-brightness source is gratefully acknowledged.

Finally, the author would like to acknowledge the financial assistance given to him by both the University of Victoria and the National Research Council (research grant NRC A 2335).

CHAPTER I

THE TWILIGHT PHENOMENON

1.1 Introduction and historical summary of twilight sodium emission

While many properties of the upper atmosphere can be determined by sampling atmospheric constituents directly using balloons or rockets, such methods are usually costly and therefore observations are often made at irregular intervals. With the discovery of the enhancement of sodium emission in the twilight sky by Bernard (1938) great impetus was given to studies of the atmospheric airglow since it then became possible to observe constituents of the atmosphere from the ground on a regular basis. Since Bernard's discovery thirty years ago, many observations of the twilight enhancement of atmospheric sodium have been made at many stations; consequently much has been learned about the role that this element plays in atmospheric chemical and photochemical reactions.

It is now generally accepted that atmospheric sodium occupies a relatively thin layer at an altitude of about 90 km. If it is assumed that the intensity of the sodium twilight emission is proportional to the abundance of illuminated sodium atoms occupying the layer, then the vertical density distribution can be deduced from observations of the rate of change of the intensity with respect to the

height of the earth's shadow in the line of sight. Using this assumption, Bernard concluded from his spectrographic observations of the suddenness of the disappearance of the emission that atomic sodium occupies a thin layer at an altitude of about 60 km. Later, however, Elvey and Farnsworth (1942) showed from spectrophotometric observations that the sodium occupies a layer having an exponential distribution paralleling that of the atmosphere as a whole in the region from 70 to 115 km.

Vegard and Kvifte (1945) extended the observations of Bernard by aiming their spectrograph towards the zenith for one observation, and towards the horizon for another. Assuming that the "disappearance" occurred at the same height, they concluded that the shadow was cast by a "screening layer" with a height of 44 km. It was natural to make the further conclusion that the "screening layer" was the top of the ozone layer and that the observed sodium emission was produced by the dissociation of sodium compounds under the action of ultraviolet light.

Bricard and Kastler (1944, 1950, 1952) showed, however, from a study of the polarization of the sodium emission itself that the radiation must arise from the resonance scattering of sunlight by neutral sodium atoms at a wavelength of 5893 Å. They explained the observations of Vegard and others by noting that the sodium layer appeared brighter near the horizon than at the zenith, and that the emission would consequently last longer before

disappearing. Dufay (1947) eliminated this error by analyzing the data for two evenings and noting the times taken for the intensity to drop to one-half of its initial value. His measurements showed that the screening height was 25 km. and the height of the sodium layer was between 80 and 90 km. Dufay also demonstrated that the screening height determined experimentally was reasonable after calculating the transmission of the atmosphere for a horizontal beam of yellow light, allowing for both ozone absorption and extinction by Rayleigh scattering.

Barbier (1948) repeated the measurements of Dufay, and from a plot of the intensity versus the dip angle of the sun concluded that the sodium layer was not only distributed exponentially with a scale height of 8 km., but also cut off sharply at the bottom at an altitude of 70 km.

The chemical equilibrium between sodium and the other constituents of the atmosphere has been examined by Hunten (1954) using the chemical reactions suggested by Chapman (1939). Hunten's analysis showed that the sodium distribution would be similar to that observed by Barbier; the bottom of the layer coinciding with the transition from molecular to atomic oxygen. Hunten also suggested that sodium is ionized by sunlight and that the recombination of ions is probably never in equilibrium. While this suggestion appeared to explain the annual intensity variation observed earlier by Bricard and Kastler (1944), it failed to explain the absence of an observed morning-

evening effect.

Later, Chamberlain, Hunten and Mack (1958) suggested that the great amplitude variation in the seasonal intensity could not be explained in terms of the transformation of sodium into ions or molecular compounds in a static atmosphere. They suggested that considerations should be given to dynamic effects, consisting either of vertical transport or exchange of air between different latitudes. Hunten and Wallace (1967) considered these dynamic effects in the atmosphere and proposed that sodium might be supplied to the upper atmosphere from dust particles by either ultraviolet light or by thermal evaporation, the observed intensity variations being due to the rate of supply. While the dust particle hypothesis has not been confirmed, Hunten and Godson (1967) have shown a correlation between increases in sodium intensity and stratospheric warming events in the northern polar and sub-polar regions. This suggests that dust particles might be injected into the 90 km. region by vertical motions associated with the warming of these regions. Furthermore, Gault (1967) has shown a correlation between the temperature of the stratosphere and the sodium intensity at Saskatoon.

Seasonal sodium intensity variations have also been observed in the southern hemisphere. Hunten, Jones, Ellyett and McLauchlan (1964) using two almost identical photometers, one in Saskatoon and the other in Christchurch, New Zealand, observed that the seasonal variation in

intensity was similar at the two stations, but displaced by six months. From these observations they concluded that the variation in intensity was actually a seasonal effect rather than an annual one.

In addition to the hemisphere effect, a latitude effect has been observed by Donahue and Blamont (1961). From observations made at three different stations (25°, 41° and 52°N latitude), they have suggested that sodium clouds exist in a belt several thousand km. wide.

A few observers have also investigated the seasonal variations of the height of maximum density. Bullock and Hunten (1961) observed a seasonal variation in the height of the sodium layer at Saskatoon of 3 to 5 km. These observers reported that observations made by Montalbetti and McEwen at Churchill (7°N of Saskatoon) showed a larger seasonal height variation than those of Saskatoon, the magnitude being about 10 km. Whereas the observations made at Saskatoon showed a single maximum in March, those made at Churchill showed maxima in May and December, and minima in February and November.

At Haute-Provence, Donahue and Blamont (1961) observed a variation in the height of the layer of about the same magnitude as that at Churchill but with a deep minimum in June. They also reported a large seasonal variation in height at Tamanrasset with maxima in the spring and summer. In addition, they observed sodium at the 150 km. level in May and August at this station.

From these observations they suggested that sodium clouds at the 85 km. level may have rifts and that a second permanent layer at approximately 150 km. may be illuminated through the gaps.

In addition to the observed seasonal variation in height reported by various observers, Blamont and Donahue (1964) reported a variation in the morning and evening heights of the sodium layer at Haute-Provence. From their published observations, it appears that generally the evening height is greater than that of the morning in the winter and early spring months, lower in the autumn months, and almost equal in the summer months. Because of the large uncertainty in their observations, however, it is difficult to determine any seasonal trends and none were suggested by these authors.

CHAPTER II

THEORETICAL DISCUSSION OF TWILIGHT SODIUM EMISSION

2.1 Resonance scattering and the excited states of the sodium atom

Bricard and Kastler (1944, 1950) have shown from a study of the characteristics of twilight sodium emission that the twilight sodium effect is produced by resonance scattering of solar radiation at a wavelength of 5893 Å by free sodium atoms. Their observations showed the emission lines to be narrow and to have a polarization of approximately 9% as would be expected for resonance excitation.

The ground state of a sodium atom is a ^2S state and the first excited states are ^2P states (cf. Herzberg, 1944, p.54 ff.). Combination of the latter with the ground state produce the characteristic yellow lines of sodium as shown in Figure II-1.

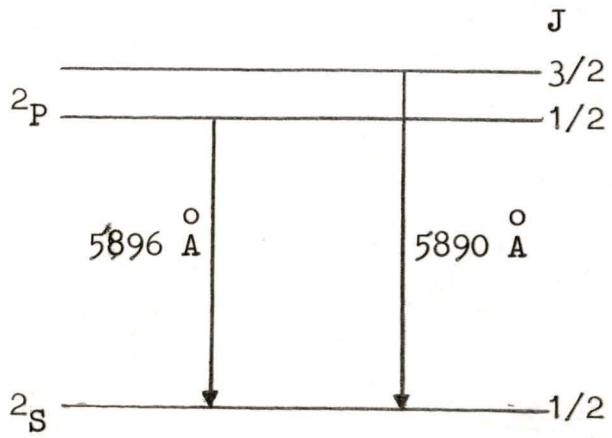

Figure II-1
Energy level diagram for sodium showing the resonance lines.

2.2 Chemical reactions of sodium in the upper atmosphere

The chemical reactions of sodium in the upper atmosphere have been discussed by many authors, including Chapman (1939), Hunten (1954), Omholt (1957), Blamont and Donahue (1964), Sullivan and Hunten (1964), and Gault (1967). Much of the following section is taken from the last three authors.

It is generally accepted that sodium reaches the upper atmosphere in the form of compounds and that these compounds are dissociated by ultraviolet light or through chemical reactions with other atmospheric constituents. Since sodium is a minor constituent of the atmosphere collisions between sodium atoms are probably rare. In addition, other constituents of the atmosphere, such as N_2 , H , and N are either relatively inactive or exist in such small concentrations as to be ineffective in any chemical reactions. Once free, sodium atoms probably react mainly with oxygen, the most important reactions being:

$$Na + O_2 + M \longrightarrow NaO_2 + M \quad \text{oxidation} \qquad 2.1$$

$$\left.\begin{array}{ll} NaO_2 + O \longrightarrow NaO + O_2 & 2.2 \\ NaO + O \longrightarrow Na + O_2 & 2.3 \end{array}\right\} \text{reduction}$$

where M represents an unspecified third body.

The rates of oxidation and reduction are thought to be nearly equal at approximately 90 km., consequently, the maximum concentration of sodium atoms would be expected

to occur at this height. Below this level, oxidation is the fastest reaction and sodium thus tends to exist predominantly in the form of oxides; reduction is the fastest reaction at higher altitudes. If complete mixing occurs above the height of maximum density and if there is no mechanism for removing free sodium at the higher altitudes, the sodium concentration should decrease at the same rate as the atmosphere as a whole, however, ionization might play an important role.

Hunten (1954) considered the ionization of sodium by sunlight and its neutralization with a negative ion:

$$Na^+ + X^- \longrightarrow Na + X \qquad 2.4$$

On this basis he predicted not only a seasonal intensity variation but also a morning-evening effect with the intensity greater in the morning and the difference largest at the equinoxes. More recently, Sullivan and Hunten (1964) have suggested that Na^+ might form ionized oxides

$$Na^+ + O + M \longrightarrow NaO^+ + M \qquad 2.5$$

$$Na^+ + O_2 + M \longrightarrow NaO_2^+ + M \qquad 2.6$$

which would be consumed by dissociative recombination to give

$$NaO_2^+ + e^- \longrightarrow Na + O_2 \qquad 2.7$$

or

$$NaO_2^+ + e^- \longrightarrow NaO + O \qquad 2.8$$

the latter reaction being rapidly followed by that given in equation (2.3).

The above reactions, if valid, would imply that atomic sodium at higher levels may not be removed rapidly by ionization. If this is so then the scale height above the peak density should be roughly equal to that of the atmosphere as a whole.

2.3 Theory of twilight sodium emission.

The theory of twilight sodium emission has been discussed in detail by Sullivan (1962) and much of this section has been taken from this author.

In section 2.2 it was shown that sodium atoms are removed through oxidation by molecular oxygen and restored through reduction by atomic oxygen. Hence at lower levels in the atmosphere, free sodium would not be expected to exist; at higher levels, the density would be expected to decrease exponentially with a scale height corresponding to that of the atmosphere as a whole. The net result is that a diffuse layer of atomic sodium will exist with a region of maximum density at some height Z_o .

During the evening twilight, for example, the diffuse layer of sodium will be illuminated by the sun and the observed intensity of emission will remain essentially constant for some time, whereas the white light intensity will decrease rapidly. As the angular solar depression, β ,

becomes larger, the earth's shadow begins to cut through the lower part of the layer in the observer's line of sight and the observed emission intensity will decrease. The rate of decrease in intensity will continue to increase until the earth's shadow passes through the densest part of the layer. As the angular depression of the sun continues to increase, only the upper reaches of the sodium layer will remain illuminated; thus the rate of decrease of intensity will continue to fall until the night sky level is reached. In the morning twilight the reverse phenomenon will, of course, be observed.

From the above discussion, it is readily apparent that the derivative of the intensity curve with respect to the height of the earth's shadow should at least approximate the vertical density distribution. Assuming that the scattered intensity, when the height of the earth's shadow in the line of sight Z_1, is proportional to the total number of sodium atoms in a $cm.^2$ column above Z_1 we may write

$$4\pi B(Z_1) = K \int_{Z_1}^{\infty} n(Z)\, dZ \qquad 2.9$$

where B is the angular surface brightness of the layer in photons/sec.-$cm.^2$ ster., Z_1 is the shadow height, $n(Z)$ is the density of sodium atoms in atoms/$cm.^3$ at the height Z, and K is a constant of proportionality.

The above discussion assumes that the sun is a point source and that the sun's rays pass through the

earth's atmosphere unaffected by refraction or scattering. In practice, however, the sun's rays are modified by the lower atmosphere and hence the shape of the twilight intensity curve will be correspondingly affected.

Figure II-2 illustrates the observational conditions during twilight for an observer situated at the point O looking at the zenith. A solar ray R_1 is shown grazing the earth. This ray would normally intersect the observer's line of sight at a height Z_1 ; but due to refraction, it is actually bent downwards by some 20 km. A ray R_2 at a height X' above the surface of the earth cuts the line of sight at a height $Z = Z_1 + X$.

Because of self-absorption by the sodium layer at the point A , both rays are attenuated. Ray R_2 is not only attenuated at A but also suffers self-absorption at the point C in the sodium layer. Rundle, Hunten and Chamberlain (1960) have described this effect by a factor $S(Z_1)$ which gives the attenuation of the absorbed radiation as a result of self-absorption. It should also be noted that ray R_2 also suffers attenuation at point B as a result of Rayleigh scattering, haze, and ozone absorption. These latter effects may be described by a transmission function $T(X')$. Note that since $X = X' \cos \beta$ and β is small for twilight observations, then $T(X') \cong T(X)$. Hunten (1954) has shown that the transmission function depends upon the following effects:

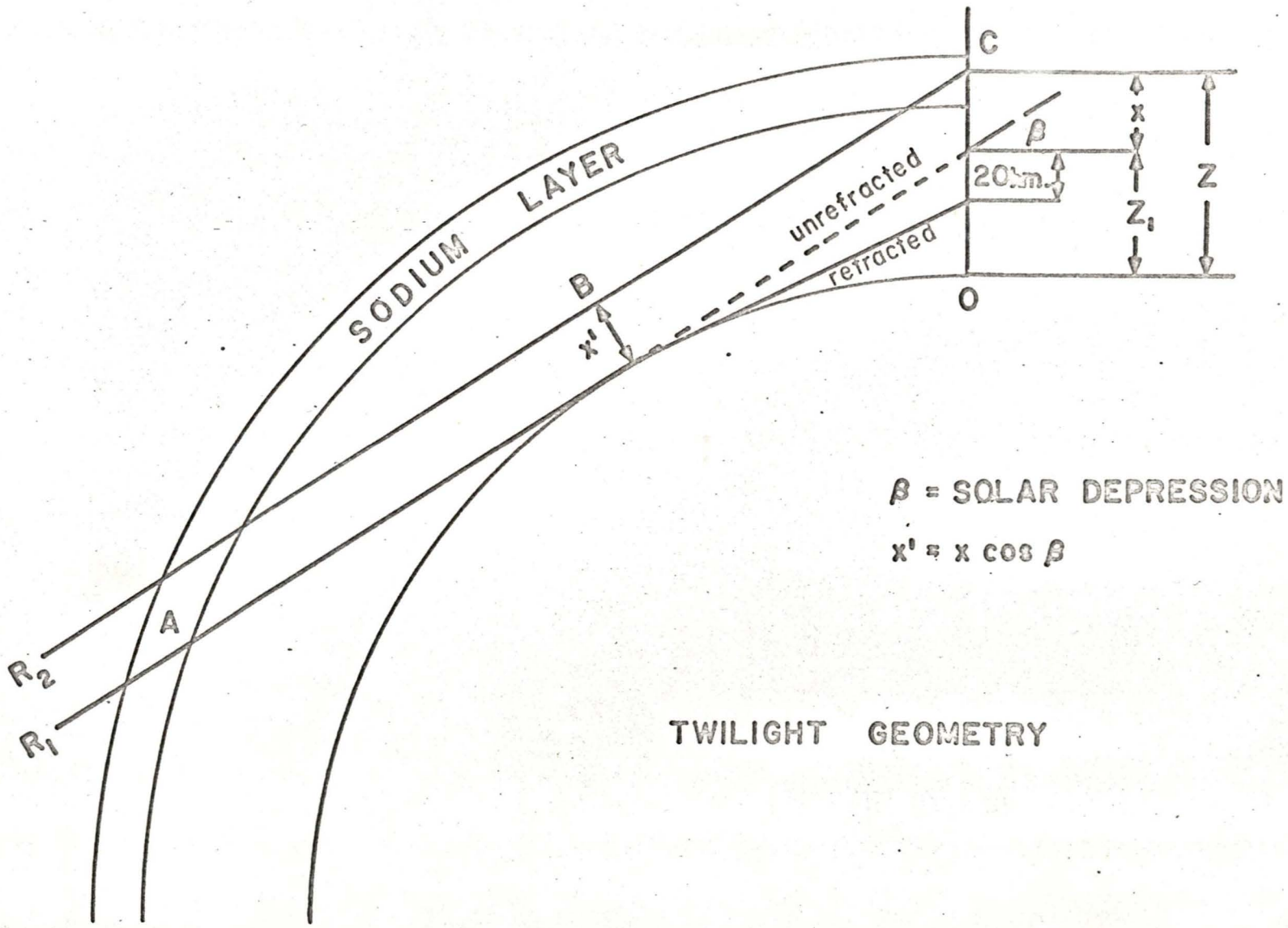

Figure II-2

Twilight Geometry

1) Extinction by molecular or Rayleigh scattering.

2) Ozone absorption.

3) Extinction by haze in the lower atmosphere.

4) Refraction.

5) Finite size of the sun.

If $B'(z_1)$ represents the surface brightness of the sodium layer when the earth's shadow cuts the observer's line of sight at a height z_1, then the observer will detect $B'(z_1)$ photons/cm.^{2}-sec.-steradian at a point O. The contribution to $B'(z_1)$ from a density $n(z)$ sodium atoms/cm.^{3} over a range dz cm. at a height z will be

$$dB'(z) = \frac{J_o \sigma}{4\pi} T(x)\, n(z)\, dz \qquad 2.10$$

photons/cm.^{2} sec-steradian, where J_o is the solar flux incident on the atmosphere measured in photons/sec.-cm.^{2} and σ is the scattering cross section of sodium atoms in cm.^{2}/atom.

Replacing x by $z - z_1$ and integrating equation (2.10) over z from $(Z_1 - 25)$ km. to infinity gives

$$4\pi B'(Z_1) = \int_{Z_1-25}^{\infty} J_o \sigma\, T(z-z_1)\, n(z)\, dz \qquad 2.11$$

where the lower limit of the integral allows for the sun's finite size (5 km.) and for refraction (20 km.). Including the self-absorption factor, $S(Z_1)$ in equation (2.11) gives

$$4\pi\, B(Z_1) = J_o \sigma\, S(Z_1) \int_{Z_1-25}^{\infty} T(z-z_1)\, n(z)\, dz \qquad 2.12$$

photons/sec.-cm.^{2} (column). Setting $J_o\sigma = g$, where g is called the g-factor or yield and has units of photons/sec. illuminated atom, gives

$$4\pi\, B(Z_1) = g\, S(Z_1) \int_{Z_1-25}^{\infty} T(z-z_1)\, n(z)\, dz \; . \qquad 2.13$$

From equation (2.13) it can be seen that if the observed intensity, $4\pi\, B(Z_1)$, is measured, and $S(Z_1)$ and $T(z-z_1)$ are calculated, then in principle the integral equation could be solved to give the density $n(z)$. Rundle, Hunten and Chamberlain (1960) have shown, however, that more information about the complete distribution can be obtained by using the derivative of the intensity rather than the intensity itself. Thus it is preferable to carry out the differentiation rather than to attempt a solution of the above integral equation directly.

Setting

$$N_{eq}(Z_1) = \int_{Z_1-25}^{\infty} T(z-z_1)\, n(z)\, dz \qquad 2.14$$

equation (2.13) can be written as

$$N_{eq}(Z_1) = \frac{4\pi\, B(Z_1)}{g\, S(Z_1)} \qquad 2.15$$

where $N_{eq}(Z_1)$ is the effective number of fully

illuminated atoms when the earth's shadow is at a height Z_1 . The units for $N_{eq}(Z_1)$ are illuminated atoms/cm.^{2} (column).

Differentiating both sides of equations (2.14) and (2.15) with respect to z_1 gives

$$\dot{N}_{eq}(Z_1) = \int_{Z_1-25}^{\infty} \dot{T}(z-z_1)\, n(z)\, dz + n(\infty)\, T(\infty) - n(Z_1-25)\, T(-25)$$

$$= \int_{Z_1-25}^{\infty} \dot{T}(z-z_1)\, n(z)\, dz \qquad 2.16$$

since $n(\infty) = T(-25) = 0$, and

$$\dot{N}_{eq}(Z_1) = \frac{4\pi}{g}\left[\frac{\dot{S}B - B\dot{S}}{S^2}\right] = \frac{4\pi}{gS}\left[\dot{B} - \frac{B\dot{S}}{S}\right] \qquad 2.17$$

where $\dot{N}_{eq}(Z_1)$ is a rough approximation to the density distribution $n(z)$ and is the derivative of the observed intensity corrected for self absorption.

Rundle, Hunten and Chamberlain (1960) have shown that the corrected derivative is not important in so far as the shape of the vertical distribution curve is concerned for abundances less than 5×10^9 atoms/cm.^{2} (column); however, if total abundances are to be determined from brightness measurements the effect of self-absorption is significant even for brightnesses as low as 2kR. Sullivan (1962) has published a curve using a g value or yield of 0.797 photons/sec. per illuminated atom (cf. Aller 1953). This curve is reproduced in figure II-3 and abundances as

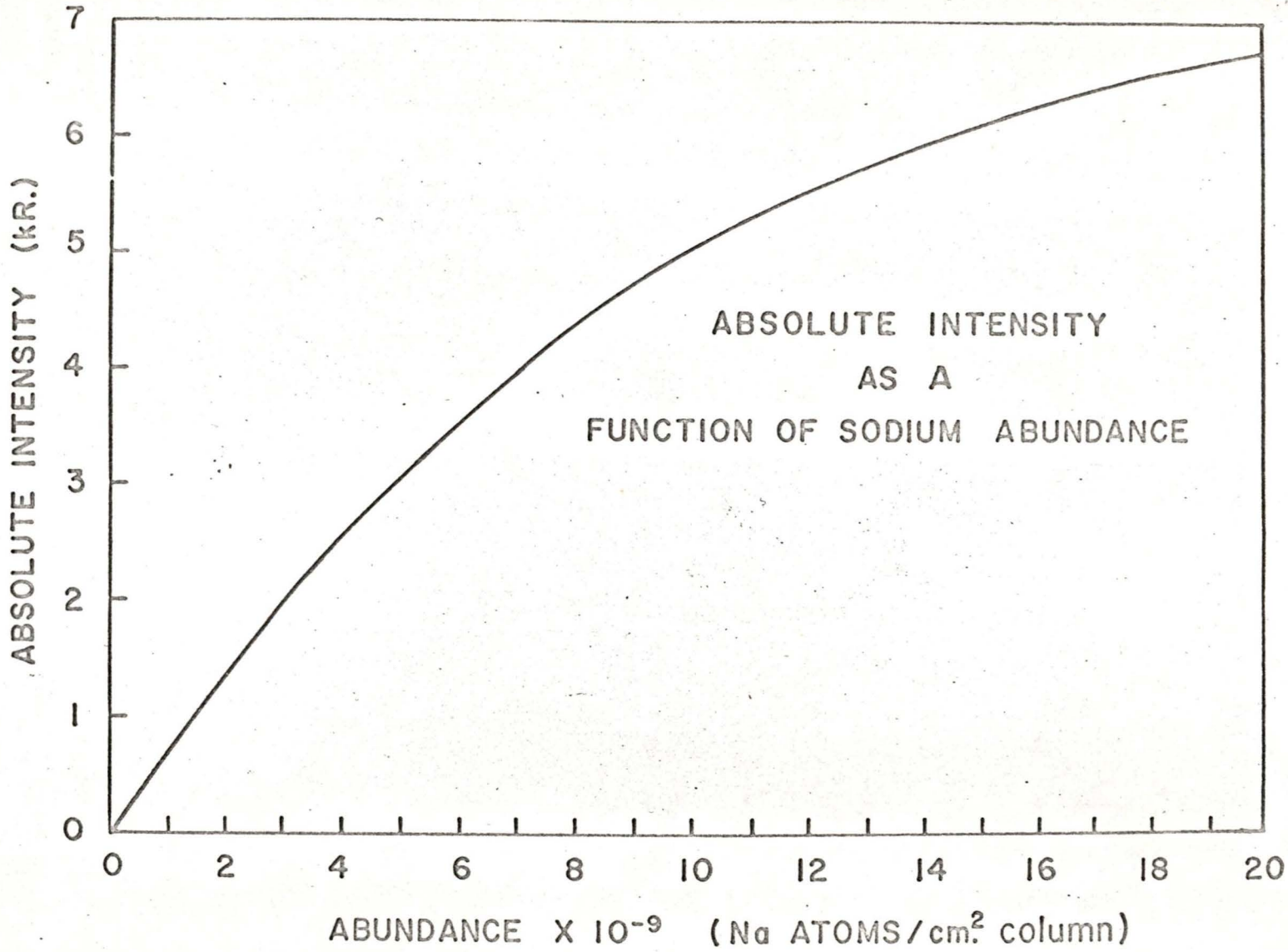

Figure II-3

Absolute intensity as a function of Na abundance for a solar depression of 6.5° and a kinetic temperature of 220°K.

a function of absolute intensity may be determined directly from it. It should be remarked that abundances determined from this curve assume a daytime to twilight abundance ratio of unity since if the sodium abundance on the day side of the terminator is much greater than the twilight value the extent of resonance absorption of incident sunlight could be much greater than has been assumed.

Equation (2.16) is a singular, linear Volterra equation of the first kind. A formal solution to this kind of equation has been derived, but higher order derivatives of both $\dot{N}_{eq}(Z_1)$ and $\dot{T}(z-z_1)$ are required and these are not known with sufficient accuracy.

Bracewell (1955) has developed a simple graphical solution for the above type of equation, and Hunten (1960) has applied the technique to the problem of determining the vertical distribution of sodium from the derivative of the measured intensity corrected for self-absorption.

Denoting the operation of the Bracewell sharpening technique by β, operating on equation (2.16) gives

$$\beta \left[\int_{Z_1-25}^{\infty} \dot{T}(z-z_1)\, n(z)\, dz \right] = \beta \left[\dot{N}_{eq}(z_1) \right] \qquad (2.18)$$

or

$$n(z) = \beta \left[\frac{4\pi}{gS} \left(\dot{B} - \frac{B\dot{S}}{S} \right) \right] \qquad (2.19)$$

atoms/cm.^{3} .

Since it is usual to express the derivative of the intensity in units of Rayleighs/km. equation (2.19) becomes

$$n\,(Z) \;=\; \beta\left[\frac{4\pi}{gS \times 10^{-1}}\left(\dot{B} - \frac{B\dot{S}}{S}\right)\right] \qquad 2.20$$

atoms/cm.^{3} . (For a discussion of the Rayleigh see Hunten, Roach and Chamberlain (1956)).

The factor $S(Z_1)$ is usually between 0.5 and 1.0 for the sodium abundances encountered (see Hunten (1960)) and hence its inclusion as a multiplying factor will not change the shape of the distribution by a large amount. Thus to a good approximation $S(Z_1)$ can be replaced by an average value $\overline{S}(Z_1)$. In this thesis the value of $\overline{S}(Z_1)$ has been set equal to unity and hence equation (2.20) can be written as

$$n\,(Z) \;=\; \beta\left[\frac{4\pi}{g \times 10^{-1}}\left(\dot{B} - \frac{B\dot{S}}{S}\right)\right] \;. \qquad 2.21$$

In chapter IV of this thesis the graphical techniques used to determine $\dot{N}_{eq}\,(Z_1)$ and $n\,(Z)$ from the observed intensity are discussed in detail.

CHAPTER III

INSTRUMENTATION AND EXPERIMENTAL TECHNIQUE

3.1 Birefringent photometer.

The birefringent photometer used throughout this investigation, which is shown in figure III-1, was built at the University of Victoria for the purpose of measuring the twilight sodium intensity and is in many respects similar to the instrument used by Sullivan in Saskatoon. Much of this section is taken from Sullivan (1962).

The theory explaining the filtering effect of birefringent quartz units has been discussed in detail by Blamont and Kastler (1951) and more recently by Sullivan (1962) and will not be discussed here.

Figure III-2 represents, schematically, the birefringent photometer used at Victoria. The instrument which is mounted vertically receives light from the zenith sky within a 5 degree (half-angle) cone by a 4-inch diameter telescope objective lens after passing through a 3 1/4-inch square interference filter. The interference filter which has a half band width of 17$\mathring{A}$ and its intensity peak at 5893$\mathring{A}$ limits the spectral region of the light entering the photometer. A birefringent unit, which includes a polarizer and an analyzer, the latter rotating at 50 Hz,, modulates the intensity of the two

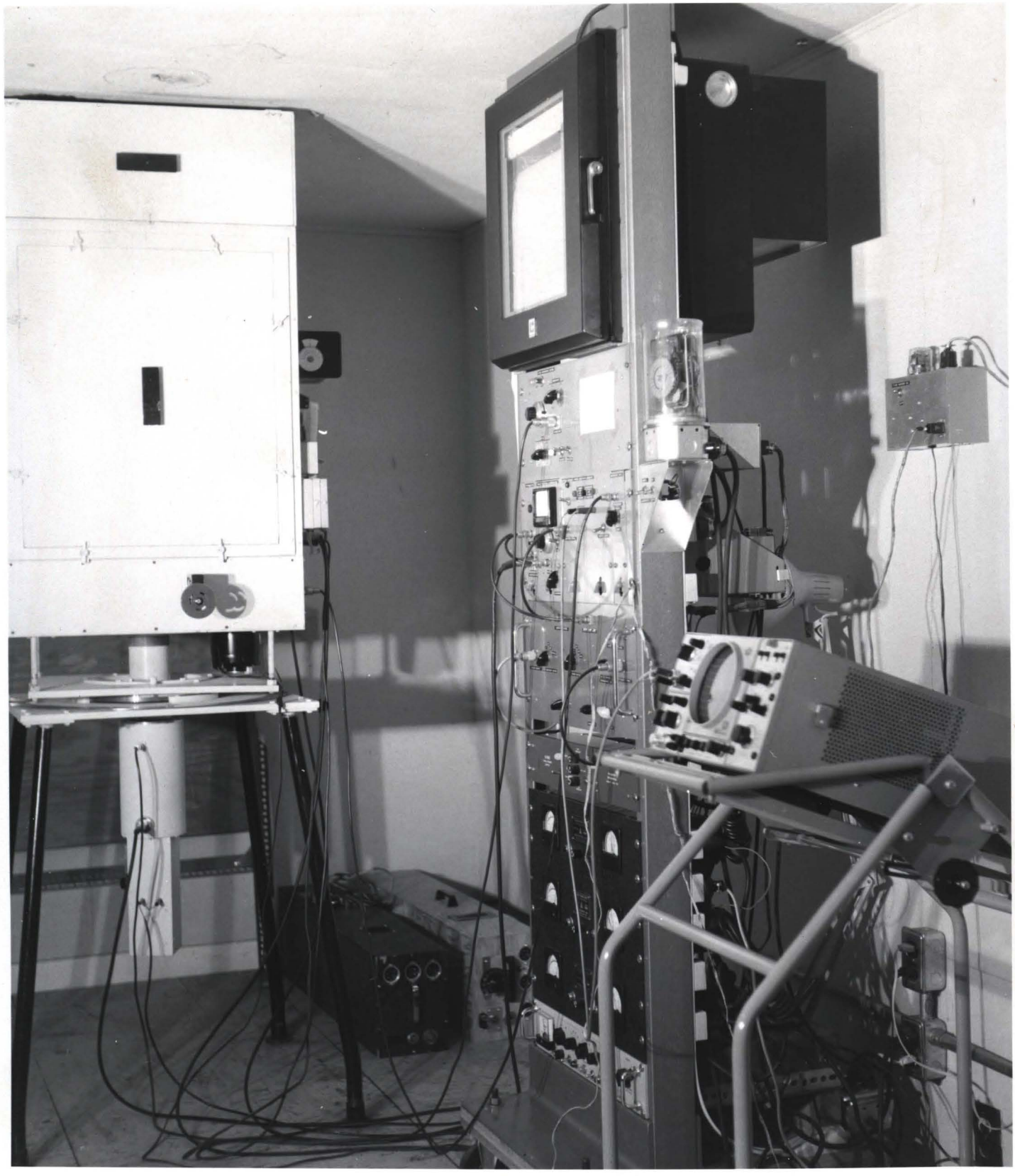

Figure III-1

Birefringent photometer and associated equipment

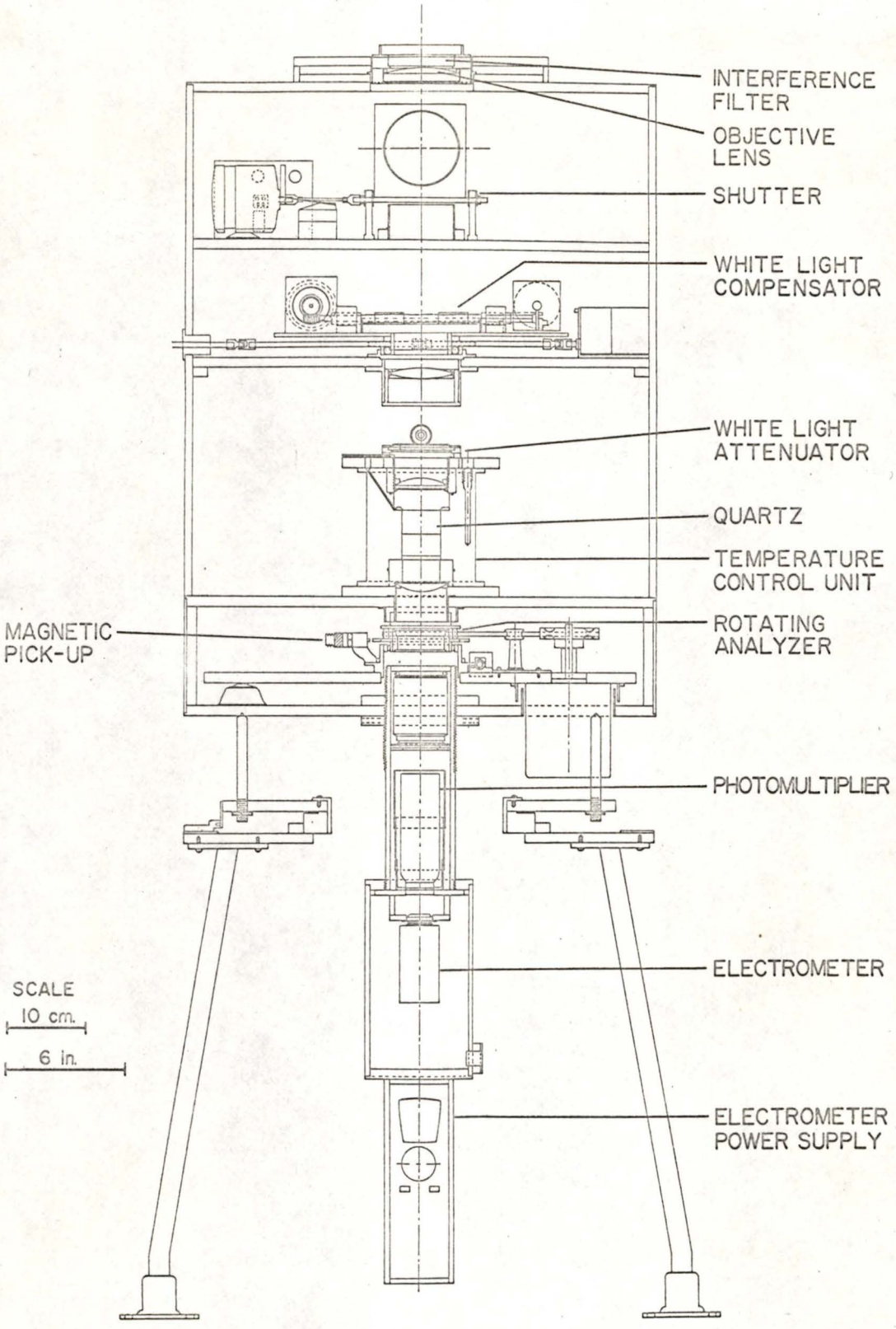

BIFRINGENT SODIUM PHOTOMETER

Figure III-2

sodium D lines simultaneously but allows the background continuum to be transmitted without modulation. Because of the presence of Fraunhofer absorption lines and other irregularities in the white light continuum, however, the background continuum is in fact modulated. To nullify this effect a white light compensator was incorporated into the optical system which, when properly adjusted, produced a signal equal in magnitude but opposite in phase to that produced by the Fraunhofer absorption lines and the other irregularities in the continuum. (See section 3.3 for a discussion of the technique of optical compensation).

When the birefringent photometer is properly compensated for the effects of Fraunhofer absorption and other irregularities in the background continuum a signal with two components is produced at the output of the photomultiplier tube. One component is the a.c. signal caused by the sodium emission and the other is the d.c. signal caused by the solar continuum. These two components are then fed into the preamplifier which serves to offer a high impedance to the signal appearing at the anode of the photomultiplier tube, transforming it with roughly unity gain to a low impedance output. (See figure III-3 for a block diagram of the electronics). In order to eliminate the d.c. component the resulting signal is fed into an a.c. amplifier tuned to 50 Hz. which passes only the a.c. component. The output from the tuned amplifier is then rectified by a phase sensitive detector which

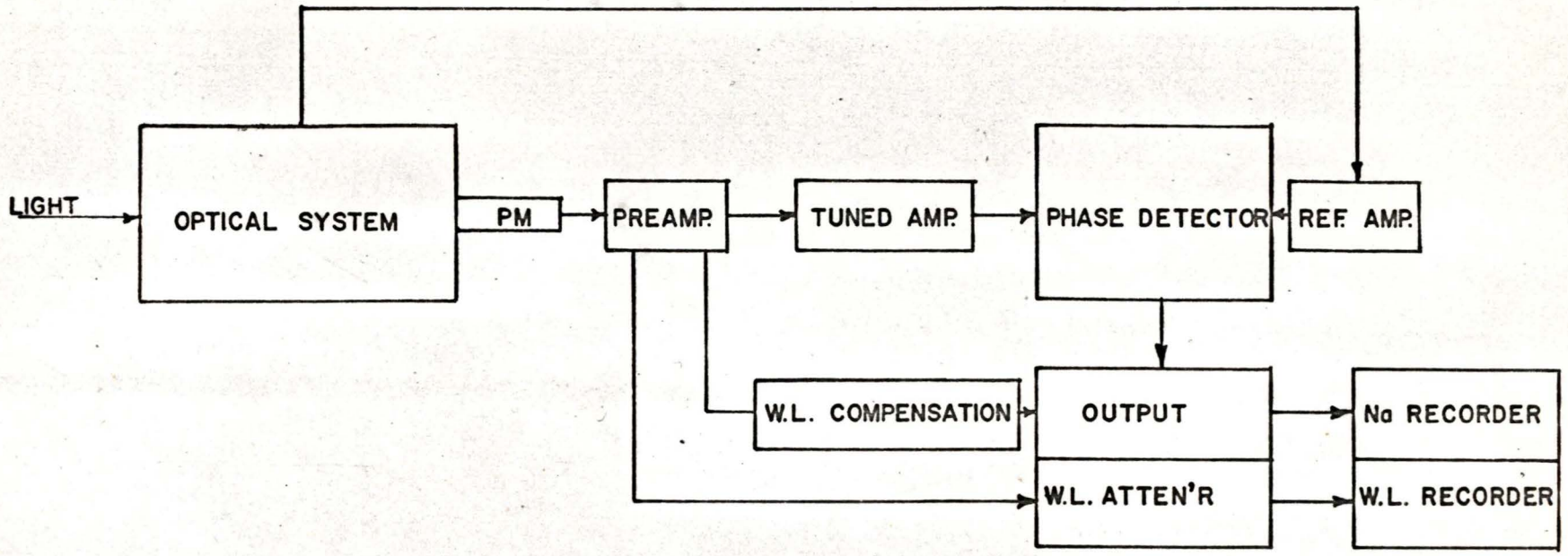

Figure III-3

BLOCK DIAGRAM OF SODIUM PHOTOMETER

is synchronized by a signal from a reference pick-up coupled to the rotating analyzer. The relative phase between the reference signal and the emission signal is adjusted so that full wave rectification of the output is obtained.

The output from the phase sensitive detector is then fed into a chopper-stabilized d.c. amplifier having a critically damped response. Finally the signal is led to the black channel input of a Leeds and Northrup Speedomax G strip-chart recorder through an attenuating range-selection switch.

While displaying the signal produced by the sodium emission, the recorder also displays the d.c. signal produced by the continuum. This is achieved by supplying the signal from the preamplifier to the second channel (red) of the Speedomax through a suitable time constant and attenuator network. This signal is extremely useful in assessing the conditions of the sky and also in correcting traces where the optical compensation settings were not properly adjusted.

Provision was also made for electronically compensating the sodium emission signal. This is achieved by applying a selected fraction of the white light signal appearing at the output of the preamplifier to the output circuit. This technique of compensation was found to be useful as a fine adjustment.

3.2 Setting the phase.

In order to adjust the photometer for maximum transmission of the two sodium D lines a sodium lamp was placed above the photometer (see figure III-2) so that scattered sodium light was directed through the optical system. Since the signal produced by modulation of the sodium light must be rectified by the phase-sensitive detector the signal appearing at the output of the reference amplifier must be synchronized with the signal appearing at the output of the tuned amplifier. This was achieved by positioning the magnetic pick-up probe until a pattern resembling full wave rectification appeared on the face of an oscilloscope connected to the output of the phase sensitive detector.

In practice the photometer was found to be extremely stable, the phase drifting only slightly over a period of several days. The phase stability of the photometer made it possible to equip the instrument with two Sauter astronomical time switches so that observations could be taken automatically. The first switch controlled the electronics, switching them on or off 15 minutes before or after each observation. The second switch controlled the shutter, (see figure III-2) opening or closing it at a solar depression of 4^{o} or 12^{o} depending upon whether the observation was an evening or morning one. Both switches automatically compensated for the daily difference in the starting or ending times of each observation due to the seasonal variation of the position of the sun.

3.3 Technique of optical compensation.

The technique of optical compensation has been discussed by Sullivan (1962) and much of this section can be attributed to this author.

A small metal disc having two areas in the shape of segments of circles diametrically opposite each other as shown in figure III-4, was fastened over the rotating analyzer (the last element of the birefringent filter) and caused to rotate with it. Above, and in the optical image plane of the rotating disc, was placed the "white light compensator" (see figure III-2) consisting of a pair of metal jaws, the aperture and azimuth setting of which could be adjusted from outside the photometer.

When properly adjusted, the net effect of these elements was to partially modulate the white light entering the photometer, producing an a.c. signal equal in magnitude but opposite in phase to that produced by the sodium Fraunhofer lines and other Fraunhofer lines and irregularities in the solar continuum.

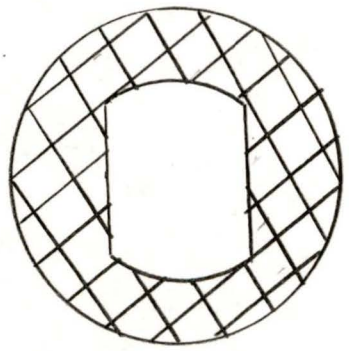

Figure III-4
Rotating mask for optical compensation

The following experimental procedure was used to obtain the correct compensation adjustments:

1) The phase of the photometer was adjusted using a sodium lamp placed above the interference filter.
2) The extra high tension (EHT) was reduced (to prevent overloading of the photomultiplier tube by white light) and the photometer orientated for minimum white light. (The transmission of white light is sensitive to photometer orientation because of the polarization due to scattering).
3) Sheets of tissue paper were then placed over the interference filter and the EHT was increased to the normal operating voltage. The thickness of the paper was determined by placing a 10.3 kR. sodium calibrator over the photometer and sheets of paper were added until the response of the photometer to the sodium calibrator was zero. With thisthickness of paper the sensitivity of the photometer was reduced to a value below the threshold for detecting atmospheric sodium.
4) The aperture of the compensator was opened and the phase of the photometer was adjusted until the signal on the cathode ray oscilloscope was shaped thus: .
5) The aperture of the compensator was partially closed and the azimuth of the compensator was adjusted until the signal on the C.R.O. was shaped thus:  .

6) The aperture of the compensator was then adjusted until no signal was visible on the C.R.O. or until no deflection of the black pen was observed.

7) The phase setting was then readjusted for the Na D lines.

Usually, the above procedure produced a reasonable plateau if the adjustments were made just prior to the evening observation. Small adjustments were made to the settings determined above on subsequent nights if the intensity curves were either slightly over or under compensated.

Once correctly set the compensator settings would generally remain satisfactory for a period of several days or several weeks. However, from time to time severe under- or over-compensation would occur. It is suggested that this effect might possibly be produced by variations in the water vapour content of the atmosphere since a strong water-vapour absorption band occurs quite close to the Na D lines in the solar spectrum.

3.4 Setting the azimuth of the photometer and determining the starting time of each observation.

Bricard, Kastler and Robley (1949) found that twilight radiation arising from resonance scattering of sunlight by sodium atoms is only about 9% polarized; hence a polarizing filter can be used to great advantage to discriminate against Rayleigh scattered white light which is strongly polarized at right angles to the sun.

Since the first element of the birefringent filter is a polaroid, it is only necessary to orient the photometer until the white light signal is a minimum. For those evening twilight observations obtained manually this was achieved by rotating the photometer about its vertical axis a few minutes before the run was due to start. To prevent the photomultiplier and/or the tuned amplifier from being overloaded while the photometer was being rotated the extra high tension (EHT) was usually reduced 20 or 30 volts below the normal operating voltage. After the photometer was orientated for minimum white light response the EHT was set to the normal operating voltage and the evening azimuth setting, α_e , was noted with respect to a circle graduate from 0^o to 360^o on the bottom of the photometer. (See appendix D for a discussion of solar azimuth). For morning observations the azimuth setting, α_m , was found using the relation $\alpha_m = 360^o - \alpha_e$.

Since the photometer was designed to operate automatically as well as manually, it was decided for the sake of convenience to write a computer program to calculate both the morning and evening azimuth settings and also the times for solar depressions of 4^o and 12^o. Using the computed azimuth setting for a particular date, the photometer was set at the correct orientation before the run started and the astronomical switch controlling the shutter was adjusted so that the shutter opened or closed at a solar depression of 4^o or 12^o depending upon whether the run

was an evening or morning one. The second astronomical switch which controlled the electronics, switched them on or off 15 minutes before or after each observation.

3.5 Calibration of the photometer.

The sodium calibrator shown in figure III-5 was designed by Sullivan to determine the absolute calibration of the photometer. Before the photometer could be calibrated, however, it was first necessary to determine the surface brightness of the sodium calibrator. This was achieved at the University of Saskatchewan using a photoelectric scanning spectrometer and a white light low-brightness source (LBS) of known surface brightness.

The output of the photoelectric scanning spectrometer was displayed on a Sanborn strip chart recorder. Figure III-6 shows schematically the triangular response to a spectral line produced by the scanning spectrometer and the steady response due to the white light LBS. The triangular response is produced because the image of the entrance slit scans over the exit slit of the scanning spectrometer.

If A is the area under the response curve produced by the sodium calibrator (in square strip chart divisions) and h is the response to the white light LBS (in vertical chart divisions), then the intensity of the sodium calibrator is given by

$$4\pi B = \frac{ADC_\lambda}{h} \text{ kilorayleighs} \qquad 3.1$$

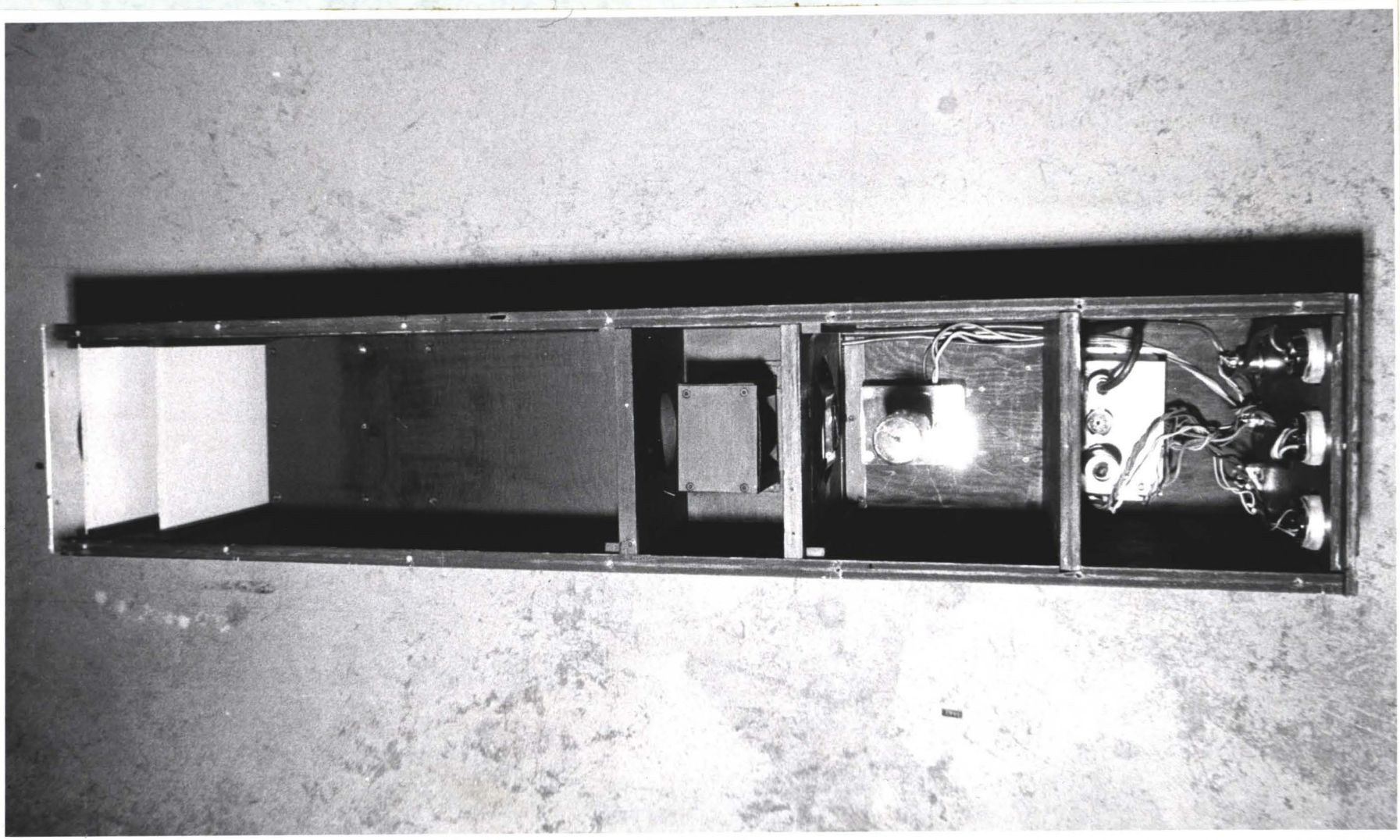

Figure III-5

Sodium Calibrator

CALIBRATION OF SODIUM CALIBRATOR

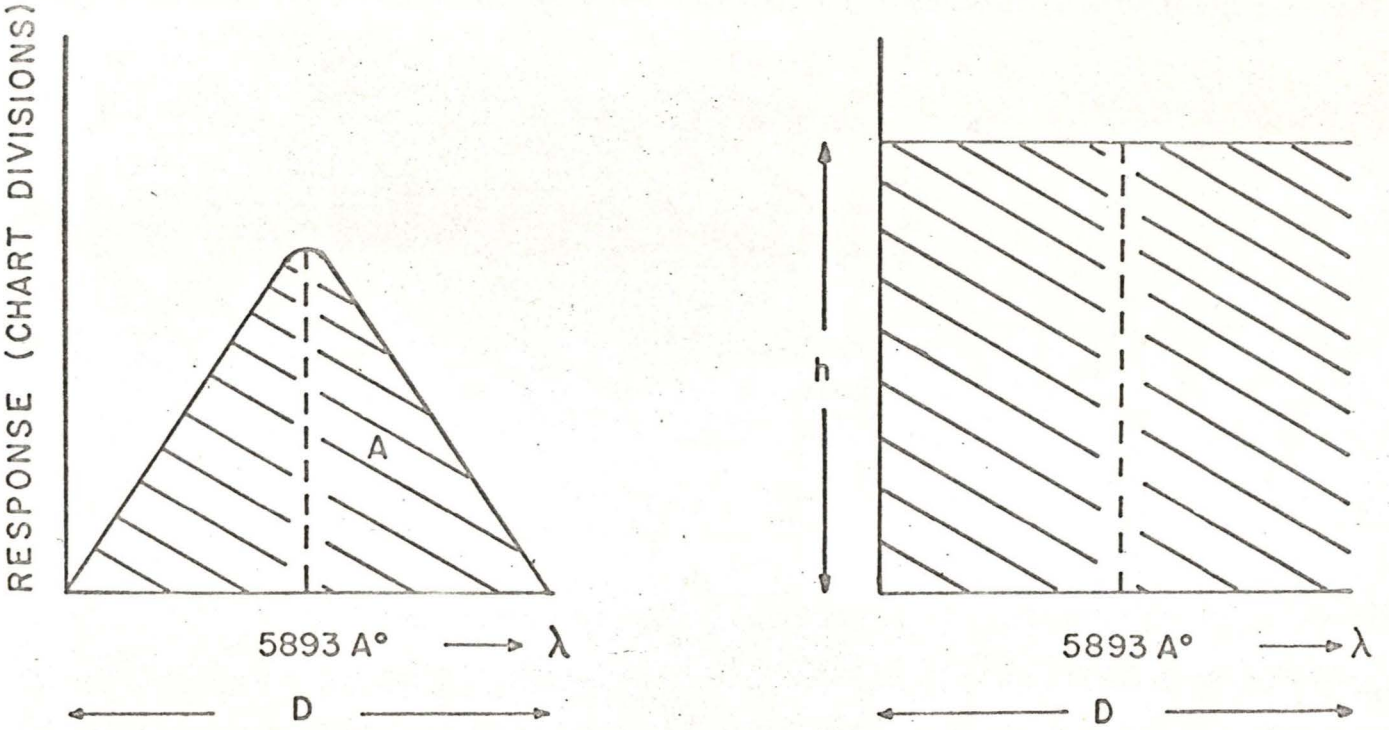

RESPONSE TO SODIUM CALIBRATOR

RESPONSE TO WHITE LIGHT LOW BRIGHTNESS SOURCE

Figure III-6

Response of photoelectric scanning spectrometer to sodium D lines and white light LBS

where D is the dispersion of the scanning spectrometer in A^{o}/horizontal chart division and C_{λ} is the differential intensity of the white light LBS in kR/A^{o}.

The value of D was calculated by scanning across the two sodium D lines after the slit of the scanning spectrometer had been adjusted to resolve them, and C_{λ}, at the wavelength 5893 $\mathring{A}$, was determined from a calibration curve of the white light LBS whose emission had been compared with that from a black body.

Three separate series of scans were made using the sodium calibrator and the white light LBS to determine the average values of A and h. (Each series usually consisted of six or more scans). Using the average values of A and h in each of the three series, the intensity of the sodium calibrator was calculated to be 11.1 $\pm$ 0.3 kR., 11.1 $\pm$ 0.3 kR. and 9.4 $\pm$ 0.4 kR. respectively, thus giving an overall average of 10.5 kR.

After determining the intensity of the calibrator using the method outlined above, it was decided to calculate the intensity by comparing the calibrator directly with the University of Saskatchewan's standard sodium calibrator. Again a series of scans was made using the two sodium calibrators and the area under each triangular response curve was calculated. Using the known surface brightness of the Saskatchewan calibrator and the ratio of the two averaged areas, the intensity of the Victoria calibrator was calculated to be 10.2 kR.

Since the calculated intensities using two independent techniques were almost identical, it was decided to adopt the average of the two values (10.3 kR.) as the intensity of the sodium calibrator.

After the intensity of the calibrator had been determined, it was possible to calibrate the photometer. This was achieved by positioning the calibrator immediately above the interference filter of the photometer. The sodium calibrator lamp was then switched on and the lamp current adjusted until the output from the monitor amplifier was 50 μa. The intensity of the sodium calibrator was then 10.3 kR. After the optical zero and the phase of the photometer were adjusted, the instrument was run for approximately 15 minutes to determine the average response in chart division produced by the calibrator. Throughout the calibration procedure the output of the monitor amplifier was observed, and if necessary, small changes were made in the lamp current to ensure that the lamp brightness remained constant.

The photometer was found to be extremely stable; the maximum deviation from the average response being less than one chart division in 50 for any one calibration run. In addition, the long term stability of the photometer was also found to be excellent. Calibration runs were made at least once a month and no significant deviation from the average response was observed.

3.6 Linearity test.

The light source shown in figure III-7 was constructed to determine whether the recorder response varied linearly as a function of the light intensity incident upon the photometer. The source is similar in many respects to the sodium calibrator discussed in section 3.5, the chief difference being the addition of a rotating disc with different apertures of known diameter. Since the light intensity falling on the large opal screen is proportional to the area of each aperture, a plot of recorder response as a function of the square of the aperture diameter will produce a curve of constant slope if the photometer response is linear. Any deviation from a straight line is a measure of the non-linearity of the instrument.

The linearity test was made by first setting the intensity of the sodium lamp to a value such that the recorder response for the largest aperture was approximately equal to that produced by the sodium calibrator (10.3 kR.). Next, the various sized apertures were rotated in front of the small opal screen, and the recorder response was noted. Throughout this procedure the intensity of the sodium lamp was monitored to ensure that the lamp intensity remained constant.

Figure III-8 shows the measured recorder response as a function of the square of the aperture diameter for the three different EHT settings used during the twilight

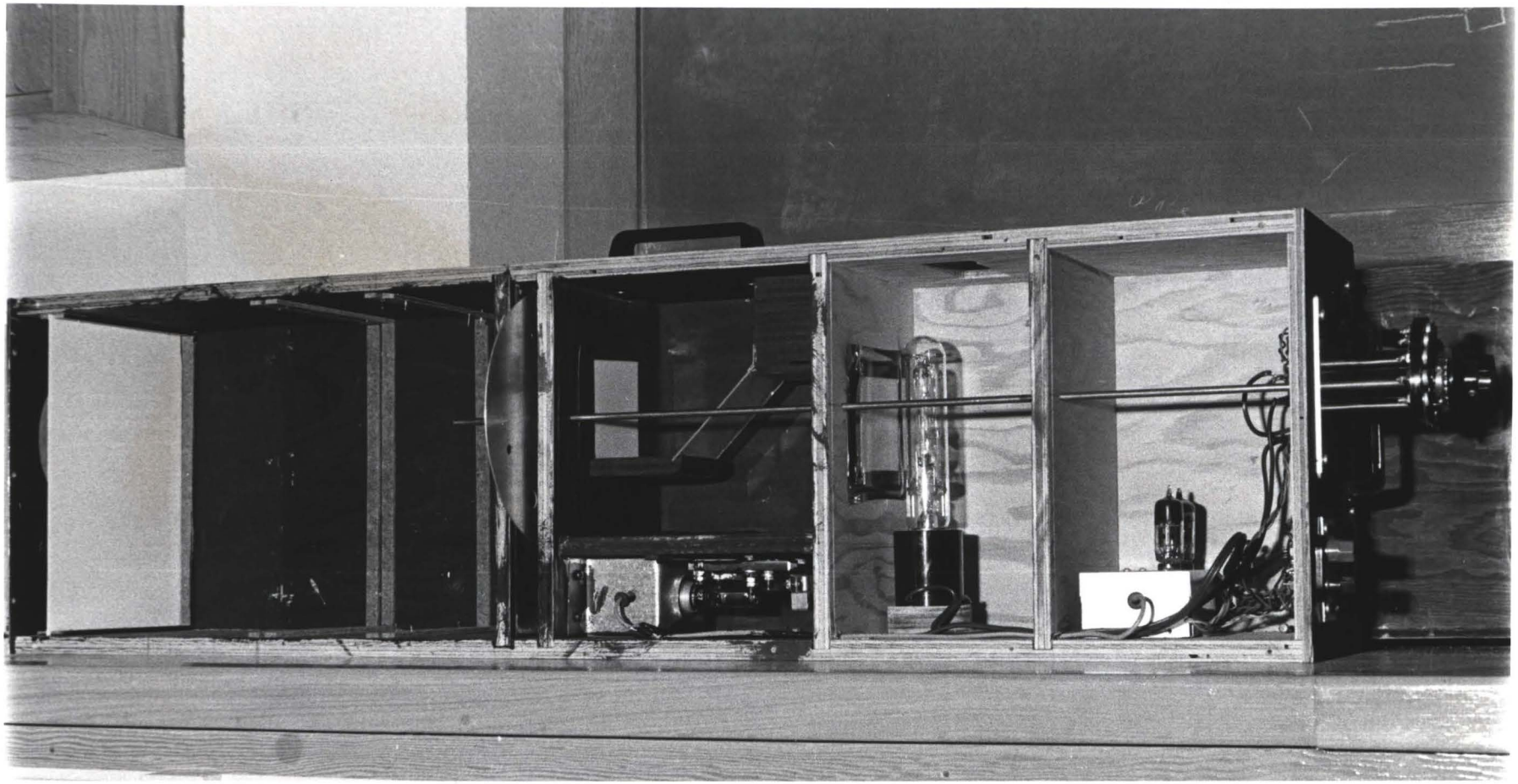

Figure III-7

Sodium light source used to test the linearity of the photometer

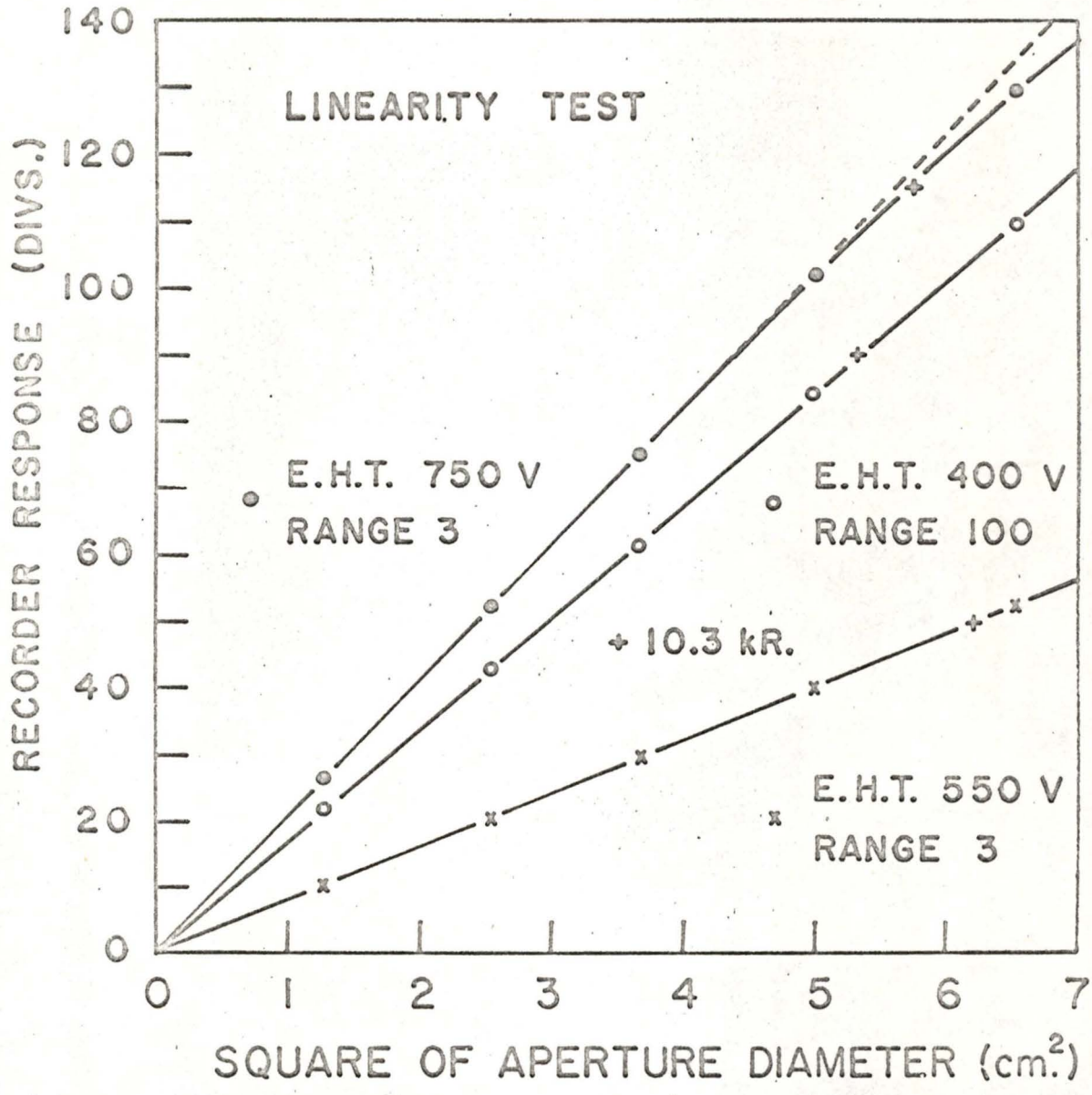

Figure III-8

Linearity test of photometer

observations. The 'plus' sign on each curve represents an intensity of 10.3 kR. determined by measuring the response of the instrument using the sodium calibrator. From this figure it can be seen that for EHT settings of 400 and 550 volts the response of the instrument was linear. However, at the EHT setting of 750 volts, the photometer response was slightly non-linear for deflections greater than 80 to 90 chart divisions. Since none of the observed twilight intensities produced deflections greater than 60 chart divisions on this EHT setting, no corrections were made to the twilight intensity curves.

While the non-linearity of the photometer on the 750 volt setting was not large enough to affect the shape of the twilight intensity curves, a small error was introduced in the calibration factor used to relate deflection in chart divisions to intensity in rayleighs. This error in the calibration factor, however, produces an error of less than 1% for deflections as great as 60 chart divisions and thus did not significantly affect either the plateau intensities or the density distribution.

CHAPTER IV

COMPUTER PROGRAM

4.1 General discussion of data analysis.

This chapter describes in detail the computer program used to determine the sodium density distribution from each recorded twilight intensity curve. The program was written in Fortran IV and the data were analyzed on the University's IBM 360/44 computer. Appendices A, B, and C contain a glossary of the symbols used in the program, a listing of the program and a typical analysis of a twilight intensity curve.

Since the calculated sodium density distribution is extremely sensitive to the shape of the twilight intensity curves, only those runs obtained during clear twilights and which were well compensated for the effects of Fraunhofer absorption of the solar continuum were analyzed. Because many observations made during clear twilights were either slightly over or under compensated the following technique was used to obtain a flat plateau region before each intensity curve was scaled. First a smooth curve was drawn on each record, following closely the sodium intensity curve. Next a fraction of the white light curve was either added to or subtracted from each sodium intensity curve, the fraction being chosen so that the resulting curve gave a flat plateau region (see figure IV-1). After each

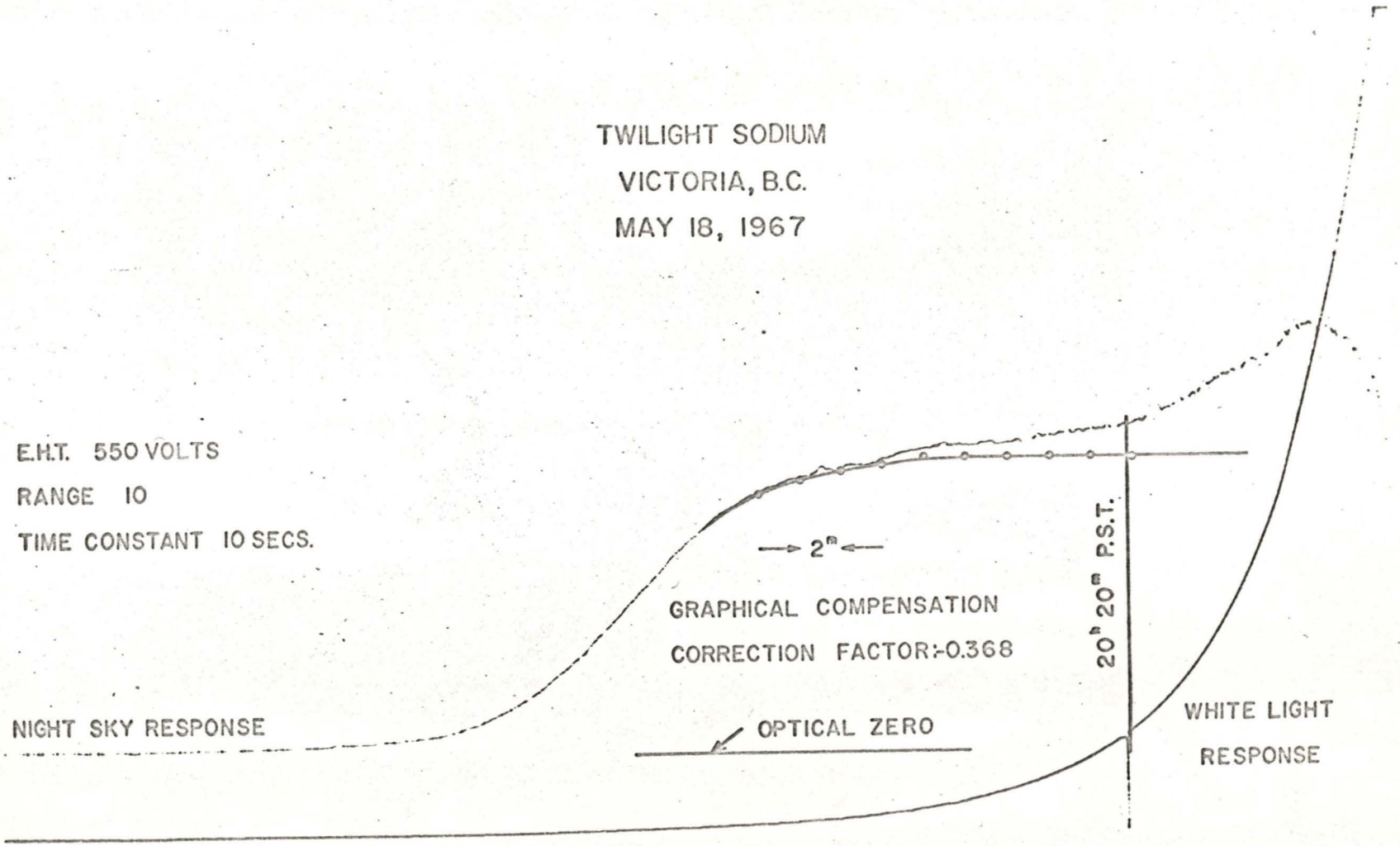

Figure IV-1

Intensity record illustrating the technique of graphical compensation

twilight curve had been corrected to give a flat plateau region, each corrected intensity curve was scaled at one minute time intervals, beginning with the highest (plateau) values first, regardless of whether the twilight observation was a morning or evening one. Each scaled value was the displacement above the optical zero of the photometer in chart divisions, the night sky correction being subtracted by the computer in each case.

In addition to the above data, the following information was provided for each twilight observation:

1. Date (IDAY, MONTH, IYEAR) and identification as to whether the run was a morning or evening observation (A.M. or P.M.).
2. Calibration factor (CALIB) to convert chart divisions to rayleighs.
3. Conversion factor (CONST) used to obtain the density from the derivative of the intensity curve with respect to the geometrical shadow height. The conversion factor is 10/g where g is the yield or g-factor and has a value of 0.797 photons/sec. per illuminated atom. See following equations (2.12) and (2.19).
4. The two Bracewell parameter $\overline{X}$ (XBAR) and 2σ(BI1). (See section 4.8 for a discussion of these parameters).
5. The range (IRANGE), the extra high tension (HV) and time constant (TC) settings of the photometer.
6. The Pacific Standard Time expressed in hours (ITIMEH)

and minutes (ITIMEM) corresponding to the first scaled chart division. The time was determined with a precission of better than ± 5 seconds.

7. The equation of time expressed in minutes (IAMM) and seconds (IAMS) at 0^h ephemeris time for the calendar day of the observation.
8. The change in the equation of time, expressed in seconds, during the subsequent 24 hour period (INCAMS).
9. The declination of the sun at 0^h ephemeris time for the calendar day of the observation expressed in degrees (IDECD), minutes (IDECM) and seconds (IDECS).
10. The change in the declination of the sun, expressed in seconds, during the subsequent 24 hour period (INCDEC).

(These last seven constantsfor any particular observation were found from the American Ephemeris and Nautical Almanac).

Using the above data the computer executed the program and the printer listed or plotted the results on thirteen pages of output.

4.2 Determination of the sodium density as a function of height.

The following operations were executed by the computer to determine the sodium density as a function of height.

1. The Pacific Standard Time corresponding to each sampled response was calculated.

2. The night sky correction was found by taking the average of the last five sampled responses read by the computer.

3. The night sky correction was subtracted from each sampled response and the result was multiplied by the appropriate calibration factor to determine the intensity in rayleighs above the night sky intensity. These calculations, while not affecting the density distribution, enabled the twilight sodium abundance to be estimated (see section 4.3).

4. The change in intensity, $\Delta 4\pi B_i$, was found as follows:

$$\Delta\, 4\pi\, B_i \;=\; 4\pi\, B_{i-2} - 4\pi\, B_{i+2} \qquad (4.1)$$

where $4\pi\, B_i$ represents the intensity expressed in rayleighs and i is a running subscript which assumes all values from 3 to N-2, where N is the total number of sampled responses read by the computer.

5. The declination of the run, the solar hour angle and the solar elevation were calculated for each sampling time. The latter was determined using equation (D.6). (See Appendix D for a discussion of the equations used to calculate both the declination of the sun and the equation of time at the time of the observation).

6. The effective shadow height of the earth was calculated for each sampling time using the relation

$$Z_i = R(\sec \beta_i - 1) + \bar{X} \text{ km.} \qquad 4.2$$

where R is the radius of the earth (6370 km.), β the solar depression and $\bar{X}$ one of the Bracewell parameters (screening height). (The factor $R(\sec \beta_i - 1)$ given in the above equation is the geometric shadow height and the factor $\bar{X}$ allows for the effect of atmospheric screening).

7. The change in height, ΔZ, corresponding to the change in intensity $\Delta 4\pi B_i$ was found using the relation

$$\Delta Z = Z_{i+2} - Z_{i-2} \qquad 4.3$$

8. A rough approximation to the density, d_i, measured in sodium atoms/cm.^{3} at the height Z_i km. was found from the relation

$$d_i = \frac{k \, \Delta 4\pi \, B_i}{\Delta Z} \qquad 4.4$$

where k is a constant equal to $10/g$ where g is the yield ($g = 0.797$ photons/sec per illuminated atom). It should be noted that the above expression is only a rough approximation to the density, the self-absorption and Bracewell corrections being applied later in the computer program. (See equation (2.9) following).

4.3 Determination of plateau intensity and abundance.

After each sampled response was multipled by an

appropriate calibration factor to convert response in chart division to rayleighs, the intensity corresponding to the first sampled scaled response was multiplied by 10^{-3} to give the intensity in kilorayleighs. Using this intensity the abundance was determined by linearly interpolating within a stored list of abundances determined from Figure II-3. This list of abundances was determined by associating each integral kilorayleigh interval in the figure with it corresponding abundance. After the computer had calculated both the intensity and the abundance corresponding to the first scaled response these two values were listed by the computer.

4.4 Interpolated densities for integral heights.

A plotting routine was incorporated into the computer program so that the sodium density as well as being determined numerically, could be plotted as a function of the height. Since an X-Y plotter was not available at the time the program was written, the density distribution was plotted using the standard printer associated with the computer (IBM 1403N1). This imposed the condition that the density distribution be expressed in terms of integral heights so that a one-to-one correspondence existed between the heights and the line numbers of the listed output. To achieve this a simple linear interpolation scheme was developed which calculated interpolated densities for integral heights from 50 to 150 km. After

the interpolated densities were calculated the densities and heights were listed and the computer then entered the plotting routine described in the next section.

4.5 Computer plotting.

Using the list of interpolated densities as a function of integral heights, the computer executed the plotting routine. This section of the program is basically as follows.

1. Each value of the density was multiplied by a constant chosen so that the resulting product was less than the total possible number of characters that could be printed on one line of printer output.
2. The constant 0.5 was added to each of the above products to correct round-off error.
3. The integer variables IDENS(I) were set equal to the values calculated in (2). I is the integral height which ran from 50 km. to 150 km.
4. Starting with IDENS (I1) where I1 was set initially to the value 149, the integer variable

$$NX = K + IDENS(I1) \qquad 4.5$$

was calculated, where K was a suitable positive integer picked to determine the position of the 'dot' on the output listing corresponding to zero density.

5. The integer variables IPLOT (I), where I ran from unity to the maximum possible value of NX (the

total number of characters that could be printed on one line), were set equal to a 'blank' with the exception of IPLOT (K), IPLOT (NX) and IPLOT (maximum possible NX), which were set to the value 'dot'.

6. Next each value of IPLOT (I) was printed across a single line producing either a 'blank' or a 'dot'. (Note that the position of the dot associated with IPLOT (NX) corresponded to the density at the height I1 in km.

7. The value of I1 was decreased by unity and the computer looped to (4) above unless I1 was equal to 49, at which point the computer executed the remainder of the program.

4.6 Self-absorption correction.

In section 2.3 (see following equation (2.17)) it was shown that the derivative of the observed intensity corrected for the effects of self-absorption may be obtained from the relation:

$$\dot{N}_{eq}\ (Z_1) = \frac{4\pi}{g \times 10^{-1}\ S}\left[\dot{B} - \frac{B\dot{S}}{S}\right] \qquad 4.6$$

where $4\pi\ B\ (Z_1)$ and $4\pi\ \dot{B}\ (Z_1)$ are the observed intensity and its derivative with respect to shadow height Z_1, and $S\ (Z_1)$ and $\dot{S}\ (Z_1)$ are the self-absorption correction factor and its derivative (cf. Rundle, Hunten and Chamberlain (1960)).

Abundance 10^9 atoms/cm.^{2} (column)	4π $\dot{BS}/S$ R/km.
1	0.42
2	1.60
3	3.33
4	5.48
5	8.00
6	10.00
7	13.70

TABLE IV-1

Values of the self-absorption correction factor, 4π $\dot{BS}/S$, at a shadow height $(43 + \bar{X})$ km. as a function of sodium abundance N . (cf. Hunten 1960). It should be noted that although Hunten stated that he plotted $\dot{SB}/S$ against abundance, constants of proportionality were dropped in his expression. The unit for 4π $\dot{BS}/S$ is in fact R/km.

Hunten (1960) has described a graphical procedure for determining $\dot{N}_{eq}(Z_1)$ which consists of the following steps:

1. Plot $4\pi \dot{B}(Z_1)/g \times 10^{-1}$ against Z where $Z = Z_1 + \bar{X}$, Z_1 is the geometric shadow height and $\bar{X}$ is the screening height.
2. Plot 4π $\dot{BS}/S$ as a zero at the height $(56 + \bar{X})$ km.
3. Plot the value of 4π $\dot{BS}/S$ given in table IV-1 at the height $(43 + \bar{X})$ km.
4. Draw a straight line through the two points found

in (2) and (3) above.

5. Add the two curves to give $\dot{N}_{eq}(Z_1)$.

Hunten's graphical technique of determining the corrected derivative was adapted to the computer program as follows:

1. The values of $4\pi B\dot{S}/S$ given in Table IV-1 were stored in the computer as the real variables S(I) where I ran from 1 to 8 .
2. The abundance corresponding to the first sampled scaled response was multipled by 10^{-9} and a linear interpolation was performed within the table to find the 'correction factor', called X4 , for the given abundance at the height $(43 + \bar{X})$ km.
3. Taking the correction factor to be zero at the height $(56 + \bar{X})$ km. the slope of the 'line' joining the above two 'points' was found using the relation,

$$\text{SLOPE} = X4/13 \quad . \qquad 4.7$$

4. Using the calculated value of the slope the corrected rough density distribution was found using the relation

$$\text{DENST (J)} = \text{DENST (J)} + (X5 - X1) \cdot \text{SLOPE} \qquad 4.8$$

where DENST (J) on the right hand side of the equation was the uncorrected density at the height J km., and (X5 - X1) was the increment in height corresponding

to the distance from the height $(56 + \bar{X})$ to the height J.

After determining the corrected rough density corresponding to all heights from $(56 + \bar{X})$ km. to 50 km. the computer determined the Bracewell correction to be added to each calculated density. This correction is discussed in the next section.

4.7 Bracewell correction

In section 2.3 the integral equation

$$\dot{N}_{eq}(Z_1) = \int_{Z_1-25}^{\infty} \dot{T}(Z - Z_1)\, n(Z)\, dZ \qquad 4.9$$

was derived, where $n(Z)$ is the density, $\dot{N}_{eq}(Z_1)$ is a rough approximation to the vertical density distribution corrected for self-absorption, and $\dot{T}(Z - Z_1)$ is the derivative of the transmission function. Bracewell (1955) showed that integral equations of the above type could be solved by a graphical technique and Hunten (1960) applied Bracewell's method to the specific problem of determining the sodium distribution from the derivative of the measured intensity. Hunten's technique is as follows:

1. $\dot{N}_{eq}(Z_1)$ is plottted against $(Z_1 + \bar{X})$ where $\bar{X}$ is the screening height given in table IV-2.
2. A chord is drawn across the curve spanning a height 2σ, where 2σ is the second Bracewell parameter.
3. The correction to be added to the curve, $\dot{N}_{eq}(Z_1)$, at the middle of the chord is equal to the distance

from the chord to the curve.

	$\overline{X}$ (km.)	2σ (km.)
Autumn (S-O-N15)	30.05	22.1
Winter 1 (N15-D-J)	30.35	20.7
Winter 2 (F-M)	31.70	19.2
Spring (A-M)	31.08	20.1
Summer (J-J-A)	30.69	21.1

TABLE IV-2

Bracewell parameters $\overline{X}$ and 2σ for different times of the year. (cf. Hunten 1962).

Hunten's graphical technique described above was adapted to the computer program as follows:

1. Starting at the height 50 km. and the corresponding density corrected for self-absorption, DENST (50), the densities at the heights (50 + 2σ) km. and (50 + σ) km. were calculated by a simple interpolation scheme. (See figure IV-2).
2. The slope of the 'chord' joining the points DENST (50) and DENST (50 + 2σ) was determined and from the slope the value of the density on the 'chord' at the height (50 + σ) km. was found.
3. The difference between the density along the 'curve' and along the 'chord' (called X in figure IV-2) was found by subtracting the appropriate densities found in (1) and (2) above.

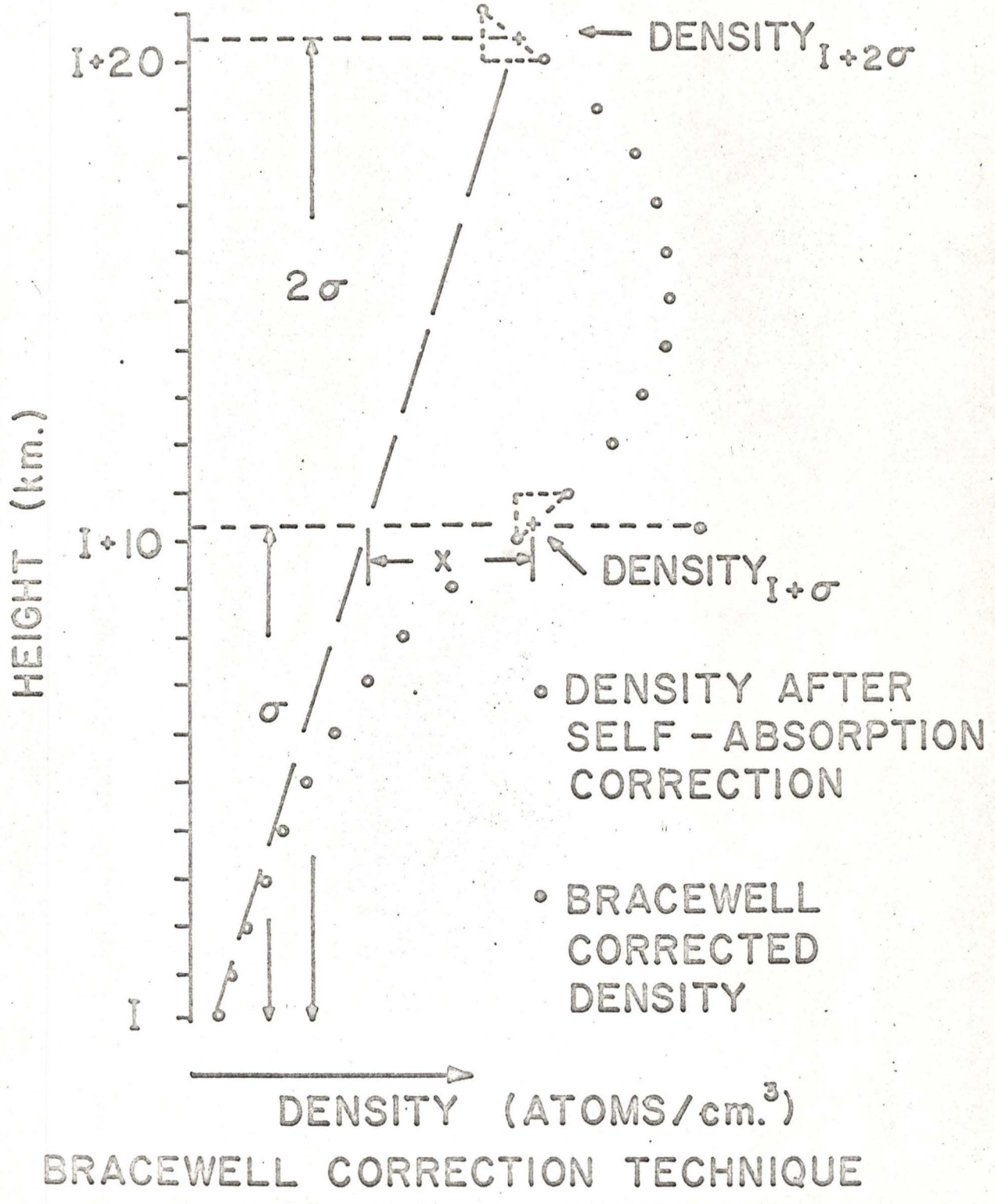

Figure IV-2

Bracewell correction technique

4. The difference found in (3) was added to the interpolated density, DENST (50 + σ) , thus giving the Bracewell corrected density at the height 50 + σ kilometers.
5. The starting height of 50 km. in (1) above was incremented by unity and the above scheme was repeated until the starting height corresponded to 130 km.
6. The list of Bracewell corrected densities, was interpolated to give the corrected density distribution for integer heights from 50 to 150 km.

After the Bracewell correction was calculated, the computer listed the densities and heights and then plotted the density distribution using the plotting routine described in section 4.5.

4.8 Scale height.

After listing and plotting the corrected sodium density distribution, the computer entered the final phase of the program. This phase listed and plotted the natural logarithm of the density distribution from which the scale height was determined as described in appendix F.

After completing the final stage of the program the computer looped back to the beginning and executed the whole program again if another set of data cards was present to be read.

CHAPTER V

DISCUSSION OF SODIUM TWILIGHT OBSERVATIONS

5.1 Seasonal variation of the plateau intensity.

Regular twilight observations of atmospheric sodium emission were made in the zenith from February 1967 to February 1968. During this period over two hundred observations were made and analyzed using the computer program discussed in Chapter IV.

The plateau intensity for each morning and evening sodium observation is plotted in figures V-1 (A) and V-1 (B). The circles represent the observations made during 1967 and the crosses those made during 1968. For convenience the circles have been joined by straight lines so that the seasonal variations of both the morning and evening plateau intensities may be more readily discerned.

The figures show that both the morning and evening plateau intensities followed the same general trend, the largest intensities occurring during the winter months and the smallest during the summer months.

In addition to the seasonal change in intensity, these figures show that both the morning and evening intensities changed by a factor of two or three over a period of several days. These changes are most obvious during the month of October (see in particular

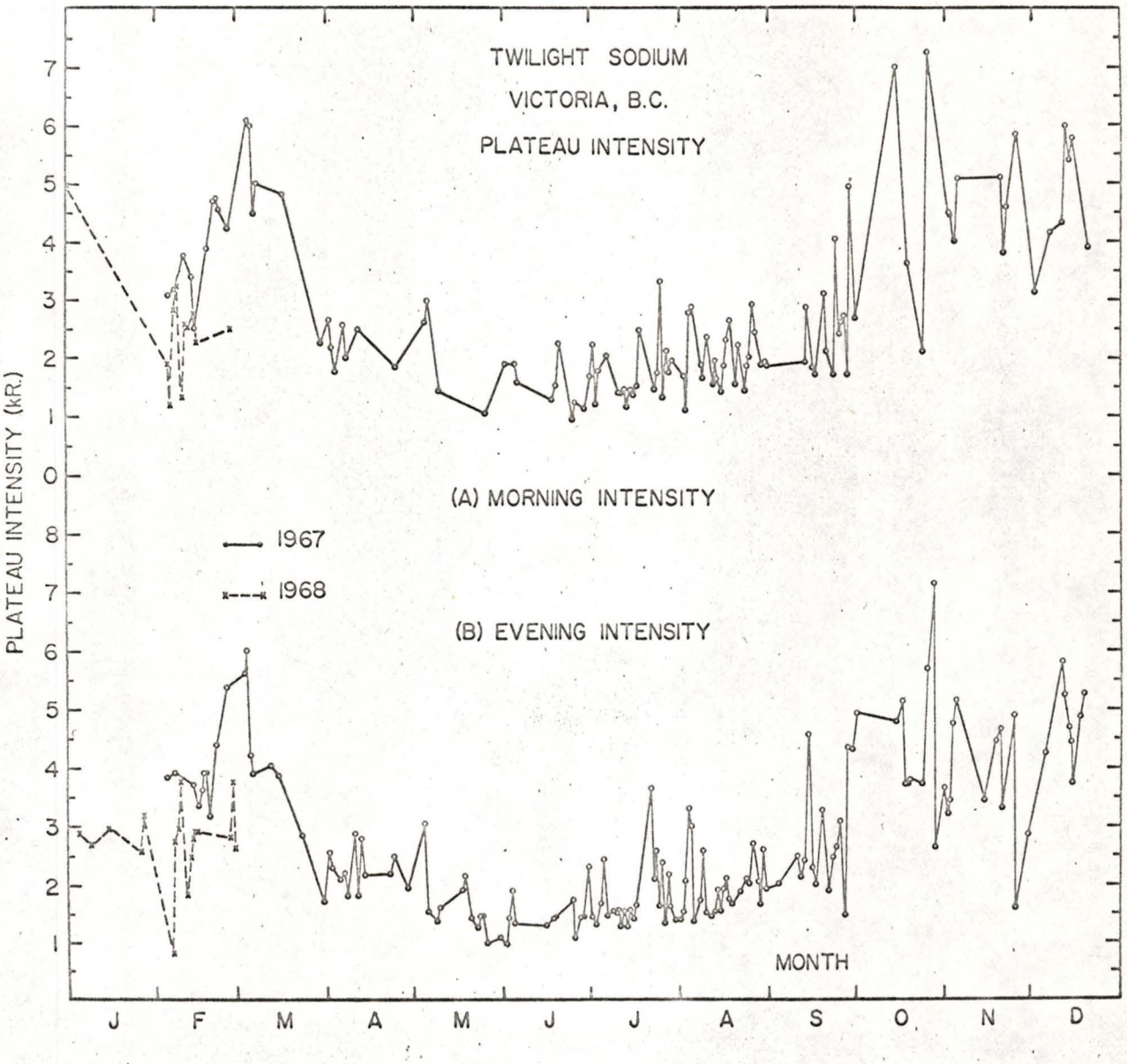

Figure V-1

Individual morning and evening plateau intensity observations

figure V-1 (A)) when the intensity varied from approximately 7 kR. to 2 kR. in a period of several days. Rapid changes of intensity such as the one mentioned here are probably real since increasing or decreasing trends were observed on more than one occasion. Such trends have also been noted by other observers. (See Bullock and Hunten (1961)). During the summer the magnitude of the fluctuations appeared to be much smaller.

The similarity of the morning and evening plateau intensity curves shown in figures V-1 (A) and V-1 (B) suggest that the average ratio of the evening to morning intensities would probably be close to unity. To check this supposition the monthly means of the evening to morning intensity ratios were computed using only pairs of observations in which a morning run was immediately preceded or followed by an evening run. Where three or more consecutive observations were possible they were considered in triplets, the intensity of the first and third members having been interpolated linearly to the time of observation of the second member in order to eliminate as much as possible any day to day intensity variation. Values of the mean monthly evening to morning intensity ratios are given in table V-1 and are plotted in figure V-2. The error bars shown in this figure represent twice the average mean deviation. It should be noted that no error bar has been assigned to the January value since very few observations were available for this month. The

Month	No. of pairs or triplets	Mean intensity ratio PM/AM	Mean deviation of ratios
1967			
February	8	1.08	0.16
March	8	0.94	0.10
April	8	1.03	0.14
May	4	1.05	0.12
June	9	1.00	0.25
July	31	1.06	0.16
August	33	1.01	0.16
September	12	1.10	0.18
October	4	1.07	0.34
November	11	0.91	0.11
December	7	1.02	0.20
1968			
January	1*	0.88	-
February	11	1.03	0.08

TABLE V-1

Mean Monthly Evening/Morning Plateau Intensity Ratios.

* No pairs of PM/AM observations were obtained during this month and only one good morning observation was obtained. The ratio was found using the morning observation and an evening observation obtained several days later.

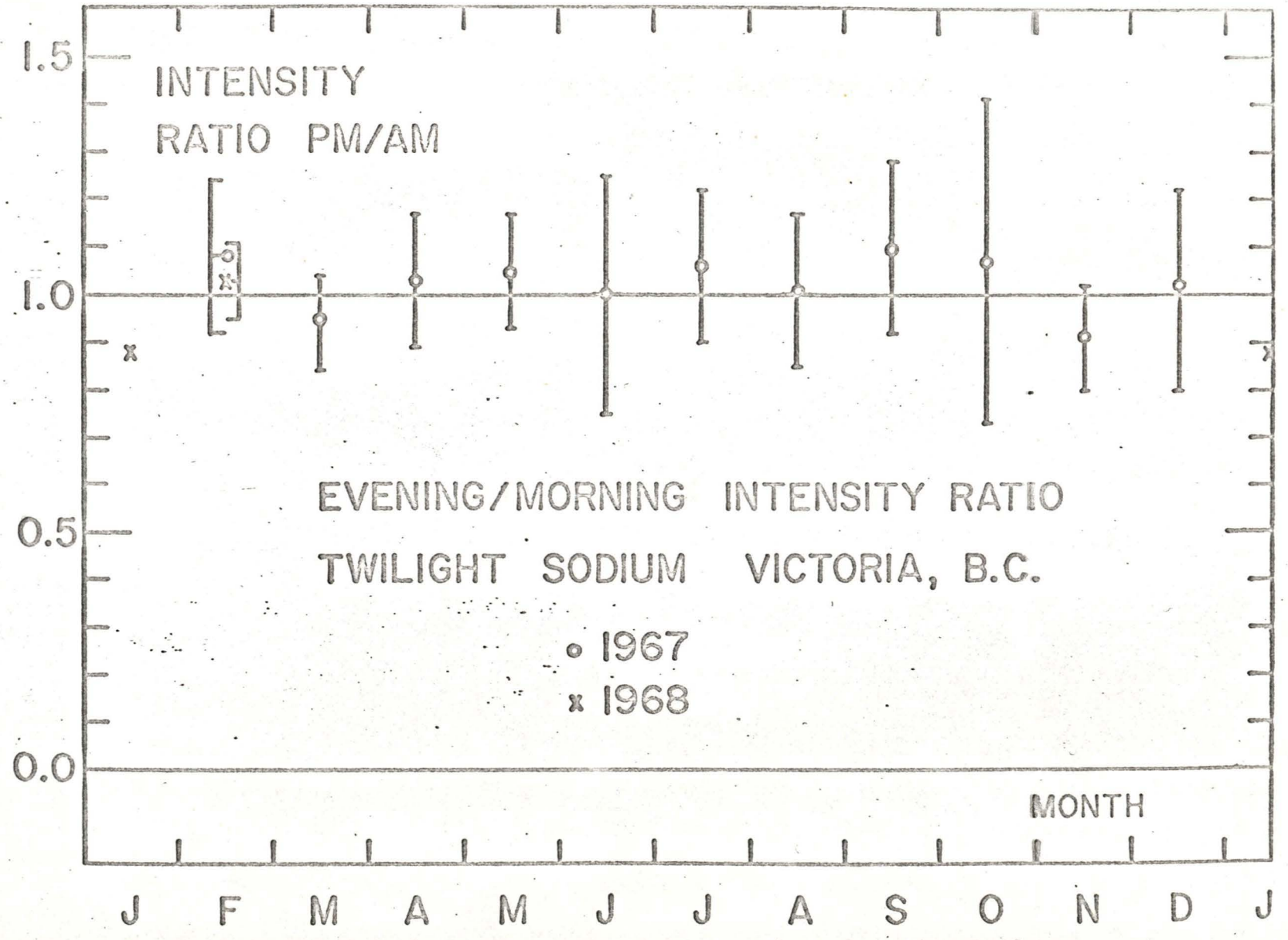

Figure V-2

Seasonal variation of mean monthly evening/morning plateau intensity ratios

figure shows clearly that the PM/AM intensity ratios do not differ from unity by more than ± 20% throughout the entire year. Since the average ratio for the entire year was 1.02 and this value is contained by all the error bars no attempt was made to draw a smooth curve through the plotted points. The absence of a significant morning-evening intensity effect confirms the observations of some other researchers. It should be noted, however, that Blamont and Donahue (1964) reported a morning/evening intensity ratio varying from unity to as much as 1.4 .

In order that the seasonal variation of the plateau intensity could be more readily discerned, the mean monthly intensities were calculated. Since there appeared to be no significant difference between morning and evening intensities, no distinction was made between them. The results of the calculations are listed in table V-2 and are plotted in figure V-3. As in the case of the evening to morning intensity ratios, the error bars represent twice the average mean deviation. The figure shows that the intensity increased to a maximum in March, decreased rapidly during this month to a summer time low in June and then increased to a maximum in November. After November, the intensity then appeared to decrease to a minimum in January. It should be pointed out that only six observations were made during January 1968 and that for February 1968 the mean intensity was approximately 1 kR. lower than the mean value for February 1967. In view of

Month	No. of Observations	Mean Intensity (kR.)	Average Mean Deviation (kR.)
1967			
February	20	3.87	0.50
March	14	4.35	1.09
April	19	2.26	0.20
May	16	1.71	0.52
June	22	1.51	0.12
July	43	1.75	0.11
August	47	2.00	0.39
September	32	2.72	0.77
October	14	4.57	1.37
November	19	4.17	0.79
December	15	4.73	0.69
1968			
January	6	3.22	0.59
February	22	2.53	0.53

TABLE V-2

Mean Monthly Combined

Morning and Evening Plateau Intensities

this, it is possible that the seasonal intensity variation may exhibit a single maximum in the winter months and a single minimum in the summer months. It is interesting to note, however, that the plot of the individual intensity

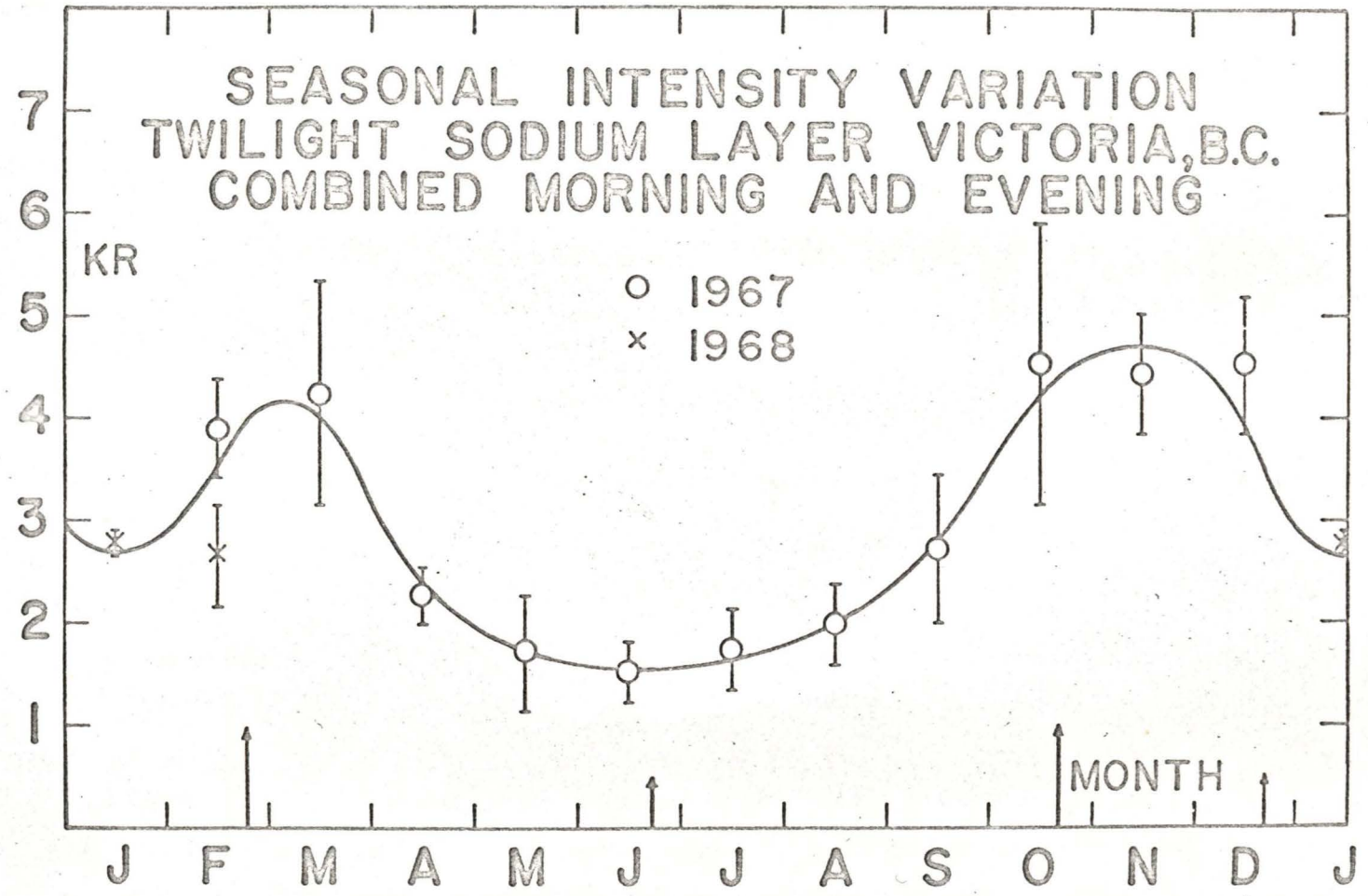

Figure V-3

Seasonal variation of the combined morning and evening plateau intensities

observations shown in figures V-1 (A) and V-1 (B) indicate an increasing trend towards the end of February 1968, thus roughly paralleling the increase observed during 1967. In addition, observations taken after February 1968 indicate that the level of intensity tended to increase during the month of March to about 3.5 kR. and then began to decrease again; thus the secondary minimum in January may in fact, be real. It is felt, however, that before it can be definitely concluded that the intensity variation exhibits two maxima and two minima, more observations should be made, especially during the winter months.

5.2 Seasonal variation of the height of maximum density.

The heights of maximum density for the morning and evening sodium observations are plotted in figures V-4 (A) and V-4 (B). As in the case of the intensity plot, the circles represent observations made during 1967 and the crosses observations made during 1968. Again, for convenience, the plotted points have been joined together by straight lines. These two figures suggest that the height of maximum density exhibits a seasonal variation.

In order that the seasonal variation of both the morning and evening heights could be more readily discerned, the mean monthly morning and evening heights were calculated. The results of these calculations are given in table V-3 and are plotted in figure V-5 (A) and V-5 (B). As in the case of the mean monthly intensity

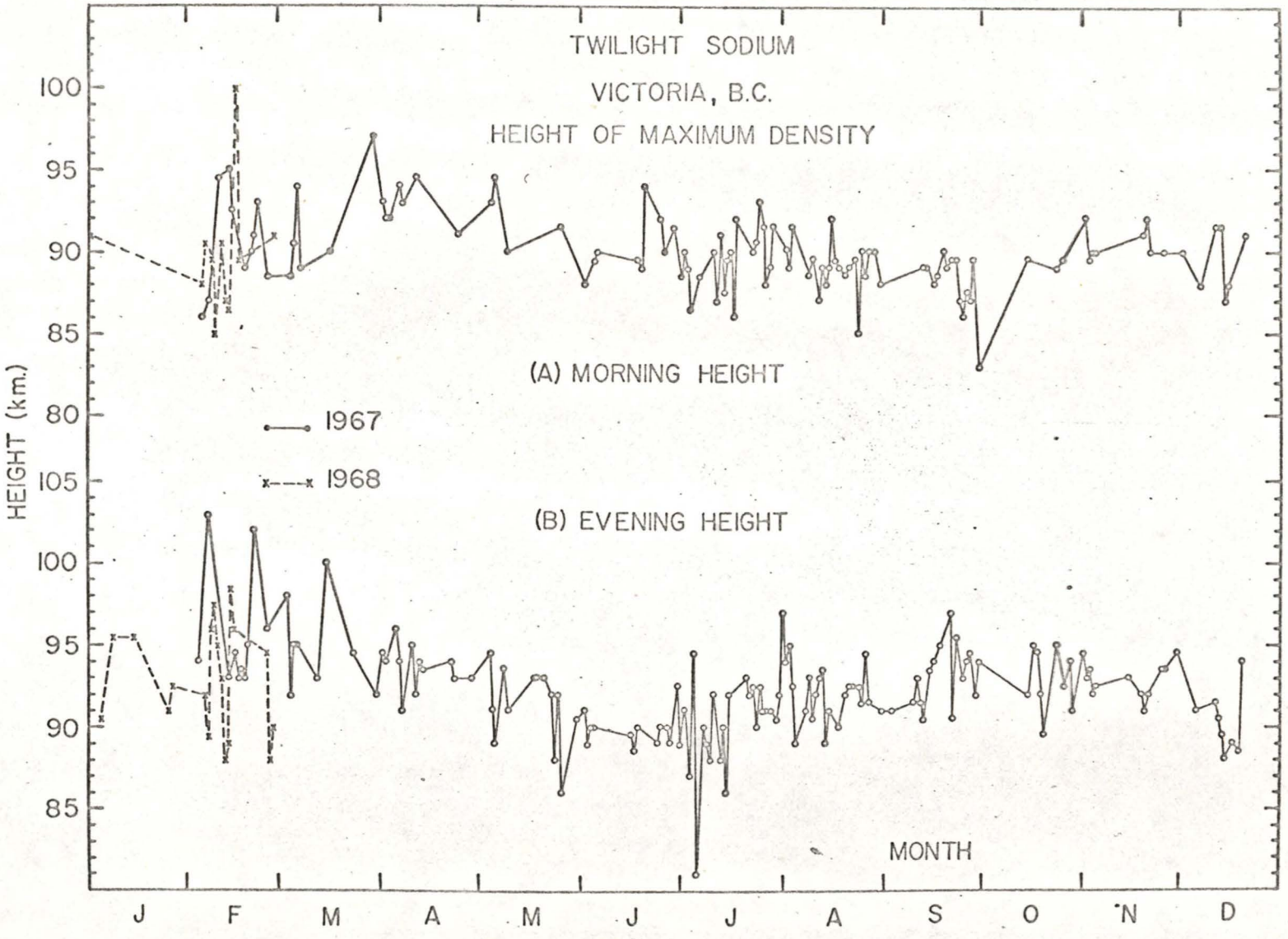

Figure V-4

Individual morning and evening heights of maximum density

MONTH	MORNING			EVENING		
	No. of Observations	Mean Height (km.)	Average Mean Deviation (km.)	No. of Observations	Mean Height (km.)	Average Mean Deviation (km.)
1967						
February	10	90.6	2.55	10	95.7	2.78
March	6	91.5	2.67	8	94.9	2.06
April	7	92.8	0.95	12	93.7	0.97
May	4	92.3	1.50	12	91.3	2.00
June	10	90.2	1.12	12	89.9	0.73
July	19	89.5	1.53	24	90.1	2.00
August	23	89.2	1.00	23	92.2	1.42
September	14	88.0	1.38	16	93.2	1.53
October	3	89.3	0.22	10	93.0	1.60
November	8	90.6	0.83	11	92.8	0.80
December	7	89.6	1.63	8	90.3	1.50
1968						
January	1	91.0	-	5	93.0	2.00
February	10	89.8	2.60	13	92.9	3.16

TABLE V-3

Mean Monthly Morning and Evening Heights of Maximum Density.

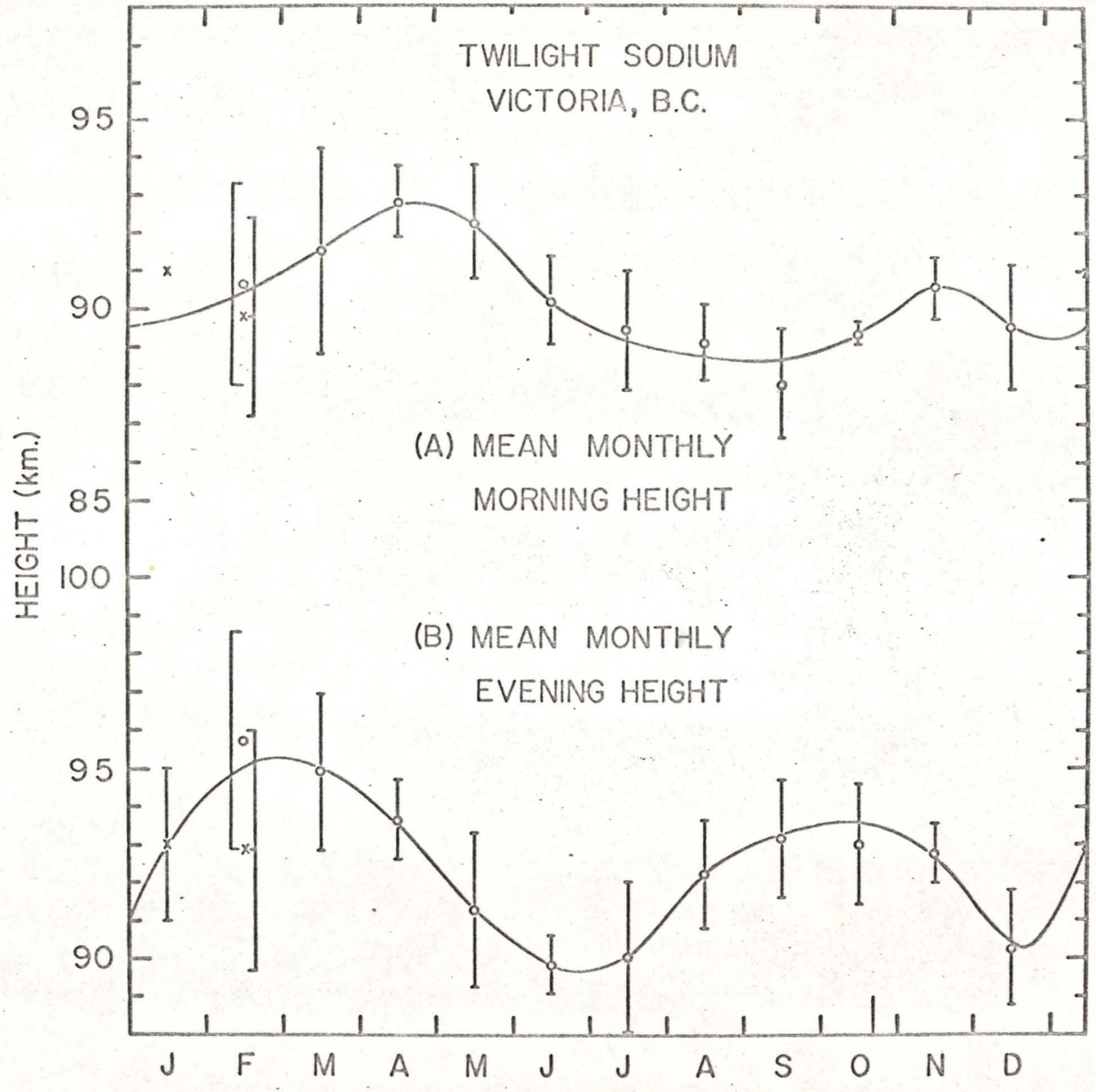

Figure V-5

Seasonal variation of the mean monthly morning and evening heights of maximum density

curve, the uncertainty bars represent twice the average mean deviation. It should be noted that no uncertainty bar has been associated with the mean morning height for January since only one morning observation was obtained during this month. Figure V-5 (A) shows that the morning height of maximum density increased during February, March and April to a maximum of approximately 92.8 km., decreased steadily to a minimum of about 88.6 km. in September, increased to a smaller secondary maximum of 90.6 km. in November, and finally decreased to a minimum of 89.2 km. near the end of December or beginning of January. The evening heights of maximum density shown in figure V-5 (B) also exhibited a seasonal variation. The evening height increased during February to a maximum of about 95.2 km. in March, decreased to a minimum of approximately 89.7 km. in June and then increased to a smaller secondary maximum of 93.5 km. in October. The height then decreased to a minimum of about 90.2 km. in December. It is interesting to note that both of these figures show trends similar to the seasonal intensity variation shown in figure V-3. These similarities are discussed in section 5.3.

An inspection of table V-3 shows that with the exception of May and June each monthly mean morning height was lower than the corresponding monthly mean evening height, thus suggesting a definite morning-evening height effect. In order to determine the seasonal variation

of any morning-evening height effect the mean difference between pairs of heights in which a morning height was immediately preceeded or followed by an evening height was calculated for each month. Where three or more consecutive observations were possible they were considered in triplets, the height of the first and third members being linearly interpolated to the time of observation of the second member in order to eliminate as much as possible any day-to-day variation. The results of these calculations are given in table V-4 and plotted in figure V-6. The error bars represent the magnitude of twice the average mean deviation for each month, and the arrows indicate the times of the vernal and autumnal equinoxes which, for a 90 km. sodium layer occur on February 22 and October 21 respectively (see Appendix E). It is clear from figure V-6 that, within the limit of experimental error, the maximum height differences occurred at the times of the equinoxes while the minimum differences occurred at the solstices. (See Sullivan and Roberts (1968)).

Although measurements of evening and morning heights have been recorded previously by Blamont and Donahue (1964), no systematic seasonal variation in their mean monthly height differences could be reported since the effect seemed to reverse several times throughout the year.

Month	No. of pairs or triplets	Mean Monthly P.M.-A.M. height difference (km.)	Average Mean deviation (km.)
1967			
February	7	7.1	3.7
March	7	4.2	2.4
April	8	1.2	0.9
May	4	0.0	1.8
June	9	-0.1	2.2
July	31	0.8	1.4
August	33	3.3	1.0
September	16	5.1	1.7
October	4	4.5	1.7
November	11	1.9	1.3
December	7	0.9	1.4
1968			
January*	1	2.6	-
February	11	4.2	2.6

TABLE V-4

Mean Monthly Evening-Morning Differences in the Height of Maximum Density.

* No pairs of PM/AM observations were obtained during this month and only one good morning observation was obtained. The PM-AM height difference was found using the morning observation and an evening observation obtained several days later.

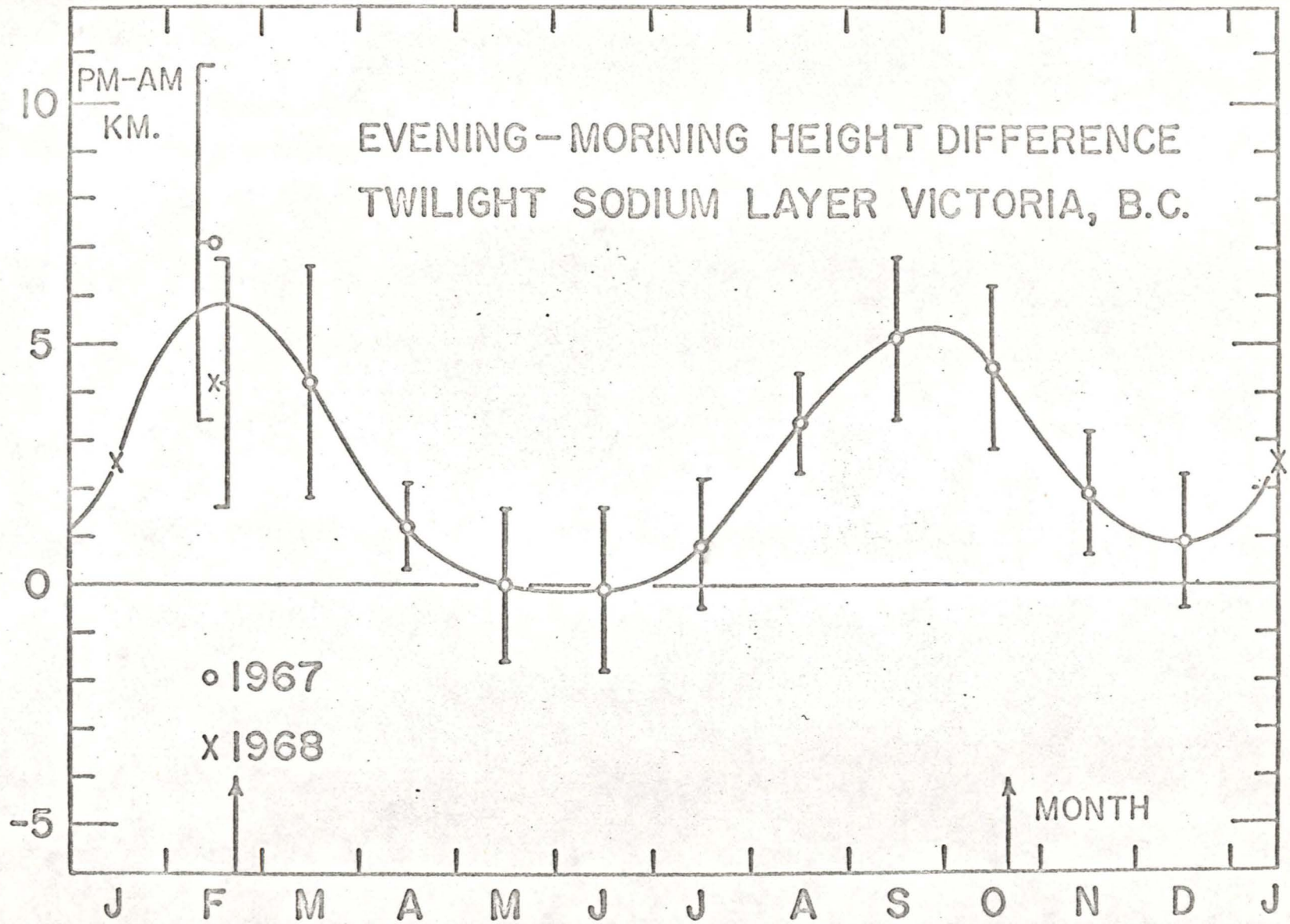

Figure V-6

Seasonal variation of the mean monthly evening-morning differences in the height of maximum density

5.3 Comparison of the seasonal variations of the height of maximum density and the plateau intensity.

A comparison of the morning and evening heights of maximum density with the plateau intensity was made after 29-day running means of the morning heights, the evening heights and the intensities were calculated. Each mean value plotted in figures V-7 (A), V-7 (B) and V-7 (C) was found by calculating the average height or intensity over a period extending 14 days on either side of the mean value. Thus a maximum of 29 observations could be included in each mean height and a maximum of 58 observations in each mean intensity since the morning and evening intensities were not distinguished. After each mean was calculated, the 29-day period was shifted by one day.

An inspection of figures V-5 and V-7 shows that there appears to be some correlation between the seasonal variations of the morning and evening heights, the morning height variation lagging behind the evening height variation by a period of from six weeks to two months. There also appears to be a correlation between the seasonal variations of the evening heights and the intensities, both variations showing maxima in March and in October or November. The minima for the evening heights occurred in June and in December, whereas the intensity minima appeared to occur in June and in late January or early February.

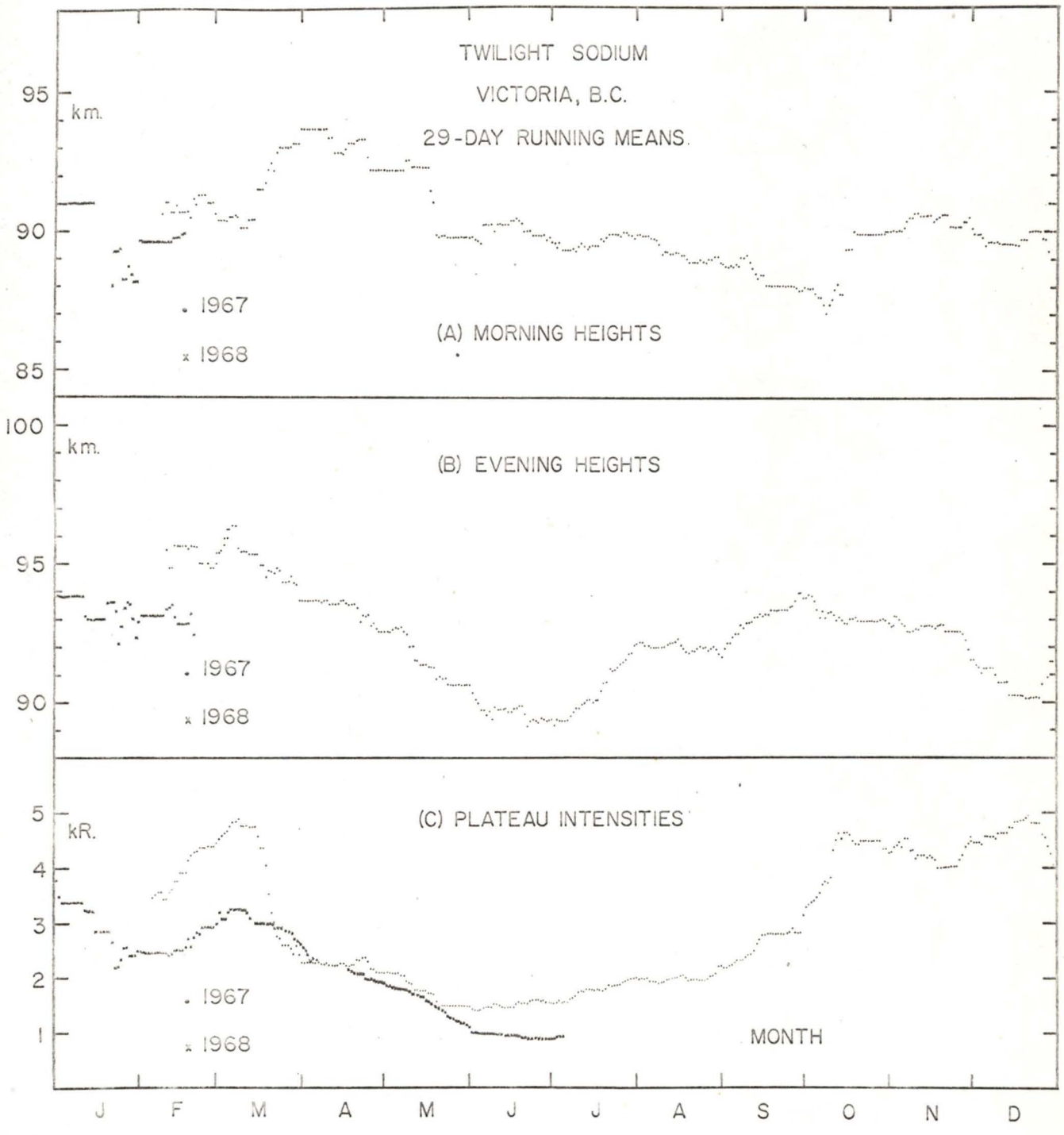

Figure V-7

Seasonal variation of the plateau intensity and the morning and evening heights of maximum density determined by calculating 29-day running means.

As was noted earlier the general level of intensity during the winter of 1968 appears to be at least 1 kR. lower than during the corresponding time of 1967. This, and the increasing trend observed in February and March 1968 (see Section 5.1), would tend to favour the suggestion of a secondary intensity minimum during the winter months. If, however, the level of sodium abundance had remained the same in 1968 as in 1967 the secondary minimum would tend to disappear. Thus the seasonal variation on a global scale might be simply a high intensity during the winter and a low intensity during the summer. If this is the case the correlation of the intensity variation with the height variations may therefore not be as pronounced as the figures suggest.

5.4 Scale height.

An attempt was made to determine the scale height of the sodium layer above the peak density from a plot of the natural logarithm of the density as a function of height for each analyzed observation. If the sodium density falls off exponentially with height above the peak, then such a plot will produce a curve of constant slope, the slope of the curve being equal to the scale height. (See appendix F for a discussion of scale height).

It was found from most observations that no unique scale height existed. Generally each plot of the logarithm of the density as a function of height produced

a smooth curve rather than a straight line. Figure V-8 is a plot of the natural logarithm of the density versus height determined from an analysis of one of the best observations. The dots and crosses show respectively the logarithm of the density distribution before and after the Bracewell-chord-correction technique was applied to the density distribution. The plot shows that the density distribution before application of the Bracewell correction was exponential in the region from 104 to 118 kilometers, whereas the Bracewell corrected density distribution in the same region appears to be non-exponential.

The non-exponential distribution after application of the Bracewell correction could be explained by postulating a mechanism for removing free sodium atoms above the peak, (other than the expected exponential decrease due to the decrease in pressure). While such a mechanism may exist it seems more likely that the magnitude of the Bracewell correction is too large in this region, thus seriously distorting the corrected distribution above the peak. Distortion is evidenced by the generation of physically meaningless negative densities in most of the chord-corrected density distributions. Figure V-9 shows the density distribution, for the same date as that given in figure V-8, both before and after the application of the chord-correction technique. It appears that the correction added to the uncorrected curve in the region from 115 to 118 kilometers was too large, thus producing negative

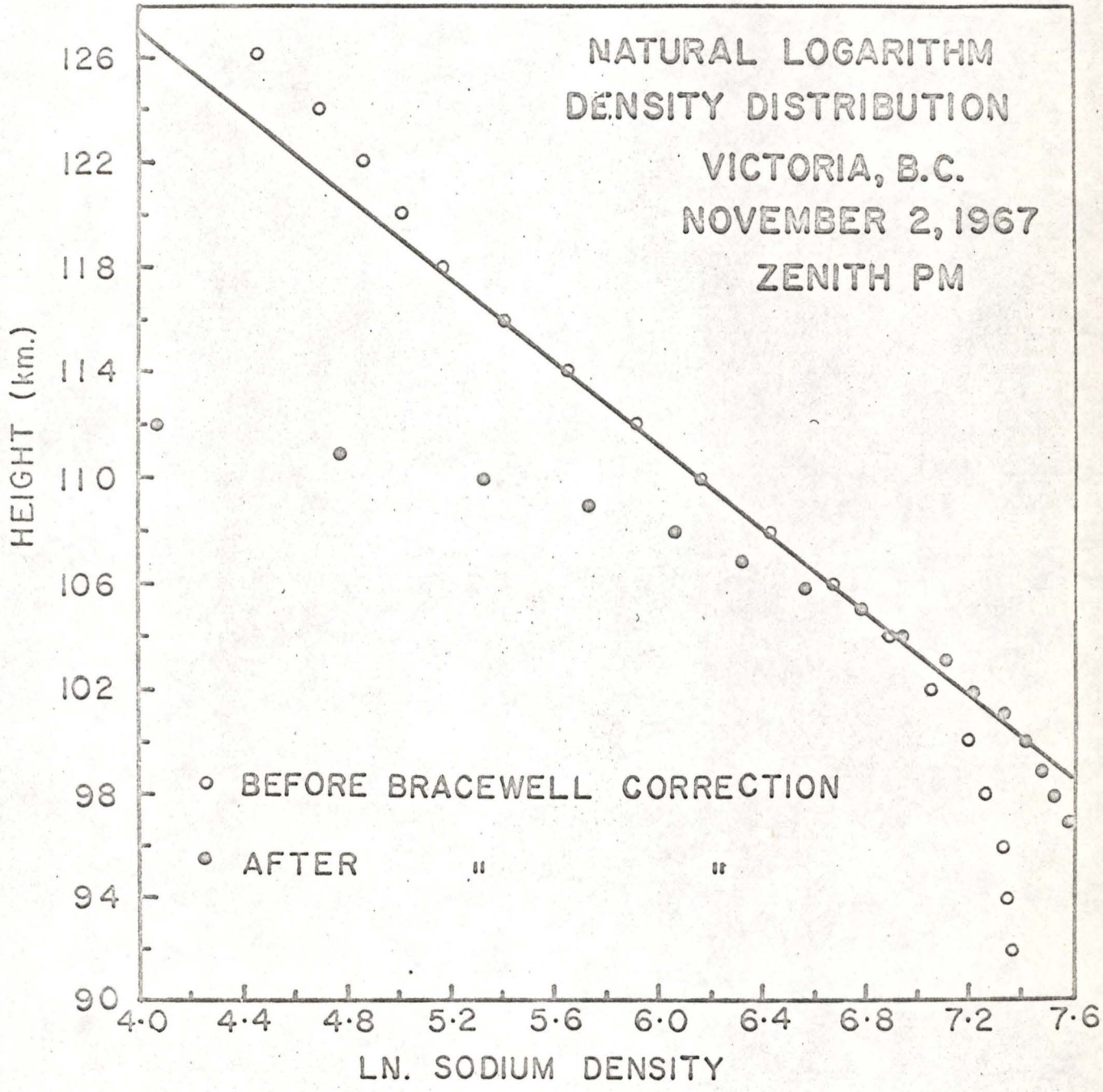

Figure V-8

Natural logarithm of the density distribution for a typical observation

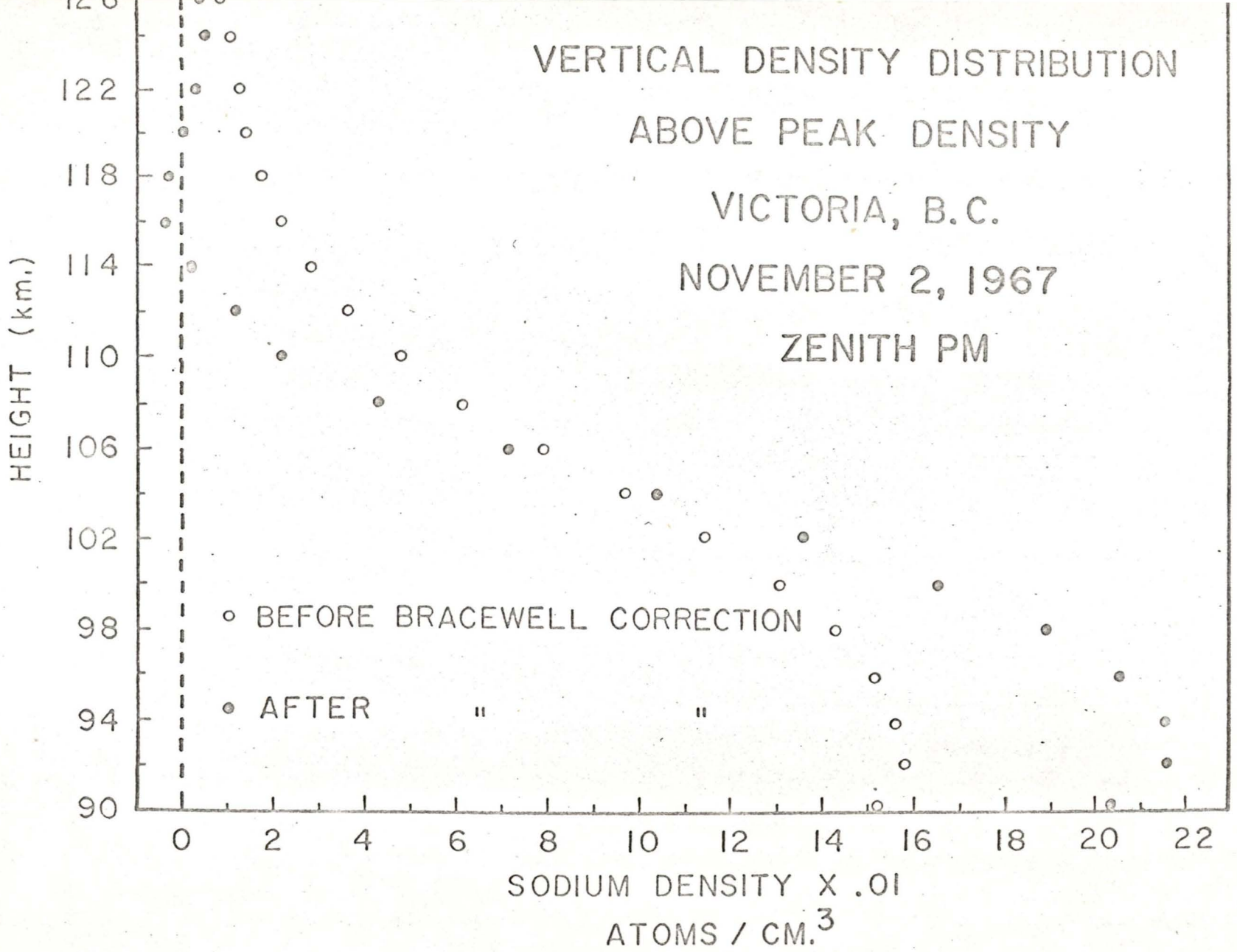

Figure V-9

Density distribution for a typical observation

densities and hence distorting the distribution not only in this region but also at lower altitudes. Because of this distortion to the density distribution curves, it was felt that density distributions and hence values of a scale height determined in this way tend to be unreliable. It should be added that although application of the Bracewell sharpening technique may distort the shape of the density distribution curve to some extent, it does not appear to alter the height at which the peak density occurs.

5.5 Possible mechanisms to explain the seasonal variations.

Twilight observations of the sodium emission have shown that the layer exhibits a seasonal variation of the height of maximum density and a seasonal variation of intensity. The evening heights and the differences between the evening and morning heights appear to be greatest in February or early March and in October (near the 90 km. equinoxes - see appendix E) and least in June and in December (near the solstices). The morning heights also exhibit a seasonal variation, but the maxima occur in April and November, the minima in September and January.

The evening - morning height effect may be partially explained in terms of solar tides in the atmosphere. Chapman (1951) has investigated such atmospheric tides and figure V-10, showing the observed pressure changes as a function of local mean time, is

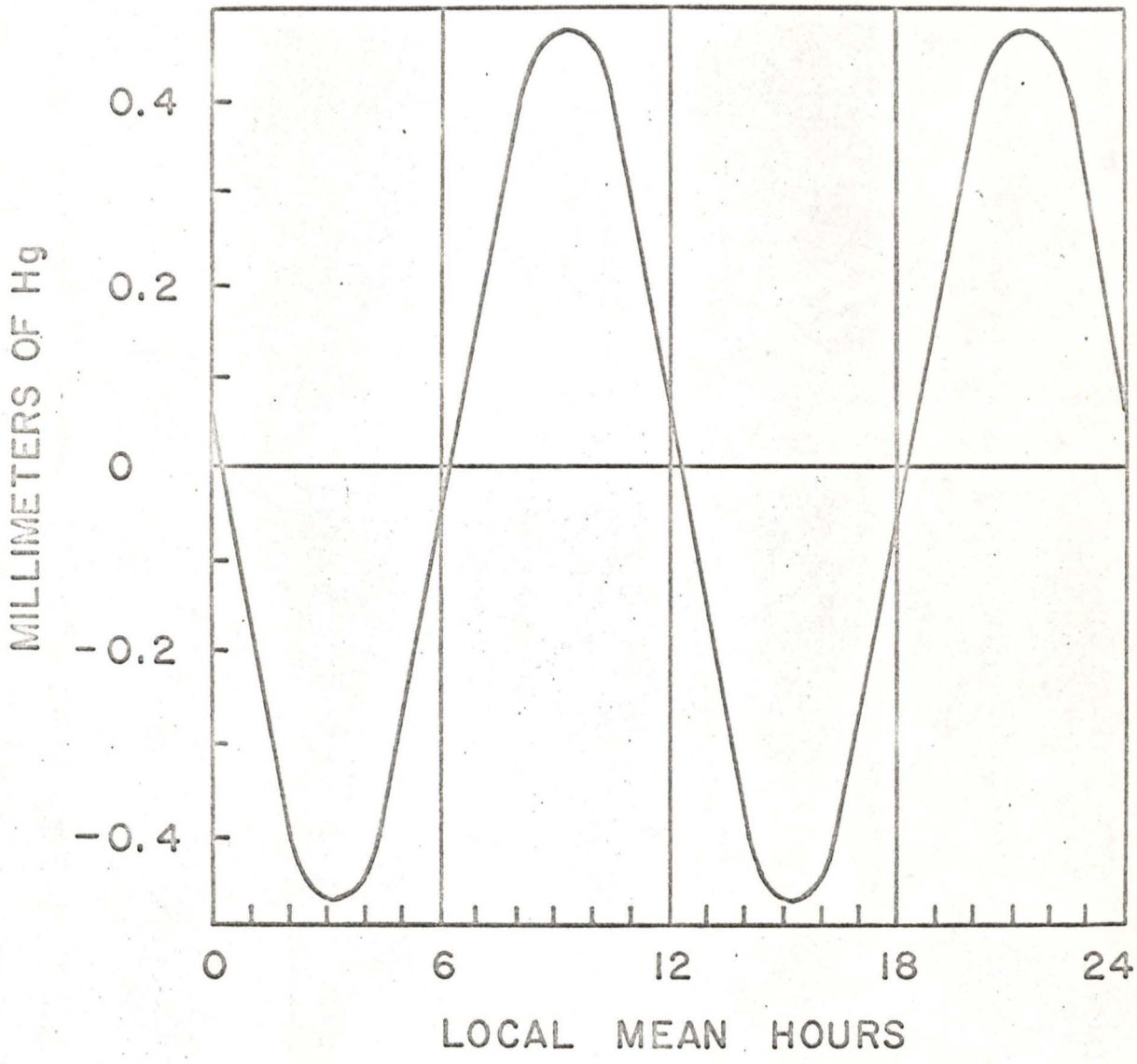

THE SOLAR SEMIDIURNAL COMPONENT (S_2) OF THE DAILY BAROMETRIC VARIATION AT WASHINGTON, D.C.

Figure V-10

The solar semidiurnal component (S_2) of the daily barometric variation at Washington, D.C.

taken from his paper. The plot shows that small variations of pressure occur in the atmosphere near the surface of the earth with a period of 12 hours (S_2 tide), the maxima occurring at about 1000 and 2200 hours, the minima at about 0400 and 1600 hours local mean time. At altitudes in the vicinity of 75 to 100 km. it has been shown that the S_2 pressure fluctuations are strongly correlated with those at ground level but that there is a difference of phase of about 6 hours between the two: thus maxima at ground level correspond to minima at higher altitudes and vice-versa. (See Butler (1962)). In addition to the above, it has been shown that the S_2 tide exhibits a seasonal variation, the maximum pressures at ground level occurring in spring and autumn and the minimum pressures in summer and winter. (See Haurwitz and Sepúlveda (1957)).

In view of the above, it seems reasonable to assume that if the S_2 tide is the cause of the morning-evening height effect the differences between evening and morning heights should correlate strongly with the differences between evening and morning pressures. Close to both equinoxes morning and evening observations are separated by a period of about 12 hours and hence the change in pressure between morning and evening is extremely small. It is at these times of the year, however, that the greatest evening-morning height differences are observed. Near the summer solstice the morning and evening observations occur around 0400 and 2000 hours respectively

while at the winter solstice they occur at 0800 and 1600 hours respectively. At these times the pressure changes are relatively large whereas the height differences are quite small. In addition, the difference in pressure between morning and evening observations would change sign at the two solstices, thus suggesting that the evening-morning height differences would reverse at these times. Such an effect is not observed. On the other hand, the amplitude of the S_2 tide varies throughout the year in accordance with the observed seasonal evening-morning height difference variation. The evening height variation also follows the same pattern.

Butler (1962) and Butler and Small (1963) have discussed the S_1 and S_2 tides in terms of insolation by atmospheric ozone at a height of 45 km. Their analysis shows that the "driving force" chiefly responsible for tidal oscillations in the atmosphere is the energy gained by the ozone layer when it absorbs ultraviolet light during the day. The driving force has, qualitatively, the form of a rectified sine wave, the first harmonic of which has a period of 24 hours (S_1 variation). Such insolation and subsequent cooling leads to expansion and contraction of the atmosphere above 45 km., resulting in an increase of pressure during a period of insolation and a decrease of pressure during cooling, extending up to 75 - 100 km. If it is assumed that the rates of warming and cooling of the ozone layer (and therefore the rates of expansion and

contraction) are roughly the same, then near both equinoxes where the days and nights are of approximately equal length, the greatest change in the thickness of the layer would be expected to occur and thus the greatest evening-morning height differences. At the summer solstice the layer would expand during the day, but possibly contract little during the night due to the few hours of cooling. Thus at these times the evening-morning height effect would be small. At the winter solstice the layer possibly expands little due to the relatively few hours of insolation and thus the evening-morning height effect would again be small. This hypothesis is in agreement with the observations in so far as the evening-morning height effect is concerned.

A difficulty arises when the seasonal height variations of the sodium layer are examined. The ozone insolation hypothesis implies a seasonal variation which should exhibit a single maximum in summer and a single minimum in winter. The observations, however, show that the evening height variations exhibit maxima at the equinoxes and minima at the solstices. The morning height variations likewise exhibit double peaks lagging behind in phase by six to eight weeks. It appears therefore, that some other explanation must be sought to account for the seasonal height variation. Armstrong (1968) has investigated the seasonal variation of temperature at the 90 km. level. Measurements appear to indicate that the temperature is greatest near the autumnal equinox and least near the

summer solstice. While the temperature measurements published by this author do not show a minimum near the winter solstice nor a maximum near the spring equinox, the uncertainties associated with the few measurements which he has made are large and could possibly mask such an effect. Thus temperature changes at the 90 km. level may be related to the seasonal height variations.

The above discussions of the morning-evening height effect and the S_1 and S_2 variations assume that these pressure variations reflect an actual change in the altitude of the sodium layer. It should be recalled, however, that the height of the sodium layer is determined by calculating the sum of the geometric shadow height, Z_1, and the screening height, $\overline{X}$, which is influenced by ozone absorption at 5893 $\mathring{A}$. Thus it is possible that the morning-evening height effect reflects a change in the screening height rather than an actual change in the altitude of the sodium layer.

The seasonal intensity variations may also be intimately related to variations in pressure and temperature in the upper atmosphere. An increase of pressure at higher levels during the day would set up a pressure gradient from the day side towards the night side resulting in a flow of air at high levels away from the day side towards the night side. Since free sodium atoms would likely be carried along as well one might expect free sodium to disappear during the day time so that the evening twilight emission would be expected to be less intense than the morning twilight

emission. No definite trend to confirm this was observed during the one year period of observations. Other observers, however, (see Blamont and Donahue (1964)) have reported high morning intensities and their day glow observations show an increase in sodium intensity after the morning twilight observation which increases to a maximum approximately two or three hours before noon, decreases to a minimum around noon, increases again until approximately two or three hours after noon, and then decreases towards evening to the twilight intensity level. This suggests a return of free sodium to the daylight region which continues until the pressure gradient reverses.

Hunten and Godson (1967) showed a correlation between intensity variations and warming events in the polar and sub-polar stratosphere. In addition, Gault (1967) reported a correlation between variations in the temperature of the stratosphere (30 mb level) and sodium intensity variations.

In summary, there appears to be some correlation between the seasonal intensity variations and changes in temperature and pressure in the stratosphere and mesosphere. The seasonal height variations, particularly the evening-morning effect, can be partially explained on the basis of insolation by atmospheric ozone; the actual seasonal height variations, however, present a problem.

Undoubtedly the effect of the day to night variations in the vertical distribution of the ozone layer would have to be taken into account and the effect on the screening height determined. One would have to work out the transmission function for the day and night ozone distributions and these would first have to be determined.

APPENDIX A

GLOSSARY OF SYMBOLS USED IN THE COMPUTER PROGRAM

RADIUS - radius of earth in kilometers

XINC - constant increment in time between each sampled chart response (1 minute of time)

S(I) - Self-absorption correction factor $\dot{S}$ B/S in R./km.

A(I) - Parameter used to relate intensity in rayleighs to abundance measured in Na atoms/cm.^{2} (column)

IDAY - Day of a particular observation

MONTH - Month of a particular observation

IYEAR - Year of a particular observation

MM - identifies observation as either A.M. or P.M.

CALIB - Calibration factor to convert sampled chart response (divisions) to intensity in rayleighs

CONST - Conversion factor (equal to 10/g where g is the yield) to convert R/km. to density in Na atoms/cm^3.

XBAR - Screening height in km. (one of the Bracewell parameters)

IRANGE - Range scale used during a particular observation

HV - Extra high tension setting of photometer

TC - Time constant used during a particular observation

ITEMEH
ITIMEM - Time of start of evening observation or end of morning observation expressed in hours and minutes (P.S.T.) on a 24 hour clock.

IAMM
IAMS - Equation of time expressed in minutes and seconds

INCAMS - Increment in the equation of time, expressed in seconds, from 0 hours ephemeris time on the date of the observation to 0 hours ephemeris time of the following day

IDECD
IDECM - Apparent declination of sun expressed in degrees,
IDECS minutes and seconds

INCDEC - Increment in the declination, expressed in seconds of arc, from 0 hours ephemeris time on the date of the observation to 0 hours ephemeris time of the following day.

DIV(I) - Recorder response in divisions

PST - Time of start of evening observation or end of morning observation expressed in hours (P.S.T.)

AM - Equation of time expressed in hours

GMT - Time of start of evening observation or end of morning observation expressed in hours (G.M.T.)

XLNGC - Longitude correction expressed in degrees

IPLOT(NX) - Variable which takes on one of two values, 'DOT' or 'NUL'.

NX - Integer which determines the position of the 'DOT' or 'NUL' in the graphical output of the computer

XLAT - Latitude of observatory expressed in degrees

T(I) - Time in hours (P.S.T.) for each sampled response

ZEROC - Night sky brightness expressed in terms of chart response measured in divisions

DELTB(I) - Change in intensity expressed in rayleighs

DEC(I) - Apparent declination of sun for each scaled chart division

TLOC(I) - Local apparent time for each sampled response

ZS(I) - Height expressed in kilometers

DELTAH - Change in height expressed in kilometers

AVGZS(I) - Same as ZS(I)

DENSTY(I) - Density in Na atoms per cubic cm. at the height 'AVGZS(I)'.

ABUND - Abundance expressed in atoms per square cm. (column)

MHIGHT(I) - Height in kilometers

DENS(IHIGHT) - Interpolated density at a height 'IHIGHT'

DENST(I)
IDENS(I) - (a) Density at the height 'I' multiplied by an appropriate constant for purposes of plotting

- (b) Natural logarithm of the density multiplied by an appropriate constant for purposes of plotting

XMAX - Parameter used to determine scale size of each graph

JJJ - Running index used to transfer control to different sections of the program.

APPENDIX B

Listing of the Computer Program

```
C       APPARENT-MEAN TIME IS FOUND FROM ALMANAC BY SUBTRACTING THE
C       EPHEMERIS TRANSIT TIME FROM  TWELVE HOURS
        DATA INUL,IDOT/' ','.'/
        DIMENSION MHIGHT(150),DENS(150),IDENS(200),IPLOT(132)
        DIMENSION DEC(200),DIV(200),T(200),TLOC(200),DELTB(200),ZS(200),
       1AVGZS(200),DENST(200),S(8),DENSTY(200),A(7)
        RADIUS=6370.
        XINC=60./3600.
        S(1)=0.0
        S(2)=0.42
        S(3)=1.60
        S(4)=3.33
        S(5)=5.48
        S(6)=8.0
        S(7)=10.8
        S(8)=13.7
        A(1)=0.0
        A(2)=1.490E+09
        A(3)=3.050E+09
        A(4)=4.880E+09
        A(5)=7.000E+09
        A(6)=9.900E+09
        A(7)=1.450E+10
  110   READ(5,100)IDAY,MONTH,IYEAR,MM
  100   FORMAT(2X,I3,5X,A4,5X,I5,5X,A4)
        IF(IYEAR)111,112,111
  112   CALL EXIT
  111   READ(5,200)CALIB,CONST,XBAR,BI1,IRANGE,HV,TC
  200   FORMAT(1X,F6.1,5X,F8.3,5X,F6.2,5X,F6.1,5X,I3,5X,I4,5X,F5.1)
        READ(5,300)ITIMEH,ITIMEM,IAMM,IAMS,INCAMS,IDECD,IDECM,IDECS,INCDEC
  300   FORMAT(4(5X,I3),2(1X,I3),2(5X,I3),5X,I5)
        NN=1
        N=7
    3   READ(5,4)(DIV(I),I=NN,N)
        IF(DIV(NN))5,6,5
    5   NN=NN+7
        N=N+7
        GO TO 3
    4   FORMAT(7(5X,F5.1))
    6   N=N-7
        DO 411 I=1,N
        DENST(I)=DIV(I)+10.5
        IDENS(I)=DENST(I)
  411   CONTINUE
        X1=ITIMEH
        X2=ITIMEM
        X2=X2/60.
        PST=X1+X2
        GMT=PST+8.
        X1=IAMM
```

```
      X1=X1/60.
      X2=IAMS
      X2=X2/3600.
      AM=X1+X2
      X1=INCAMS
      X1=X1/3600.
      AM=AM+GMT*X1/24.
      X1=IDECD
      X2=IDECM
      X3=IDECS
      X2=X2/60.
      X3=X3/3600.
      DEC(1)=X1+X2+X3
      X1=INCDEC
      X1=X1/3600.
      DEC(1)=DEC(1)+GMT*X1/24.
      XLNGC=13./60.+12.9/3600.
      WRITE(6,14)
   14 FORMAT(1H1)
      WRITE (6,8)MM,IDAY,MONTH,IYEAR
    8 FORMAT(10X, ' SODIUM Z',2X,A4,5X,I3,2X,A4,1X,I5,5X,' VICTORIA, B.C
     1.')
      WRITE(6,7)
    7 FORMAT(1H0)
      WRITE(6,9)HV,TC,IRANGE
    9 FORMAT(' E.H.T. =',I4,' VOLTS',5X,' TIME CONSTANT =',F5.1,' SECS.'
     1,5X,' RANGE ='I3)
      IF(PST-12.)407,16,406
  406 WRITE(6,400)ITIMEH,ITIMEM
  400 FORMAT(' START OF RUN =',I3,'H',2X,I3,'M',2X,'P.S.T.')
      GO TO 408
  407 WRITE(6,409)ITIMEH,ITIMEM
  409 FORMAT(' END OF RUN =',I3,'H',2X,I3,'M',2X,'P.S.T.')
  408 WRITE(6,401)CALIB,IRANGE
  401 FORMAT(' CALIBRATION FACTOR =',F6 .1,' R/DIV. ON RANGE',I3)
      WRITE(6,402)CONST
  402 FORMAT(' CONVERSION FACTOR =',F8 .3,' ATOMS/CUBIC CM. PER R/KM.')
      WRITE(6,403)XBAR
  403 FORMAT(' SCREENING HEIGHT =',F6.2,' KM.')
      WRITE(6,404)AM
  404 FORMAT(' (A - M) =',F8.5,' H')
      WRITE(6,405)BIL
  405 FORMAT(' BRACEWELL INTERVAL =',F8 .1,' KM.')
      WRITE(6,7)
      WRITE(6,97)
   97 FORMAT(' CHART DIVISIONS TAKEN AT  60 SECOND TIME INTERVALS'/)
      IN=1
      NN=12
  202 IF(NN-N)13,13,201
  201 NN=N
```

```
 13 WRITE(6,10)(DIV(I),I=IN,NN)
 10 FORMAT(12(3X,F7.3))
    IF(NN-N)11,12,12
 11 IN=IN+12
    NN=NN+12
    GO TO 202
 12 WRITE(6,14)
    WRITE (6,8)MM,IDAY,MONTH,IYEAR
    WRITE(6,7)
    WRITE(6,410)
410 FORMAT('                PLOT OF RECORDER RESPONSE IN DIVISIONS AS A F
   1UNCTION OF TIME '/)
    WRITE(6,412)
412 FORMAT('          0    5   10   15   20   25   30   35   40   45
   150   55   60   65   70   75   80   85   90   95  100')
    DO 413 I=10,110
    IPLOT(I)=IDOT
413 CONTINUE
    JJJ=1
    WRITE(6,414)JJJ,(IPLOT(KK),KK=10,110)
414 FORMAT(2X,I5,2X,110A1)
    IN=N-1
    NN=2
417 DO 415 I=11,109
    IPLOT(I)=INUL
415 CONTINUE
    JJJ=JJJ+1
    NX=IDENS(NN)
    IPLOT(NX)=IDOT
    WRITE(6,414)JJJ,(IPLOT(KK),KK=10,110)
    IF(NN.EQ.IN)GO TO 416
    NN=NN+1
    GO TO 417
416 DO 418 I=11,109
    IPLOT(I)=IDOT
418 CONTINUE
    JJJ=JJJ+1
    WRITE(6,414)JJJ,(IPLOT(KK),KK=10,110)
    WRITE(6,412)
    WRITE(6,14)
    XLAT=48.+27.42/60.
    X1=3.14159/180.
    X2=15.*X1
    X3=XLAT*X1
    SLAT=SIN(X3)
    CLAT=COS(X3)
    IF(PST-12.)35,16,36
 16 WRITE(6,18)
 18 FORMAT(' ERROR IN CALCULATION OF TIME')
    GO TO 110
```

```
   35 DO 40 I=1,N
      I1=I-1
      X3=I1
      T(I)=PST-XINC*X3
   40 CONTINUE
      GO TO 41
   36 DO 37 I=1,N
      I1=I-1
      X3=I1
      T(I)=PST+XINC*X3
   37 CONTINUE
C     CORRECTION FOR NIGHT SKY ZERO
   41 I1=N
      I2=N-1
      I3=N-2
      I4=N-3
      I5=N-4
      ZEROC=(DIV(I1)+DIV(I2)+DIV(I3)+DIV(I4)+DIV(I5))*0.2
      DO 50 I=1,N
      DIV(I)=(DIV(I)-ZEROC)*CALIB
   50 CONTINUE
C     CHANGE IN INTENSITY IN UNITS OF RAYLEIGHS BETWEEN READINGS
      NN=N-2
      DO 51 I=3,NN
      J=I+2
      K=I-2
      DELTB(I)=DIV(K)-DIV(J)
   51 CONTINUE
C     DECLINATION FOR EACH READING
      X3=INCDEC
      X3=X3/3600.
      DO 60 I=2,N
      DEC(I)=DEC(1)+(T(I)-T(1) )*X3/24.
   60 CONTINUE
      IF(PST-12.)61,16,62
   61 DO 63 I=1,N
      TLOC(I)=12.-T(I)+XLNGC-AM
   63 CONTINUE
      GO TO 69
   62 DO 64 I=1,N
      TLOC(I)=T(I)-12.-XLNGC+AM
   64 CONTINUE
   69 DO 65 I=1,N
      SDEP=SIN(DEC(I)*X1)*SLAT+COS(DEC(I)*X1)*CLAT*COS(TLOC(I)*X2)
      CDEP=SQRT(1.-SDEP*SDEP)
      ZS(I)=(1.-CDEP)/CDEP*RADIUS+XBAR
   65 CONTINUE
      DO 66 I=3,NN
      J=I+2
      K=I-2
```

```
      DELTAH=ZS(J)-ZS(K)
      DENSTY(I)=DELTB(I)*CONST/DELTAH
      AVGZS(I)=ZS(I)
   66 CONTINUE
      WRITE (6,8)MM,IDAY,MONTH,IYEAR
      WRITE(6,7)
      WRITE(6,2201)
 2201 FORMAT('           HEIGHT IN KM. VERSUS DENSITY IN ATOMS/CUBIC CM.'
     1/)
      WRITE(6,70)
   70 FORMAT(' HEIGHT  DENSITY    HEIGHT  DENSITY    HEIGHT  DENSITY
     1HEIGHT  DENSITY    HEIGHT  DENSITY    HEIGHT  DENSITY    HEIGHT  D
     2ENSITY')
      WRITE(6,7)
      IN=3
      JN=9
  102 IF(JN-NN)74,74,75
   75 JN=NN
   74 WRITE(6,71)(AVGZS(I),DENSTY(I),I=IN,JN)
   71 FORMAT(1X,6(F7.2,1X,F8.2,3X),F7.2,1X,F8.2,/)
      IF(JN-NN)72,73,73
   72 IN=IN+7
      JN=JN+7
      GO TO 102
C     CALCULATION OF INTENSITY AND ABUNDANCE
   73 XINTEN=DIV(1)
      X3=XINTEN*1.0E-03
      I3=X3
      J=I3+1
      K=J+1
      IF(K-8)76,77,77
   77 WRITE(6,78)
   78 FORMAT(' INTENSITY GREATER THAN ALLOWABLE RANGE - ABUNDANCE NOT CA
     1LCULATED')
      WRITE(6,7)
      ABUND=0.0
      GO TO 4002
   76 X4=I3
      X5=X3-X4
      ABUND=A(J)+(A(K)-A(J))*X5
      WRITE(6,7)
 4002 WRITE(6,4000)XINTEN
 4000 FORMAT(' INTENSITY CALCULATED AT TIME OF FIRST SCALE DIVISION  =',
     1 F6.0,' RAYLEIGHS')
      WRITE(6,7)
      WRITE(6,58)ABUND
   58 FORMAT(' ABUNDANCE CALCULATED AT TIME OF FIRST SCALE DIVISION  =',
     1E11.4,' ATOMS/SQUARE CM. (COLUMN)')
      WRITE(6,14)
      DO 620 I=50,150
```

```
      MHIGHT(I)=I
      DENS(I)=0.0
  620 CONTINUE
      IHIGHT=150
  607 DO 603 I=3,NN
      IF(I.EQ.NN)GO TO 604
      I1=AVGZS(I)
      IF(IHIGHT-I1)606,606,603
  603 CONTINUE
  606 J=I-1
 6101 IF(J.LE.2)GO TO 611
      J1=AVGZS(J)
      IF(I1-J1)608,608,609
  608 J=J-1
      GO TO 6101
  609 X1=AVGZS(I)-AVGZS(J)
      X2=DENSTY(I)-DENSTY(J)
      X3=IHIGHT
      X4=X3-AVGZS(J)
      MHIGHT(IHIGHT)=IHIGHT
      DENS(IHIGHT)=DENSTY(J)+X2*X4/X1
  604 IHIGHT=IHIGHT-1
      IF(IHIGHT-49)611,611,607
  611 WRITE (6,8)MM,IDAY,MONTH,IYEAR
      WRITE(6,7)
      WRITE(6,2201)
      WRITE(6,612)
  612 FORMAT(' INTERPOLATED DENSITIES')
      WRITE(6,7)
      WRITE(6,613)
  613 FORMAT(' HEIGHT    DENSITY         HEIGHT    DENSITY         HEIGHT
     1   DENSITY         HEIGHT    DENSITY         HEIGHT    DENSITY')
      WRITE(6,7)
      IN=50
      JN=54
  615 WRITE(6,614)(MHIGHT(J),DENS(J),J=IN,JN)
  614 FORMAT(1X,5(I6,3X,F8.2,8X)/)
      IN=IN+5
      JN=JN+5
      IF(IN-150)615,616,616
  616 WRITE(6,14)
      IF(DENS(95).LE.100.0)GO TO 110
      WRITE(6,8)MM,IDAY,MONTH ,IYEAR
      WRITE(6,7)
      WRITE(6,701)
  701 FORMAT('                                                        DENSITY
     1OF SODIUM ATOMS PER CUBIC CENTIMETRE X 0.01'/)
      WRITE(6,702)
  702 FORMAT('          -5  -4  -3  -2  -1   0   1   2   3   4   5   6
     1 7   8   9  10  11  12  13  14  15  16  17  18  19  20  21  22  23
```

```
   2  24  25')
    DO 703 I=50,150
    DENST(I)=DENS(I)*0.04+0.5
    IDENS(I)=DENST(I)
703 CONTINUE
    XMAX=1.0
    JJJ=0
803 DO 704 I=12,132
    IPLOT(I)=IDOT
704 CONTINUE
    JJJ=JJJ+1
    WRITE(6,705)(IPLOT(KK),KK=12,132)
705 FORMAT(5X,'150',3X,132A1)
    I1=149
718 DO 706 I=12,131
    IPLOT(I)=INUL
706 CONTINUE
    NX=32+IDENS(I1)
    IPLOT(32)=IDOT
    IPLOT(NX)=IDOT
    IF(JJJ-2)740,740,746
746 IF(I1-62)752,740,740
752 IPLOT(NX)=INUL
    IPLOT(32)=IDOT
    GO TO 741
740 IF(I1.EQ.140)GO TO 707
    IF(I1.EQ.130)GO TO 707
    IF(I1.EQ.120)GO TO 707
    IF(I1.EQ.110)GO TO 707
    IF(I1.EQ.90)GO TO 707
    IF(I1.EQ.80)GO TO 707
    IF(I1.EQ.70)GO TO 707
    IF(I1.EQ.104)GO TO 708
    IF(I1.EQ.103)GO TO 709
    IF(I1.EQ.102)GO TO 710
    IF(I1.EQ.101)GO TO 711
    IF(I1.EQ.100)GO TO 712
    IF(I1.EQ.99) GO TO 713
    IF(I1.EQ.97) GO TO 714
    IF(I1.EQ.96)GO TO 715
741 IF(I1.EQ.60)GO TO 707
    WRITE(6,716)(IPLOT(KK),KK=12,132)
716 FORMAT(11X,132A1)
    I1=I1-1
    IF(I1.EQ.50)GO TO 717
    GO TO 718
707 WRITE(6,719)I1,(IPLOT(KK),KK=12,132)
719 FORMAT(5X,I3,3X,132A1)
    I1=I1-1
    GO TO 718
```

```
708 WRITE(6,720)(IPLOT(KK),KK=12,132)
720 FORMAT(2X,'H',8X,132A1)
    I1=I1-1
    GO TO 718
709 WRITE(6,721)(IPLOT(KK),KK=12,132)
721 FORMAT(2X,'E',8X,132A1)
    I1=I1-1
    GO TO 718
710 WRITE(6,722)(IPLOT(KK),KK=12,132)
722 FORMAT(2X,'I',8X,132A1)
    I1=I1-1
    GO TO 718
711 WRITE(6,723)(IPLOT(KK),KK=12,132)
723 FORMAT(2X,'G',8X,132A1)
    I1=I1-1
    GO TO 718
712 WRITE(6,724)(IPLOT(KK),KK=12,132)
724 FORMAT(2X,'H',2X,'100',3X,132A1)
    I1=I1-1
    GO TO 718
713 WRITE(6,725)(IPLOT(KK),KK=12,132)
725 FORMAT(2X,'T',8X,132A1)
    I1=I1-1
    GO TO 718
714 WRITE(6,726)(IPLOT(KK),KK=12,132)
726 FORMAT(2X,'K',8X,132A1)
    I1=I1-1
    GO TO 718
715 WRITE(6,727)(IPLOT(KK),KK=12,132)
727 FORMAT(2X,'M',8X,132A1)
    I1=I1-1
    GO TO 718
717 DO 730 I=12,131
    IPLOT(I)=IDOT
730 CONTINUE
    NX=32+IDENS(50)
    IF(JJJ-3)747,748,748
747 IPLOT(NX)=IDOT
    GO TO 749
748 IPLOT(NX)=IDOT
    IPLOT(32)=IDOT
749 WRITE(6,731)(IPLOT(KK),KK=12,132)
731 FORMAT(6X,'50',3X,132A1)
    IF(XMAX-2500.)960,960,961
960 WRITE(6,702)
    GO TO 962
961 WRITE(6,955)
962 WRITE(6,14)
    IF(JJJ.EQ.2)GO TO 804
    IF(JJJ.EQ.3)GO TO 2000
```

```
      WRITE (6,8)MM,IDAY,MONTH,IYEAR
      WRITE(6,7)
      WRITE(6,801)
  801 FORMAT(' SMOOTHED PLOT OF SODIUM DENSITY AS A FUNCTION OF HEIGHT F
     1OUND BY TAKING THE AVERAGE OF 3 CONSECUTIVE POINTS')
      WRITE(6,7)
      WRITE(6,701)
      WRITE(6,702)
      X1=0.04/3.
      DO 802 I=50,148
      I1=I
      I2=I+1
      I3=I+2
      DENST(I2)=(DENS(I1)+DENS(I2)+DENS(I3))*X1+0.5
      IDENS(I2)=DENST(I2)
  802 CONTINUE
      IF(JJJ.EQ.1)GO TO 803
  804 DO 901 I=50,150
      DENST(I)=DENST(I)-0.5
  901 CONTINUE
C     SELF ABSORPTION CORRECTION
      ABUND1=ABUND*1.0E-09
      IABUND=ABUND1
      I=IABUND+1
      J=I+1
      X1=S(J)-S(I)
      X2=IABUND
      X3=ABUND1-X2
      X4=(S(I)+X1*X3)*CONST*0.04
      X5=56.0+XBAR
      I=XBAR
      J=56+I
      X2=1./13.
  924 X1=J
      DENST(J)=DENST(J)+   (X5-X1)*X2*X4
      J=J-1
      IF(J.EQ.49)GO TO 923
      GO TO 924
C     BRACEWELL CORRECTION
  923 IB1=BI1
      BI2=IB1
      BI3=BI1-BI2
      BI4=BI1*0.5
      IB4=BI4
      BI5=BI4+1.
      IB5=BI5
      BI5=IB4
      BI6=BI4-BI5
      DO 900 I=50,129
      J1=I+IB1
```

```
      J2=J1+1
      X1=DENST(J2)-DENST(J1)
      X2=X1*BI3+DENST(J1)
      X3=(X2+DENST(I))*0.5
      J3=IB4+I
      J4=IB5+I
      X4=DENST(J4)-DENST(J3)
      X5=DENST(J3)+BI6*X4
      X6=X5-X3
      X7=X5+X6
      DENSTY(J3)=X7
  900 CONTINUE
      J3=IB4+50
      J4=IB4+128
      X5=1.0-BI6
      DO 902 I=J3,J4
      J=I+1
      X1=DENSTY(J)-DENSTY(I)
      X2=X1*X5+DENSTY(I)
      DENST(J)=X2
  902 CONTINUE
      DO 903 I=50,150
      DENST(I)=DENST(I)*25.
  903 CONTINUE
      WRITE (6,8)MM,IDAY,MONTH,IYEAR
      WRITE(6,7)
      WRITE(6,904)
  904 FORMAT(' INTERPOLATED DENSITIES AFTER SELF ABSORPTION AND BRACEWEL
     1L CORRECTIONS')
      WRITE(6,7)
      WRITE(6,613)
      WRITE(6,7)
      IN=50
      JN=54
  905 WRITE(6,614)(MHIGHT(J),DENST(J),J=IN,JN)
      IN=IN+5
      JN=JN+5
      IF(IN-150)905,906,906
  906 WRITE(6,14)
      WRITE (6,8)MM,IDAY,MONTH,IYEAR
      WRITE(6,7)
      WRITE(6,907)
  907 FORMAT('                    SODIUM DENSITY AS A FUNCTION OF HEIGHT A
     1FTER APPLYING SELF ABSORPTION AND BRACEWELL CORRECTIONS')
      WRITE(6,7)
      WRITE(6,701)
      XMAX=DENST(50)
      DO 950 I=51,150
      IF(DENST(I)-XMAX)950,952,952
  952 XMAX=DENST(I)
```

```
  950 CONTINUE
      IF(XMAX-2500.)953,953,954
  953 WRITE(6,702)
      DO 908 I=50,150
      DENST(I)=DENST(I)*0.04+0.5
      IDENS(I)=DENST(I)
  908 CONTINUE
      GO TO 803
  954 WRITE(6,955)
  955 FORMAT('          -10  -8  -6  -4  -2   0   2   4   6   8  10  12
     114  16  18  20  22  24  26  28  30  32  34  36  38  40  42  44  46
     2  48  50')
      DO 956 I=50,150
      DENST(I)=DENST(I)*0.02+0.5
      IDENS(I)=DENST(I)
  956 CONTINUE
      GO TO 803
C     DETERMINATION OF SCALE HEIGHT
 2000 IF(XMAX-2500.)2001,2001,2002
 2001 DO 2003 I=50,150
      DENST(I)=(DENST(I)-0.5)*25.
 2003 CONTINUE
      GO TO 2005
 2002 DO 2004 I=50,150
      DENST(I)=(DENST(I)-0.5)*50.
 2004 CONTINUE
 2005 DO 2006 I=62,150
      IF(DENST(I)-100.)2006,2007,2007
 2006 CONTINUE
 2007 J1=I
      I1=I+1
      XMAX=DENST(J1)
      DO 3000 J=I1,85
      IF(DENST(J)-XMAX)3001,3001,3000
 3000 CONTINUE
      GO TO 3004
 3001 J1=J
      XMAX=DENST(J1)
      I1=J+1
      DO 3003 I=I1,85
      IF(DENST(I)-XMAX)3003,3003,3004
 3003 CONTINUE
 3004 I1=I
      DO 2026 I=90,150
      IF(DENST(I)-100.)2021,2021,2026
 2026 CONTINUE
 2021 I2=I
      DO 2008 I=I1,I2
      DENST(I)=ALOG(DENST(I))
 2008 CONTINUE
```

```
      WRITE(6,8)MM,IDAY,MONTH,IYEAR
      WRITE(6,7)
      WRITE(6,2200)
 2200 FORMAT('            NATURAL LOGARITHM OF DENSITY AS A FUNCTION OF HE
     1IGHT IN KM.'/)
      WRITE(6,7)
      WRITE(6,2059)
 2059 FORMAT(' HEIGHT    LOG DENS        HEIGHT    LOG DENS        HEIGHT
     1   LOG DENS        HEIGHT    LOG DENS        HEIGHT    LOG DENS')
      WRITE(6,7)
      IN=I1
      JN=I1+4
 2024 IF(JN-I2)2022,2022,2023
 2023 JN=I2
 2022 WRITE(6,614)(MHIGHT(J),DENST(J),J=IN,JN)
      IF(JN-I2)2027,2025,2025
 2027 IN=IN+5
      JN=JN+5
      GO TO 2024
 2025 WRITE(6,14)
      DO 2030 I=I1,I2
      DENST(I)=DENST(I)*20.-49.5
      IDENS (I)=DENST(I)
 2030 CONTINUE
      WRITE(6,8)MM,IDAY,MONTH,IYEAR
      WRITE(6,7)
      WRITE(6,2009)
 2009 FORMAT('                                NATURAL LOGARITHM OF DENSITY AS A
     1 FUNCTION OF HEIGHT'/)
      WRITE(6,2020)
 2020 FORMAT('                          10 X NATURAL LOG. OF THE DENSITY OF SO
     1DIUM ATOMS PER CUBIC CENTIMETRE'/)
      WRITE (6,2010)
 2010 FORMAT('          30  32  34  36  38  40  42  44  46  48  50  52  54
     1  56  58  60  62  64  66  68  70  72  74  76  78  80  82  84  86
     288  90')
      DO 2011 I=10,130
      IPLOT(I)=IDOT
 2011 CONTINUE
      NX=IDENS (I2)
      IPLOT(NX)=IDOT
      GO TO 2019
 2012 FORMAT(4X,I3,2X ,130A1)
 2017 I2=I2-1
      DO 2013 I=11,129
      IPLOT(I)=INUL
 2013 CONTINUE
      NX=IDENS (I2)
      IPLOT(NX)=IDOT
 2019 IF(I2.EQ.140)GO TO 2014
```

```
      IF(I2.EQ.I1)GO TO 2015
      IF(I2.EQ.130)GO TO 2014
      IF(I2.EQ.120)GO TO 2014
      IF(I2.EQ.110)GO TO 2014
      IF(I2.EQ.100)GO TO 2014
      IF(I2.EQ.80)GO TO 2014
      IF(I2.EQ.70)GO TO 2014
      IF(I2.EQ.60)GO TO 2014
      IF(I2.EQ. 94)GO TO 2040
      IF(I2.EQ. 93)GO TO 2041
      IF(I2.EQ. 92)GO TO 2042
      IF(I2.EQ. 91)GO TO 2043
      IF(I2.EQ. 90)GO TO 2044
      IF(I2.EQ. 89)GO TO 2045
      IF(I2.EQ. 87)GO TO 2046
      IF(I2.EQ. 86)GO TO 2047
      WRITE(6,2016)(IPLOT(KK),KK=10,130)
2016  FORMAT(9X,130A1)
      GO TO 2017
2014  WRITE(6,2012)I2,(IPLOT(KK),KK=10,130)
      GO TO 2017
2040  WRITE(6,2050)(IPLOT(KK),KK=10,130)
2050  FORMAT(2X,'H',6X,130A1)
      GO TO 2017
2041  WRITE(6,2051)(IPLOT(KK),KK=10,130)
2051  FORMAT(2X,'E',6X,130A1)
      GO TO 2017
2042  WRITE(6,2052)(IPLOT(KK),KK=10,130)
2052  FORMAT(2X,'I',6X,130A1)
      GO TO 2017
2043  WRITE(6,2053)(IPLOT(KK),KK=10,130)
2053  FORMAT(2X,'G',6X,130A1)
      GO TO 2017
2044  WRITE(6,2054)I2,(IPLOT(KK),KK=10,130)
2054  FORMAT(2X,'H',I4,2X,130A1)
      GO TO 2017
2045  WRITE(6,2055)(IPLOT(KK),KK=10,130)
2055  FORMAT(2X,'T',6X,130A1)
      GO TO 2017
2046  WRITE(6,2056)(IPLOT(KK),KK=10,130)
2056  FORMAT(2X,'K',6X,130A1)
      GO TO 2017
2047  WRITE(6,2057)(IPLOT(KK),KK=10,130)
2057  FORMAT(2X,'M',6X,130A1)
      GO TO 2017
2015  DO 2018 I=10,130
      IPLOT(I)=IDOT
2018  CONTINUE
      NX=IDENS(I1)
      IPLOT(NX)=IDOT
```

```
      X1=I1
      X1=X1*0.1
      J=X1
      X2=J
      IF(X1-X2)2060,2061,2060
2061  WRITE(6,2012)I1,(IPLOT(KK),KK=10,130)
      WRITE(6,2010)
      GO TO 110
2060  WRITE(6,2016)(IPLOT(KK),KK=10,130)
      WRITE(6,2010)
      GO TO 110
      END
```

TYPICAL OUTPUT FROM THE PRINTER

SODIUM Z P.M. 1 NOV. 1967 VICTORIA, B.C.

E.H.T. = 750 VOLTS TIME CONSTANT = 25.0 SECS. RANGE = 3
START OF RUN = 17H 20M P.S.T.
CALIBRATION FACTOR = 90.4 R/DIV. ON RANGE 3
CONVERSION FACTOR = 12.550 ATOMS/CUBIC CM. PER R/KM.
SCREENING HEIGHT = 30.05 KM.
(A - M) = 0.27307 H
BRACEWELL INTERVAL = 22.1 KM.

CHART DIVISIONS TAKEN AT 60 SECOND TIME INTERVALS

36.700	36.700	36.700	36.700	36.700	36.700	36.700	36.700	36.700	36.500	36.200	35.700
34.900	34.000	32.600	30.900	28.900	26.600	24.100	21.200	18.200	15.000	12.000	9.300
7.100	5.100	3.900	3.100	2.500	2.100	1.900	1.600	1.400	1.300	1.200	1.100
1.000	1.000	1.000	1.000	1.000	1.000						

SODIUM Z P.M. 1 NOV. 1967 VICTORIA, B.C.

PLOT OF RECORDER RESPONSE IN DIVISIONS AS A FUNCTION OF TIME

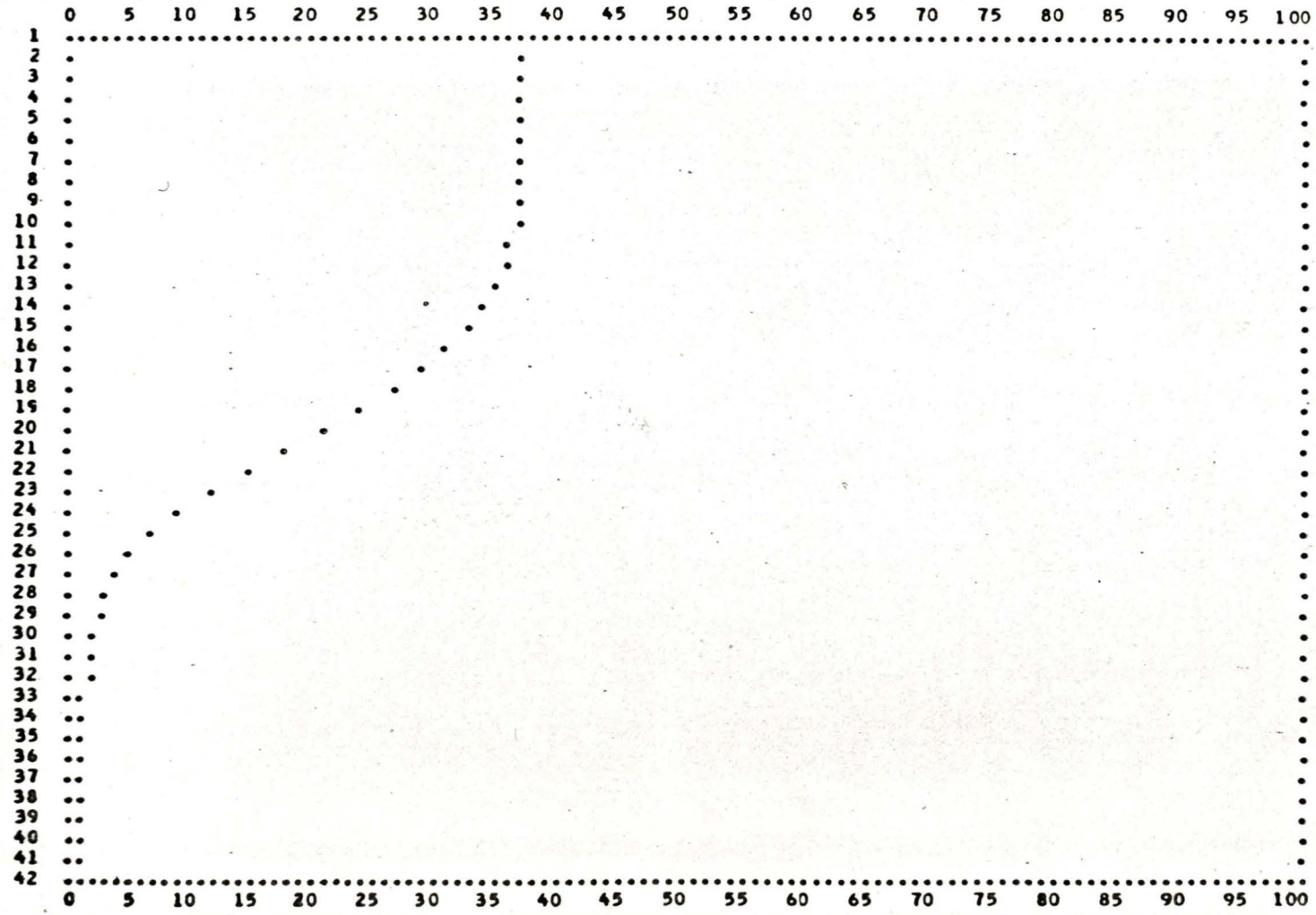

SODIUM 2 P.M. 1 NOV. 1967 VICTORIA, B.C.

HEIGHT IN KM. VERSUS DENSITY IN ATOMS/CUBIC CM.

HEIGHT	DENSITY	HEIGHT	DENSITY	HEIGHT	DENSITY	HEIGHT	DENSITY	HEIGHT	DENSITY	HEIGHT	DENSITY	HEIGHT	DENSITY
55.96	0.0	57.59	0.0	59.27	0.0	61.01	0.0	62.80	0.0	64.64	30.35	66.54	73.80
68.49	143.63	70.49	251.73	72.54	340.65	74.65	478.23	76.81	621.96	79.03	758.75	81.30	913.73
83.62	1025.25	86.00	1143.21	88.43	1233.28	90.92	1307.73	93.47	1334.89	96.06	1285.14	98.72	1173.98
101.43	1025.82	104.19	822.46	107.01	617.12	109.89	448.98	112.83	287.23	115.82	187.90	118.86	138.31
121.97	99.58	125.13	71.12	128.35	61.12	131.63	42.90	134.96	33.73	138.35	24.87	141.80	16.30
145.31	8.02	148.88	0.0	152.51	0.0								

INTENSITY CALCULATED AT TIME OF FIRST SCALE DIVISION = 3227. RAYLEIGHS

ABUNDANCE CALCULATED AT TIME OF FIRST SCALE DIVISION = 0.5362E 10 ATOMS/SQUARE CM. (COLUMN)

SODIUM 2 P.M. 1 NOV. 1967 VICTORIA, B.C.

HEIGHT IN KM. VERSUS DENSITY IN ATOMS/CUBIC CM.

INTERPOLATED DENSITIES

HEIGHT	DENSITY	HEIGHT	DENSITY	HEIGHT	DENSITY	HEIGHT	DENSITY	HEIGHT	DENSITY
50	0.0	51	0.0	52	0.0	53	0.0	54	0.0
55	0.0	56	0.0	57	0.0	58	0.0	59	0.0
60	0.0	61	0.0	62	0.0	63	3.28	64	19.76
65	38.53	66	61.44	67	90.31	68	126.16	69	171.34
70	225.37	71	273.90	72	317.19	73	370.52	74	435.73
75	501.38	76	567.88	77	633.49	78	695.25	79	757.00
80	825.11	81	893.41	82	947.41	83	995.36	84	1043.93
85	1093.54	86	1143.14	87	1180.18	88	1217.21	89	1250.20
90	1280.10	91	1308.54	92	1319.22	93	1329.90	94	1324.67
95	1305.53	96	1286.39	97	1245.97	98	1204.06	99	1158.57
100	1103.92	101	1049.27	102	983.82	103	910.25	104	836.68
105	763.73	106	690.94	107	618.14	108	559.50	109	501.07
110	442.99	111	387.90	112	332.81	113	281.49	114	248.27
115	215.04	116	184.92	117	168.64	118	152.37	119	136.61
120	124.13	121	111.65	122	99.28	123	90.29	124	81.30
125	72.30	126	68.42	127	65.31	128	62.20	129	57.50
130	51.94	131	46.38	132	41.87	133	39.12	134	36.37
135	33.63	136	31.02	137	28.40	138	25.79	139	23.26
140	20.78	141	18.30	142	15.84	143	13.48	144	11.11
145	8.75	146	6.47	147	4.23	148	1.98	149	0.0

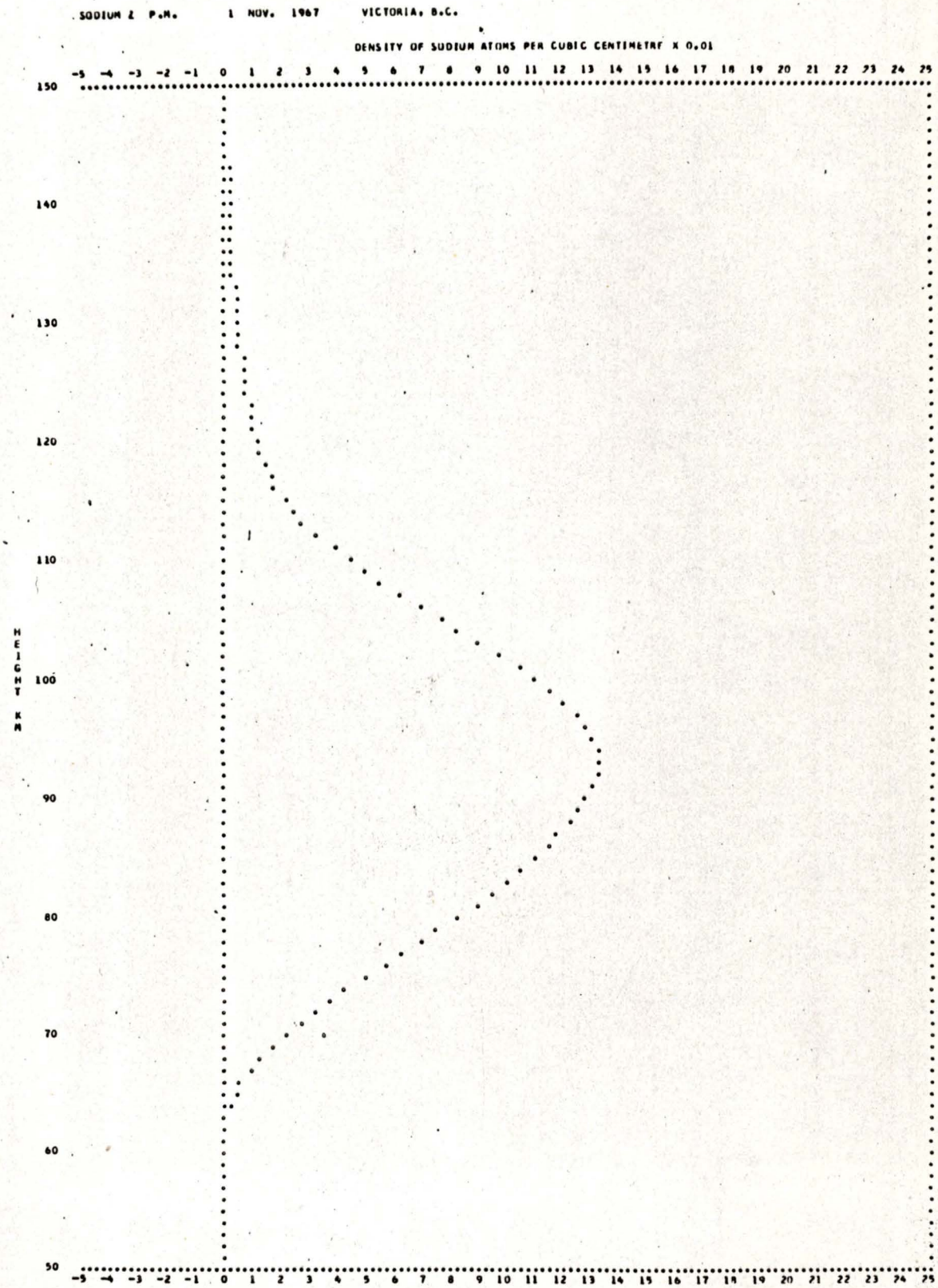
SODIUM 2 P.M. 1 NOV. 1967 VICTORIA, B.C.
DENSITY OF SODIUM ATOMS PER CUBIC CENTIMETRE X 0.01
-5 -4 -3 -2 -1 0 1 2 3 4 5 6 7 8 9 10 11 12 13 14 15 16 17 18 19 20 21 22 23 24 25
150
140
130
120
110
100
90
80
70
60
50
HEIGHT KM

SODIUM 2 P.M. 1 NOV. 1967 VICTORIA, B.C.

SMOOTHED PLOT OF SODIUM DENSITY AS A FUNCTION OF HEIGHT FOUND BY TAKING THE AVERAGE OF 3 CONSECUTIVE POINTS

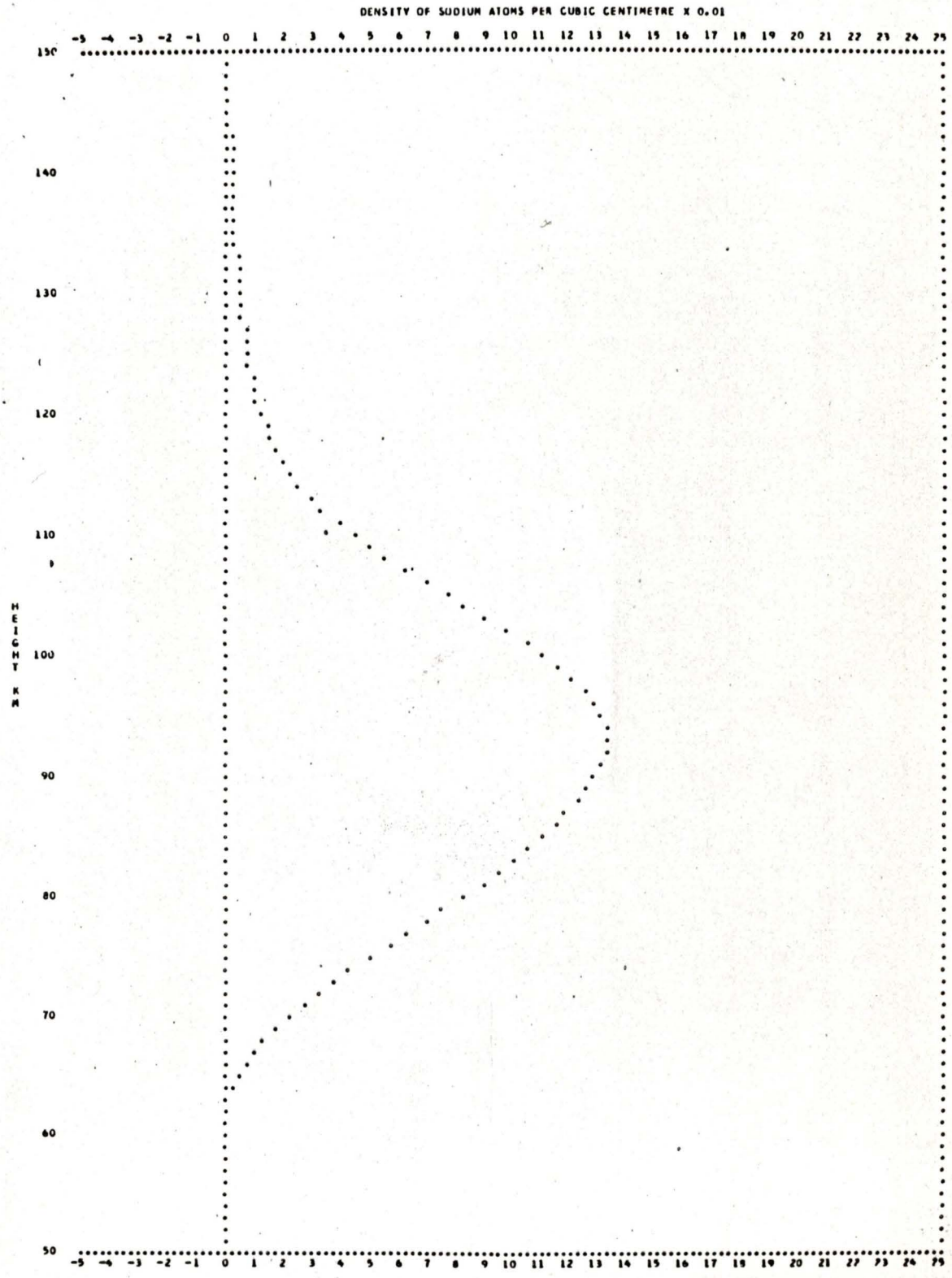

SODIUM Z P.M. 1 NOV. 1967 VICTORIA, B.C.

INTERPOLATED DENSITIES AFTER SELF ABSORPTION AND BRACEWELL CORRECTIONS

HEIGHT	DENSITY	HEIGHT	DENSITY	HEIGHT	DENSITY	HEIGHT	DENSITY	HEIGHT	DENSITY
50	313.68	51	304.97	52	296.27	53	287.57	54	278.87
55	270.17	56	261.47	57	252.77	58	244.07	59	235.37
60	226.66	61	217.96	62	23.03	63	-3.17	64	-18.95
65	-22.01	66	-15.79	67	2.50	68	35.13	69	83.22
70	141.07	71	201.43	72	264.88	73	339.32	74	425.53
75	518.74	76	607.80	77	694.47	78	776.70	79	858.46
80	943.39	81	1024.46	82	1098.12	83	1164.23	84	1229.55
85	1297.30	86	1360.21	87	1433.64	88	1501.05	89	1566.43
90	1628.59	91	1678.52	92	1719.22	93	1742.52	94	1749.03
95	1736.02	96	1697.59	97	1642.90	98	1567.02	99	1482.97
100	1390.79	101	1285.65	102	1167.94	103	1037.58	104	904.13
105	773.09	106	645.17	107	529.94	108	427.48	109	338.21
110	253.55	111	172.79	112	99.59	113	43.06	114	3.39
115	-21.89	116	-36.67	117	-40.25	118	-36.39	119	-31.68
120	-26.96	121	-21.10	122	-13.93	123	-5.81	124	1.06
125	7.64	126	14.56	127	22.32	128	26.84	129	27.35
130	25.57	131	23.27	132	22.17	133	22.32	134	23.02
135	23.29	136	22.79	137	21.32	138	18.57	139	15.62
140	12.84	141	18.30	142	15.87	143	13.48	144	11.11
145	8.78	146	6.48	147	4.23	148	2.07	149	0.66

SODIUM 2 P.M. 1 NOV. 1967 VICTORIA, B.C.

SODIUM DENSITY AS A FUNCTION OF HEIGHT AFTER APPLYING SELF ABSORPTION AND BRACEWELL CORRECTIONS

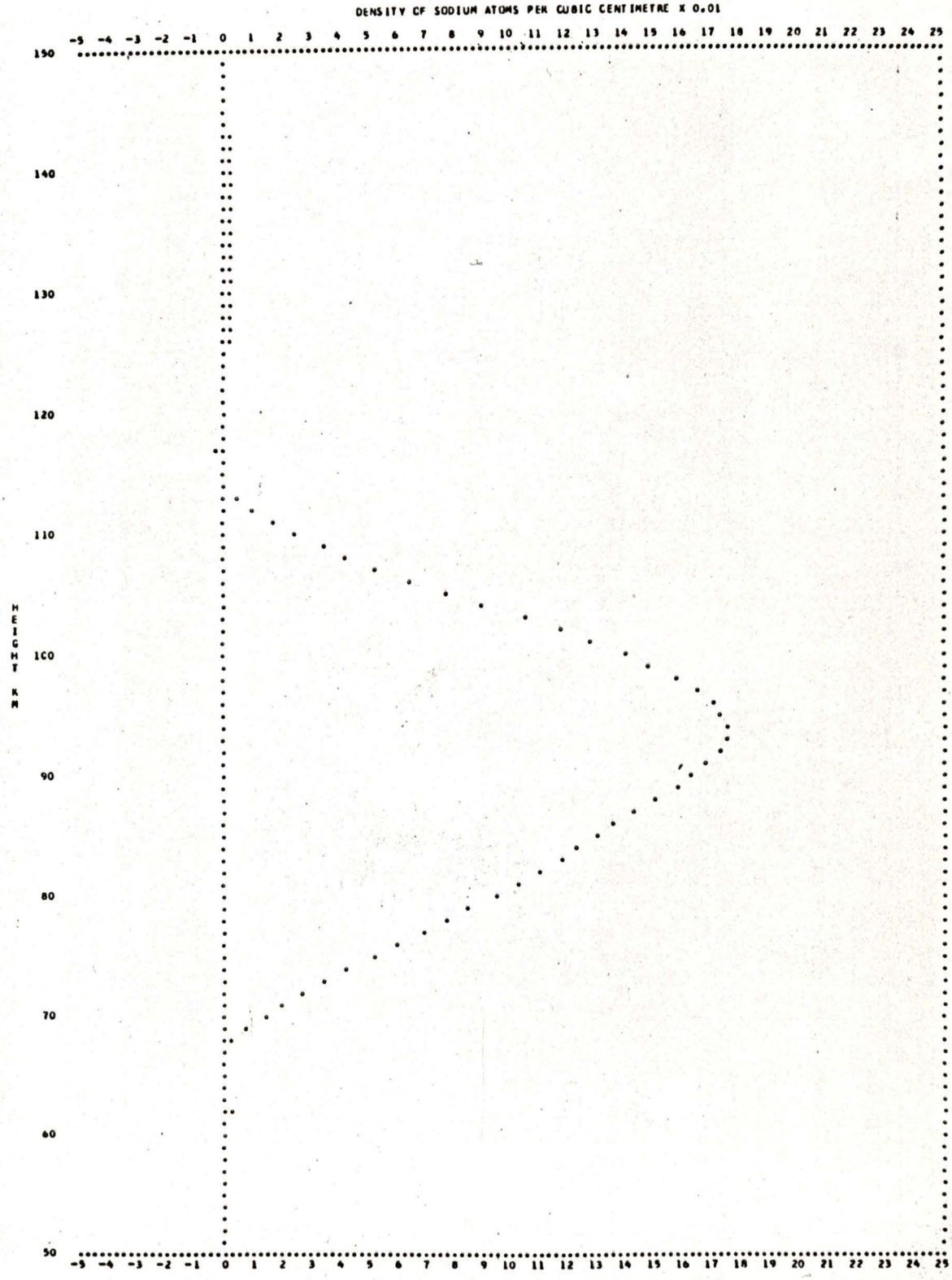

SODIUM Z P.M. 1 NOV. 1967 VICTORIA, B.C.

NATURAL LOGARITHM OF DENSITY AS A FUNCTION OF HEIGHT IN KM.

HEIGHT	LOG DENS	HEIGHT	LOG DENS	HEIGHT	LOG DENS	HEIGHT	LOG DENS	HEIGHT	LOG DENS
70	4.95	71	5.31	72	5.58	73	5.83	74	6.05
75	6.25	76	6.41	77	6.54	78	6.66	79	6.76
80	6.85	81	6.93	82	7.00	83	7.06	84	7.11
85	7.17	86	7.22	87	7.27	88	7.31	89	7.36
90	7.40	91	7.43	92	7.45	93	7.46	94	7.47
95	7.46	96	7.44	97	7.40	98	7.36	99	7.30
100	7.24	101	7.16	102	7.06	103	6.94	104	6.81
105	6.65	106	6.47	107	6.27	108	6.06	109	5.82
110	5.54	111	5.15	112	4.60				

SODIUM Z P.M. 1 NOV. 1967 VICTORIA, B.C.

NATURAL LOGARITHM OF DENSITY AS A FUNCTION OF HEIGHT

10 X NATURAL LOG. OF THE DENSITY OF SODIUM ATOMS PER CUBIC CENTIMETRE

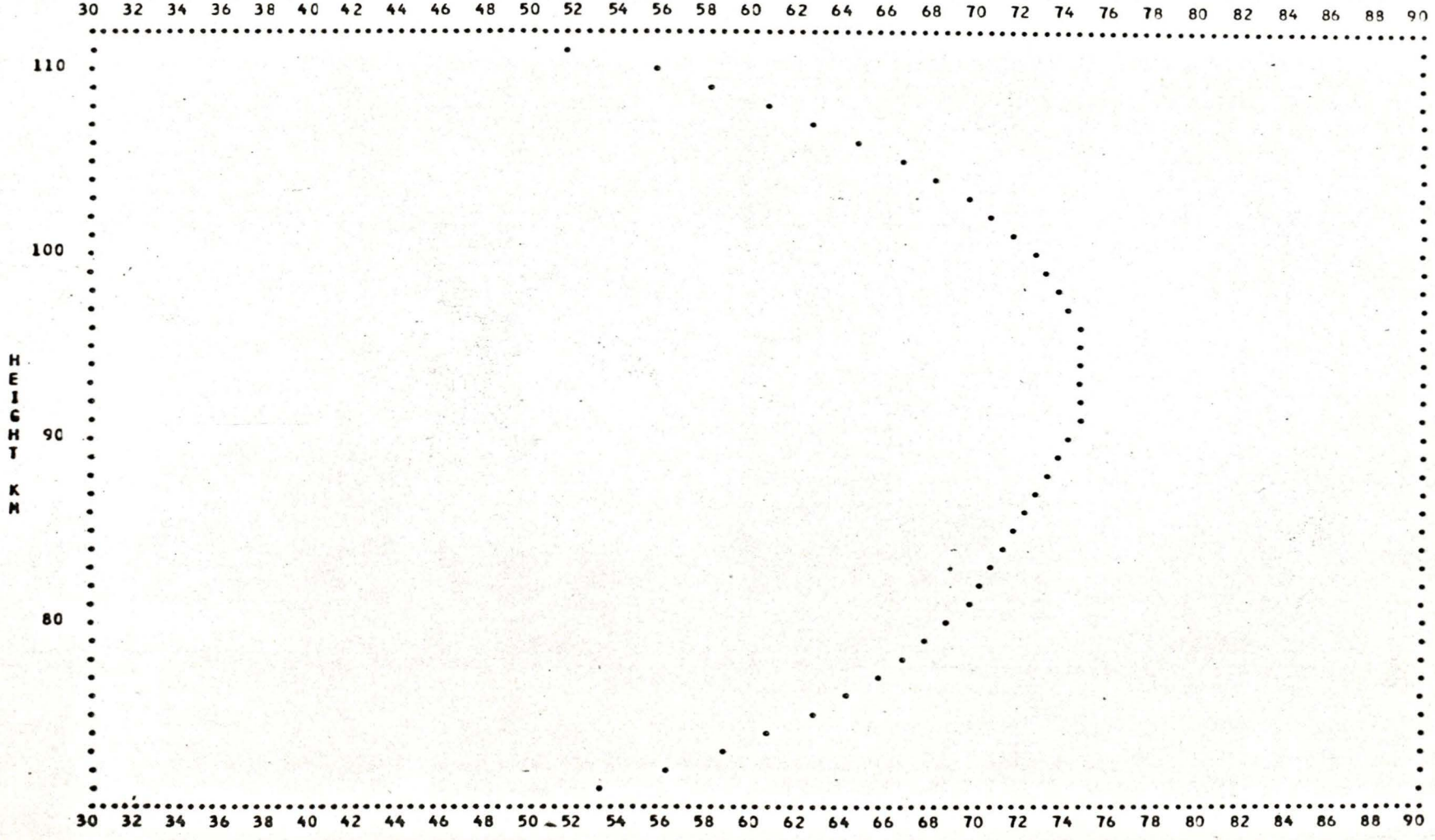

APPENDIX D

CALCULATION OF THE SOLAR DEPRESSION β AND THE AZIMUTH ANGLE α

1. Calculation of β

The solar depression, β , represents the angular depression of the sun below the horizon, measured along a great circle on the celestial sphere through the observer's zenith. Defining h to be the solar elevation, then:

$$\beta = -h \qquad \text{D1}$$

From figure D1 it can be seen that h and thence β can be determined if the quantities ϕ , δ and θ are known in the spherical triangle PZS , where ϕ is the observer's latitude, δ is the declination of the sun and θ is the solar hour angle.

The solar hour angle, θ , is given by the relation,

$$\theta = 12 - PST + LNGC - (A-M)_{obs} \qquad \text{D2}$$

for morning observations, and

$$\theta = PST - 12 - LNGC + (A-M)_{obs} \qquad \text{D3}$$

for evening observations, where PST is the Pacific Standard Time expressed in terms of a 24 hour clock, LNGC is the longitude correction for the observer

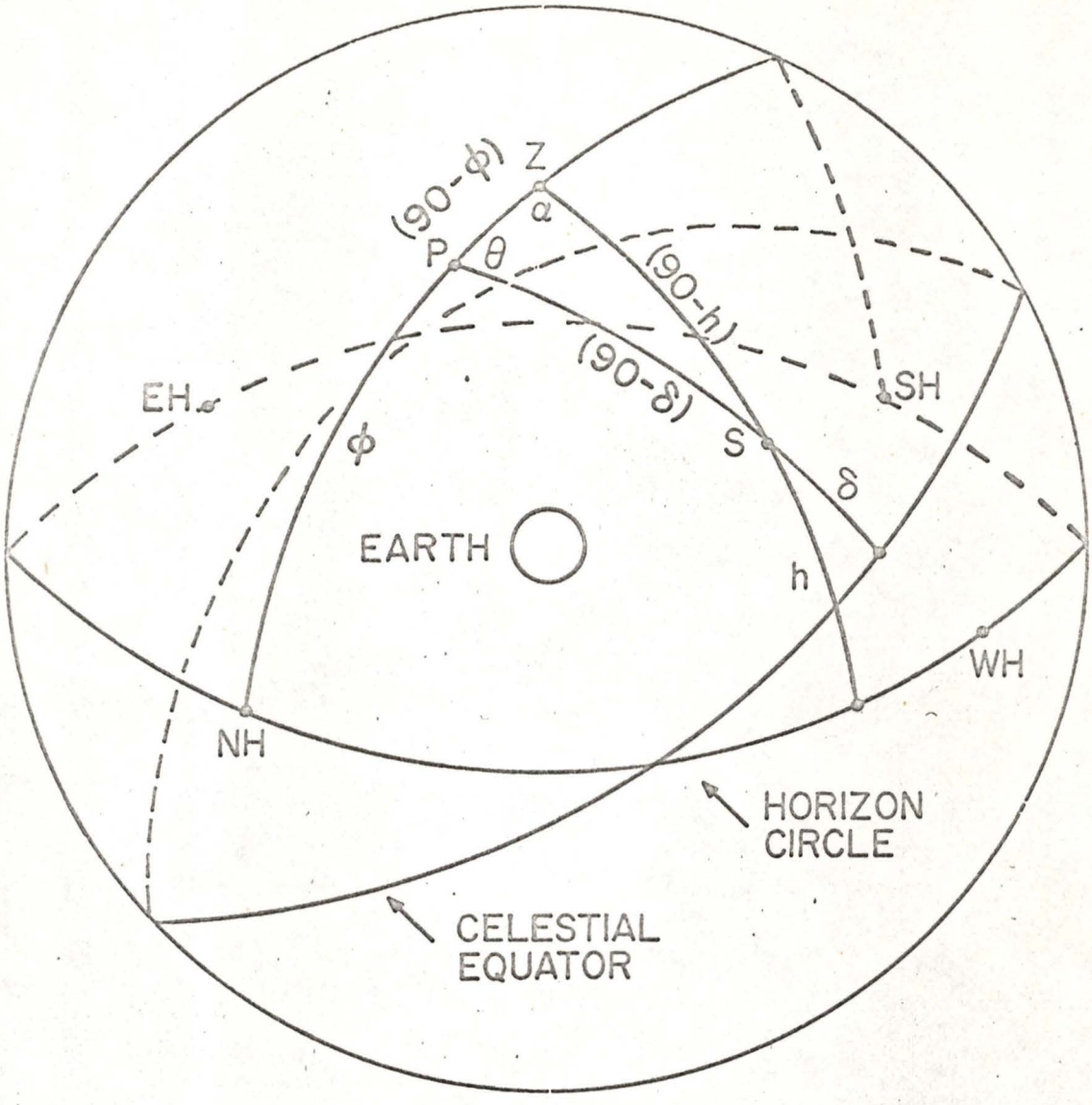

THE CELESTIAL SPHERE

P CELESTIAL POLE
Z OBSERVER'S ZENITH
S SUN
α SOLAR AZIMUTH MEASURED EAST OF NORTH
θ SOLAR HOUR ANGLE
δ SOLAR DECLINATION
h SOLAR ELEVATION
ϕ OBSERVER'S LATITUDE

Figure D1

The celestial sphere

and $(A-M)_{obs}$ is the equation of time at the time of the observation.

The value of $(A-M)_{obs}$ is easily calculated from

$$(A-M)_{obs} = (A-M)_{0} + \frac{(G.M.T.)[\Delta(A-M)]}{24} \qquad D4$$

where $(A-M)_{0}$ and $\Delta(A-M)$ are found from the American Ephemeris and Nautical Almanac and are respectively the equation of time at 0^h ephemeris time and the increment in the equation of time during the subsequent 24 hour period. (The equation of time is determined by subtracting the ephemeris transit time given in the Almanac from 12 hours). G.M.T. is the time of the observation expressed in hours of Greenwich Mean Time. (See figure D2). (A similar calculation is performed to determine the declination of the sun at the time of the observation).

Applying the cosine law to the spherical triangle PZS in figure D1 gives,

$$\cos(90^\circ-h) = \cos(90^\circ-\delta)\cos(90^\circ-\phi) + \sin(90^\circ-\delta)\sin(90^\circ-\phi)\cos\theta \qquad D5$$

or,

$$\sin h = \sin\delta\sin\phi + \cos\delta\cos\phi\cos\theta \qquad D6$$

from which h and thence β may be readily calculated.

2. Calculation of α

Again referring to the PZS triangle in figure D1 and applying the cosine law

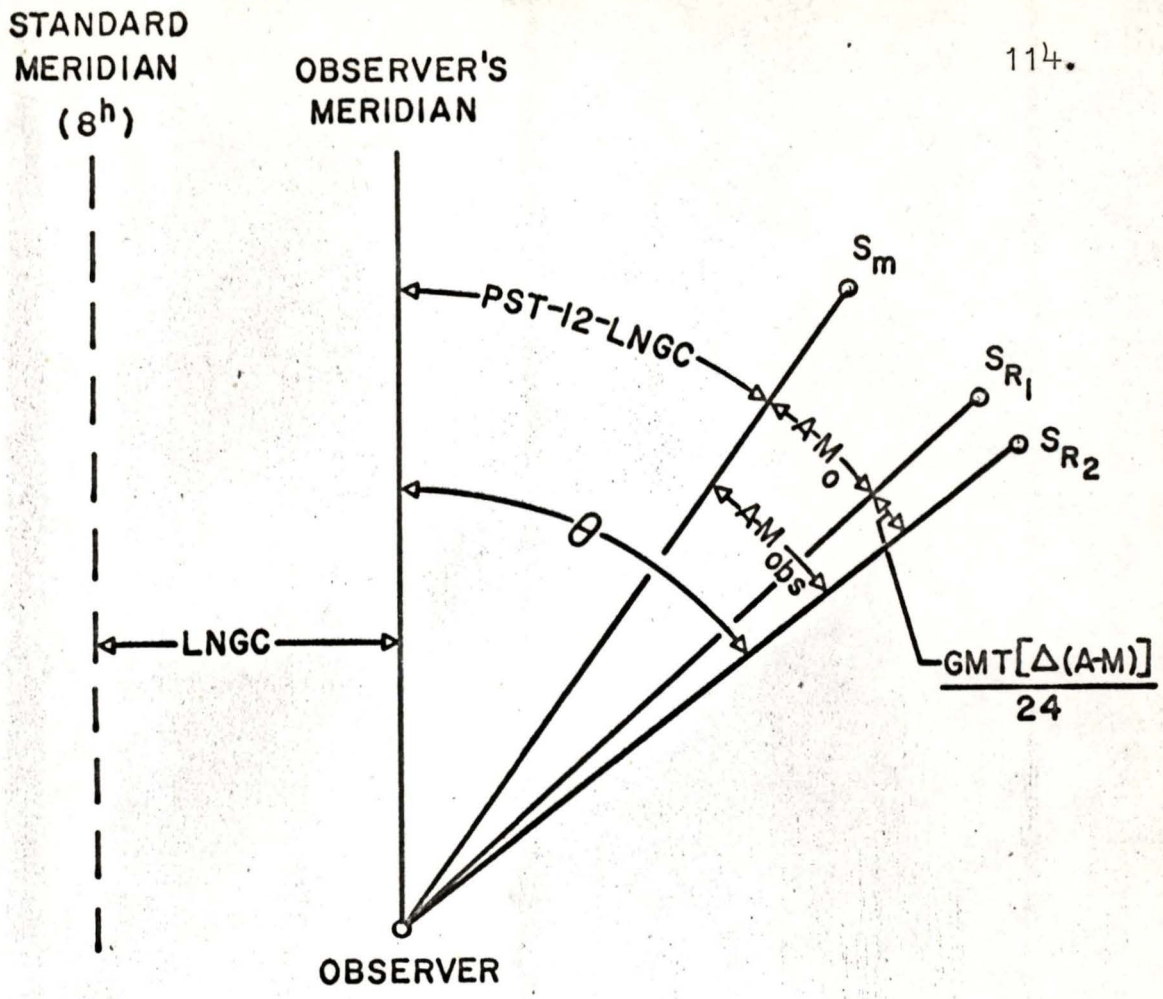

S_m	Position of the mean sun at the time of the observation.
S_{R_1}	Position of the real sun calculated using the value of the equation of time at 0^h ephemeris time
S_{R_2}	Position of the real sun at the time of the observation
PST	Pacific Standard Time
GMT	Greenwich Mean Time
LNGC	Longitude correction
$A-M_o$	Equation of time at 0^h ephemeris time
$\Delta(A-M)$	Change in the equation of time during 24^h period
$A-M_{obs}$	Equation of time at the time of the observation
θ	Solar hour angle

Figure D2

Schematic diagram showing the relation between Pacific Standard Time and Solar Hour Angle for an evening observation

$$\cos (90^\circ-\delta) = \cos (90^\circ-h) \cos (90^\circ-\phi) + \sin (90^\circ-h) \sin (90^\circ-\phi) \cos \alpha$$

or

$$\sin \delta = \sin h \sin \phi + \cos h \cos \phi \cos \alpha \qquad D7$$

where α is the solar azimuth angle measured east or west of north along a horizon circle.

The azimuth, α , may also be obtained by applying the law of sines:

$$\sin \alpha = \frac{\sin \theta}{\cos h} \cos \delta \quad . \qquad D8$$

If, for convenience, α is redefined as the solar azimuth angle measured east of north along a horizon circle, then the morning azimuth angle, α_m , is given by

$$\alpha_m = \sin^{-1}\left[\frac{\sin \theta \cos \delta}{\cos h}\right] \qquad D9$$

for hour angles greater than or equal to six hours and

$$\alpha_m = 180^\circ - \sin^{-1}\left[\frac{\sin \theta \cos \delta}{\cos h}\right] \qquad D10$$

for hour angles less than or equal to six hours.

The corresponding evening azimuth angle, α_e , may be expressed approximately in terms of the morning azimuth angle as follows,

$$\alpha_e = 360^\circ - \alpha_m \quad . \qquad D11$$

APPENDIX E

CALCULATION OF THE DATES OF THE EQUINOXES AT AN ALTITUDE OF 90 KILOMETERS

Chamberlain (1961) has shown that the earth's geometric shadow height, Z_S, is given by,

$$Z_S = R (\sec \beta - 1) \qquad E1$$

where R is the radius of the earth and β is the solar depression.

Thus from equation (E1)

$$\cos \beta = \frac{R}{Z_S + R} \quad . \qquad E2$$

In appendix D it was shown that,

$$\sin h = \sin \delta \sin \phi + \cos \delta \cos \phi \cos \theta \qquad E3$$

where h is the solar elevation, δ is the declination of the sun, ϕ is the observer's latitude, and θ is the solar hour angle.

Now at the equinoxes the solar hour angle is six hours and hence equation E3 reduces to,

$$\sin h = \sin \delta \sin \phi \qquad E4$$

or,

$$\sin \delta = \sin h / \sin \phi \quad . \qquad E5$$

Using the values R = 6,400 km. which is the radius of the earth plus a factor of 30 km. to allow for the screening height, and Z_S = 60 km. the angle β was found from equation (E2) to be $7^{o}49'$. Taking the latitude of Victoria to be 48.457^{o} the declination of the sun for an effective altitude of 90 km. at the equinoxes was found from equation (E5) to be $-10^{o}28'$. From the American Ephemeris and Nautical Almanac the dates when the sun had the above declinations were found to be February 22 and October 21, 1967.

APPENDIX F

DETERMINATION OF THE SCALE HEIGHT

If sodium atoms are thoroughly mixed with the other constituents of the atmosphere and if it is assumed that there is no mechanism for removing sodium atoms at altitudes above the peak density, then the decrease in density of sodium atoms above the peak should be given by the exponential law,

$$n(Z) = n_o \exp\left[-\frac{Z - Z_o}{H}\right] \qquad F1$$

where $n(Z)$ is the density of sodium atoms/cm.^{3} at the height Z in km., n_o is the density at the height Z_o and H is the scale height.

Taking the natural logarithm of both sides of equation (F1) gives,

$$H\left\{\ln\left[n(Z)\right] - \ln n_o\right\} = Z_o - Z \qquad F2$$

which is seen to be the equation of a straight line having slope H.

Thus above the peak density it would be expected, assuming the above conditions, that a plot of the natural logarithm of the density as a function of height would produce a straight line of slope H.

APPENDIX G

(Reprinted from Nature, Vol. 220, No. 5165, pp. 361-362, October 26, 1968)

Height of the Twilight Sodium Layer: Evening–Morning Effect observed at Victoria, British Columbia, from February 1967 to February 1968

An interesting variation in the height of maximum density of the twilight sodium layer was observed at Victoria, British Columbia, during a year long series of observations, between February 4, 1967, and February 29, 1968, using a birefringent photometer directed towards the zenith sky. It has been found that, in general, the height of the sodium layer during the morning twilight period is lower than the evening twilight layer by an amount which varies throughout the year. The difference in height appears to be greatest around the times of the equinoxes amounting to approximately 5 km, and least near the solstices, when the difference diminishes to zero.

The seasonal variation of this observed evening–morning height effect is illustrated in Fig. 1, in which the mean monthly height differences have been plotted throughout the year. The error bars represent the magnitude of twice the average mean deviation for each month, and the arrows indicate the times of the vernal and autumnal equinoxes which, for a 90 km sodium layer, occur on February 22 and October 21 respectively, due account being taken of the effect of atmospheric screening. It is clear from Fig. 1 that, within the limit of experimental error, the maximum height differences occur at the times of the equinoxes while the minimum differences occur at the solstices.

Although measurements of evening and morning heights have been recorded by Blamont and Donahue[1], no systematic seasonal variation in their mean monthly height differences could be reported, because the effect seemed to reverse several times throughout the year.

The observations made at Victoria have been very carefully corrected for the contaminating effects resulting from Rayleigh scattering so that the resulting intensity curves represent a very pure signal. Only observations made under clear or slightly hazy skies, and adequately corrected for the effects of white light, have been included in the analysis; furthermore, only pairs of observations, in which a morning run was immediately preceded or followed by an evening run, were considered. Where three or more consecutive observations were possible they were considered in triplets, the heights of the first and third members having been interpolated linearly to the time of

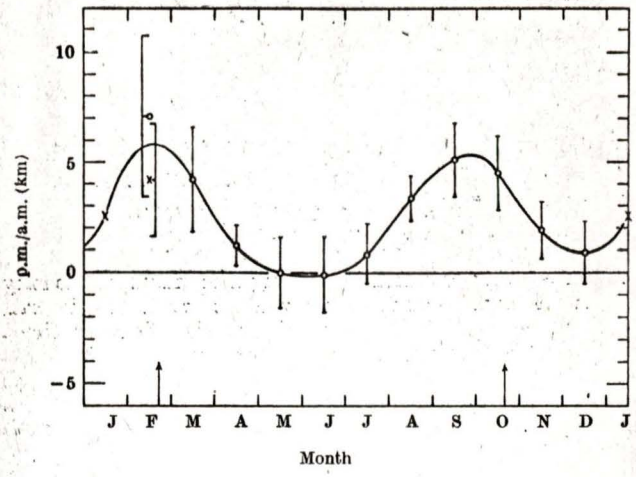

Fig. 1. Seasonal variation of the evening–morning difference in the heights of the twilight sodium layer at Victoria, from February 1967 to February 1968. The error bars represent twice the magnitude of the average mean deviation of the differences for each month, and the arrows indicate the times of the vernal and autumnal equinoxes at the 90 km level. No error bar has been assigned to the January value because very few observations were available for this month. ○, 1967; ×, 1968.

observation of the second member in order to eliminate as much as possible any day to day height variation.

Although Hunten[2] predicted an evening/morning intensity effect on the basis of photoionization of sodium and neutralization of sodium ions, and Blamont and Donahue[1] have actually reported such an effect, no such effect has been observed at Victoria. The same observations as those which were used for a study of the height variations were used to determine whether an evening/morning intensity effect could be observed. In Fig. 2 is plotted the average of the evening to morning ratios of the plateau intensities for each month. The error bars again represent twice the average mean deviation. It is clear from this figure that the p.m./a.m. plateau intensity ratios do not differ from unity by more than ± 20 per cent throughout the year. Because the average ratio for the entire year was 1·02 and this value is contained by all the error bars, no attempt was made to draw a smooth curve through the plotted points.

It is remarkable that no discernible evening/morning intensity effect could be observed in view of the corresponding apparent variation in the height of maximum density. If the evening–morning height effect is a consequence of a subsidence of the atmosphere as a whole during the night, free sodium atoms might be expected to disappear because atomic oxygen would move down into

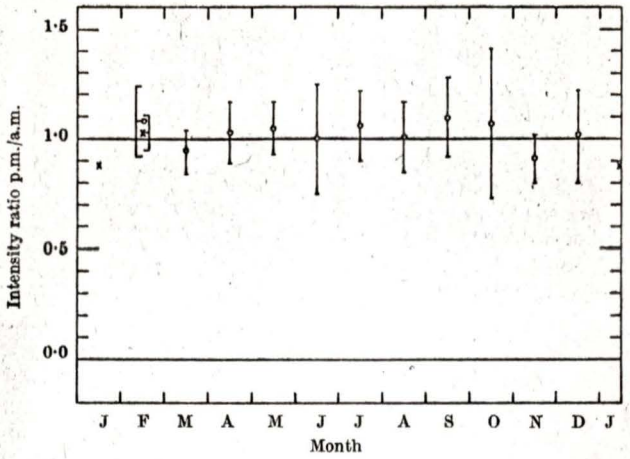

Fig. 2. Seasonal variation of the evening/morning plateau intensity ratio for twilight emission at Victoria, from February 1967 to February 1968. The error bars represent twice the magnitude of the average mean deviation of the ratios for each month. No error bar has been assigned to the January value because very few observations were available for this month. ○, 1967; ×, 1968.

a region more favourable for recombination. This, however, does not seem to happen between evening and morning. On the other hand, for longer periods there does seem to be a direct correlation between height and intensity, as a study of the seasonal height variation at Victoria carried out during the same period has revealed. Results of this study will be summarized later.

Although in general the morning heights have been found to be lower than the evening heights, this need not imply that every morning height should necessarily be lower than the immediately preceding or following evening height, for it is conceivable that some atmospheric process raises or lowers the height of the layer in either the morning or the evening. Several cases have been found in which the morning height was greater than that for the previous evening or the following evening, even at about the times of the equinoxes when the differences are great; however, near these times the cases are rare, as can be seen by examination of Table 1 which indicates the total

Table 1. SUMMARY OF THE TOTAL NUMBER OF EVENING–MORNING COMPARISONS FOR EACH MONTH AND THE NUMBER OF INSTANCES IN WHICH THE P.M.–A.M. HEIGHT DIFFERENCE WAS NEGATIVE

No. of p.m.–a.m. comparisons	1967 F	M	A	M	J	J	A	S	O	N	D	1968 J	F
Total	7	8	8	4	9	31	33	16	4	11	7	1	11
Negative height differences	1*	0	2	2	5	10	0	0	0	2	2	0	0

* In this case the difference was only 0·8 km.

number of evening–morning comparisons for each month as well as the number of cases in which the p.m.–a.m height difference was negative.

In November, for example, of eleven triplets only two showed negative p.m.–a.m. differences.

If a suitable explanation can be found for the usual evening–morning height effect, then those cases which exhibit an abnormal effect might be related to meteorological phenomena. In any event, twilight sodium observations seem to be able to provide some information about atmospheric dynamics in the 90 km region, information which might be of considerable interest to meteorologists.

This work was supported by the National Research Council of Canada, and by funds made available by the University of Victoria through a faculty research grant. The observations were made by Mr J. Sommers.

H. M. Sullivan
M. G. Roberts

Department of Physics,
University of Victoria,
British Columbia.

Received September 16, 1968.

[1] Blamont, J. E., and Donahue, T. M., *J. Geophys. Res.*, **69**, 4093 (1964).
[2] Hunten, D. M., *J. Atmos. Terr. Phys.*, **5**, 44 (1954).

Printed in Great Britain by Fisher, Knight & Co., Ltd., St. Albans.

LIST OF REFERENCES

Aller, L. H. 1953. Astrophysics: The atmospheres of the sun and stars. Ronald Press Co., N.Y.

Armstrong, E. B. 1968. Planetary and Space Science 16, No. 2, 211-229.

Barbier, D. 1948. Ann. de Géophys. 4, 193-210.

Bernard, R. 1938. Z. Phys. 110, 291-302.

Blamont, J.E., and Donahue, T. M. 1964. J. Geophys. Res. 69, 4093-4127.

Blamont, J. E., and Kastler, A. 1951. Ann. de Géophys. 7, 73.

Bracewell, R. N. 1955. J. Opt. Soc. Am. 45, 873.

Bricard, J. and Kastler, A. 1944. Ann. de Géophys. 1, 53.

Bricard, J. and Kastler, A. 1950. Ann. de Géophys. 6, 286-299.

Bricard, J. and Kastler, A. 1952. Mem. Soc. Roy. Sci. Liège 12, No. 1-2, 87-96.

Bricard, J., Kastler, A. and Robley, R. 1949. C.R. 228, 1601.

Bullock, W. R. and Hunten, D. M. 1961. Can. J. Phys. 39, 976.

Butler, S. T. 1962. Sci. Amer., 49-55.

Butler, S. T. and Small, K. A. 1963. Proc. Roy. Soc. (A). 274, 91-121.

Chamberlain, J. W. 1961. Physics of the Aurora and Airglow, No. 2, Academic Press, N.Y.

Chamberlain, J. W., Hunten, D. M. and Mack, J. E. 1958. J. Atmos. Terr. Phys. 12, 153.

Chapman, S. 1939. Astrophys. J. 90, 309-316.

Chapman, S. 1951. Compendium of Meteorology, American Meteorological Society, 510-530.

Donahue, T. M. and Blamont, J. E. 1961. Ann. de Géophys. 17, 116.

Dufay, J. 1947. C. R. Acad. Sci. (Paris) 225, 690-692.

Elvey, C. T. and Farnsworth, A. H. 1942. Astrophys. J. 96, 451-467.

Gault, W. A. 1967. Ph.D. Thesis, University of Saskatchewan.

Haurwitz, B. and Sepúlveda, G. M. 1957. Archiv für Meteorologie, Geophysik und Bioklimatologie Serie A: Meteorologie und Geophysik, Band 10, 1. Heft, 29-42.

Herzberg, G. 1944. Atomic Spectra and Atomic Structure, Dover Pub., N.Y.

Hunten, D. M. 1954. J. Atmos. Terr. Phys. 5, 44.

Hunten, D. M. 1960. J. Atmos. Terr. Phys. 17, 295.

Hunten, D. M. 1962. J. Atmos. Terr. Phys. 24, 333.

Hunten, D. M. and Godson, W. L. 1967. J. Atmos. Sci. 24, No. 1

Hunten, D. M., Vallance Jones, A., Ellyett, C. D. and McLauchlan, E. C. 1964. J. Atmos. Terr. Phys. 26, 67.

Hunten, D. M., Roach, F. E. and Chamberlain, J. W. 1956. J. Atmos. Terr. Phys. 8, 345-346.

Hunten, D. M. and Wallace, L. 1967. J. Geophys. Res. 72, 69.

Omholt, A. 1957. J. Geophys. Res. 20, 106.

Rundle, H. N., Hunten, D. M. and Chamberlain, J. W. 1960. J. Atmos. Terr. Phys. 17, 205.

Sullivan, H. M. 1962. Ph.D. Thesis, University of Saskatchewan.

Sullivan, H. M. and Hunten, D. M. 1964. Can. J. Phys. 42, 937.

Sullivan, H. M. and Roberts, M. G. 1968. Nature 220, 361-362.

Vegard, L. and Kvifte, G. 1945. Geofys. Publ. 16, No. 7.

Surname: ROBERTS Given Names: MICHAEL GEORGE

Place of Birth: BIRMINGHAM, ENGLAND

Date of Birth: SEPTEMBER 17, 1940

Educational Institutions Attended, with Dates of Entering and Leaving:

VICTORIA COLLEGE	1958	to	1963
UNIVERSITY OF BRITISH COLUMBIA	1963	to	1964
UNIVERSITY OF VICTORIA	1965	to	1969

Degrees, Diplomas, Etc., Awarded, with Dates and Names of Institutions:

B.Sc. (Majors)	1963	University of British Columbia at Victoria College, Victoria, B.C.

Honours and Awards:

University of Victoria Bursary, 1966/67

Publications:

Height of the Twilight Sodium Layer; Evening-Morning Effect observed at Victoria, British Columbia, from February 1967 to February 1968. Sullivan, H. M. and Roberts, M. G. Nature 220, 361-2.

THE UNIVERSITY OF VICTORIA LIBRARY

MANUSCRIPT THESIS

AUTHORITY TO DISTRIBUTE

AUTHOR: This thesis may be lent or microfilm copies made available:

(signature of the author in one of the spaces below)

(a) Without restriction [redacted]

(b) With the restriction that, for a period of five years (until . . . . . .) the date written approval of the following is required:

(1) The Dean, Faculty of Graduate Studies .....

(2) The Author .....

(3) both the Dean, Faculty of Graduate Studies, and the Author .....

BORROWERS: The borrower undertakes, by signing below, to give proper credit for any use made of the thesis, and to obtain the consent of the author if it is proposed to make extensive quotations, or to reproduce the thesis in whole or in part.

Signature of Borrower	Address	Date